EXPERIMENTAL EVOLUTION OF PEPTIDOGLYCAN BIOSYNTHESIS IN *VIBRIO FISCHERI*

By

MACEY N COPPINGER

(Under the Direction of ERIC V STABB)

ABSTRACT

The bacterial cell wall is largely comprised of peptidoglycan (PG), a bacteria-specific molecule that is sturdy and protective, yet fluid enough to allow for cellular growth and division. PG structure is highly conserved, though there are examples of natural variation. Elucidating the mechanisms of this PG variation will inform our understanding of antibiotic resistance, PG signaling within hosts, and the evolution of the bacterial cell wall. We are interested in PG structure in *Vibrio fischeri*, because of PG's role in the model symbiosis between *V. fischeri* and the Hawaiian bobtail squid. Specifically, PG monomers released from *V. fischeri* trigger normal host development of the symbiotic organ. In this dissertation, I altered *V.* fischeri's PG biosynthesis via isolation of spontaneous suppressor mutants from strains that were previously auxotrophic for PG-specific D-amino acids. First, I detail the characterization of a D-glutamate suppressor with a novel biosynthesis pathway to wildtype PG structure. Fusion of two proteins buries the secretion signal of BsrF, a periplasmic broad-spectrum

racemase. When relegated to the cytoplasm, BsrF produces the D-glu and D-ala necessary biosynthesis of wild-type PG structure. Next, I describe a set of D-glu suppressors that have mutations in *gltS*, which encodes a sodium:glutamate symporter. These mutations lead to increased D-glu transport and permissive transport of toxic glutamate structural analogues. I then characterize D-ala auxotrophy in *V. fischeri*, and the extent to which it can be suppressed. Finally, I describe our work to develop a novel method for transiently colonized *Euprymna scolopes* through use of a D-ala auxotrophic strain. Together, these discoveries and insights broaden our understanding of D-amino acids and the evolution of PG structure.

INDEX WORDS: *Aliivibrio,* peptidoglycan, D-glutamate, D-alanine, racemase

EXPERIMENTAL EVOLUTION OF PEPTIDOGLYCAN BIOSYNTHESIS IN *VIBRIO FISCHERI*

By

MACEY N COPPINGER

B.S., University of Illinois Urbana-Champaign, 2017

A Dissertation Submitted to the Graduate Faculty of The University of Georgia in Partial Fulfillment of the Requirements for the Degree

DOCTOR OF PHILOSOPHY

ATHENS, GA

2023

EXPERIMENTAL EVOLUTION OF PEPTIDOGLYCAN BIOSYNTHESIS IN *VIBRIO FISCHERI*

By

MACEY N COPPINGER

Major Professor: Eric V Stabb
Committee: Ellen Neidle
Christine Szymanski
Stephen Trent

Electronic Version Approved:

Ron Walcott
Dean of the Graduate School
The University of Georgia
December 2023

DEDICATION

I dedicate this dissertation to a younger Macey. The Macey who wasn't allowed to learn evolution in school. The one who took summer science courses through the community college, because the high school didn't have AP sciences. To the college girl who wanted to give up, when she got her lowest grade in molecular genetics. And to the Macey who, for so many years, couldn't see any future for herself. To that girl: I still may not know what I want to be when I grow up, but I'm out of the fog and apparently, I'm a pretty smart scientist now!

Miss Macey, we did it.

ACKNOWLEDGEMENTS

First, I want to thank all the Real Adult Scientists that have seen me through this:

I thank Dave Popham for working with me since my first day as a roton in Stabb Lab, for all his ideas and advice, and for hosting me in his lab to show me HPLC. To my committee members, Ellen Neidle, Christine Szymanski, and Stephen Trent: thank you for working with us through these projects! And of course, I am grateful for my mentor Eric, who's always quick to remind me that I am smart, my time is valuable, and I **am** a scientist.

To my family and friends:

I'd like to thank my parents for going through this with me. Without their support I couldn't have gotten to this point, let alone through it. For helping me to become who I am, for all their love and support, and for all the work they've done for my education.

Abby and Alex: the best friends I could ever dream of having. Words cannot express how much I love and appreciate them, for all that they are and all that they do. I'm immensely proud of and thankful for you both.

Bellissimo: the kindest person I know. I'm truly grateful for everything she is.

To my countless friends from home, from college, from UGA and Chicago: your friendships have supported and motivated me through everything.

Finally, I thank Maxis and Blaise for their unconditional love and support.

TABLE OF CONTENTS

Page

ACKNOWLEDGEMNETS v

LIST OF TABLES ix

LIST OF FIGURES x

CHAPTER

1 Introduction and Literature Review 1

Overview 1

Vibrio-Euprymna symbiosis as a model system 2

Light organ colonization 4

Signaling molecules in squid-*Vibrio* 7

PG biosynthesis and recycling in *V. fischeri* 9

Variations in PG structure 12

D-amino acids in bacteria 15

Bacterial amino acid racemases 17

Rationale and scope of this work 21

2 A prototrophic suppressor of a *Vibrio fischeri* D-glutamate auxotroph reveals a member of the periplasmic broad-spectrum racemase family, BsrF 22

Abstract 23

Importance 24

Introduction 24

Results 26
Discussion 36
Materials and methods 40
Acknowledgements 48
3 Mutant *glts* alleles enable a *Vibrio fischeri* D-glutamate auxotroph to grow with lower requirements for exogenous D-glutamate 49
Abstract 50
Importance 51
Introduction 51
Results 53
Discussion 64
Materials and methods 69
Acknowledgements 77
4 Transient infection of *Euprymna scolopes* with an engineered D-alanine auxotroph of *Vibrio fischeri* 78
Abstract 79
Importance 80
Introduction 80
Results 83
Discussion 91
Materials and methods 95
Acknowledgements 102
5 Conclusions and Future Directions 103

Altering the broad-spectrum racemase, BsrF 105

Characterization of mutants with altered glutamate transport 106

D-ala auxotrophy in culture and in symbiosis 109

Future study of the DAP branch of PG biosynthesis 111

Final conclusions 112

REFERENCES..... 113

LIST OF TABLES

Page

Table 1.1: Examples of well-characterized bacterial broad-spectrum racemases 19

Table 2.1: Selection for prototrophic suppressors in D-glu auxotroph RMJ13 28

Table 2.2: Strains and plasmids used in this study 42

Table 2.3: Oligonucleotides used in this study 43

Table 3.1: RMJ13 derivative strains and mutations 55

Table 3.2: Average D-amino acid concentrations in various media and solutions 56

Table 3.3: Strains used in this study 70

Table 3.4: Plasmids and oligonucleotides used in this study 71

Table 4.1: Strains used in this study 87

Table 4.2: Selection of prototrophic suppressors of D-ala auxotrophy 88

Table 4.3: Plasmids and primers used in this study 97

LIST OF FIGURES

Page

Figure 1.1: Organization of the juvenile *E. scolopes* light organ 5

Figure 1.2: *E. scolopes* light organ morphogenesis 6

Figure 1.3: Diagram of peptidoglycan structure in *V. fischeri* 10

Figure 1.4: Enantiomeric structures of PG-specific D-amino acids 18

Figure 2.1: D-glu independent prototrophy of suppressor RMJ13S10 29

Figure 2.2: Genotype of RMJ13S10 30

Figure 2.3: Removal of putative secretion signal sequence from BsrF 32

Figure 2.4: Removing the secretion signal from BsrF increases resistance to DCS 33

Figure 2.5: Expression of ΔSS-*bsrF* suppresses multiple auxotrophies 34

Figure 2.6: Cytoplasmic BsrF does not affect PG composition 35

Figure 3.1: RMJ13 and suppressor mutants grow with varied supplementation 54

Figure 3.2: Mutant *gltS* alleles lower D-glu requirement of D-glu auxotroph 58

Figure 3.3: Expressing mutant *gltS* increases sensitivity to HCA 59

Figure 3.4: Muropeptide profiles of *V. fischeri strains* 61

Figure 3.5: Diagrams of predicted GltS protein structures 62

Figure 3.6: D-glu auxotrophic *V. fischeri* appears to transiently colonize *E. scolopes*, dependent upon D-glu 63

Figure 3.7: *V. fischeri* D-glu auxotroph lyses without D-glu 64

Figure 4.1: Generation and recovery of D-ala auxotrophy 84

Figure 4.2: Expression of *metC* in an *alr* mutant can enable growth without D-ala 85

Figure 4.3: MetC is involved in L-met and D-ala synthesis..... 85

Figure 4.4: Expression of *metC* leads to PG structure 86

Figure 4.5: D-ala auxotrophic *V. fischeri* requires D-ala to maintain cell morphology .. 90

Figure 4.6: *V. fischeri* colonization of *E. scolopes* requires D-alanine 91

CHAPTER 1

INTRODUCTION AND LITERATURE REVIEW

OVERVIEW

We believe today that simple, anucleate microbes were the first life-forms to inhabit the earth. Microbial Eukaryotes then arose from these bacterial and archaeal species, surrounded by these Prokaryotes. Importantly, this evolutionary history led to integration of bacteria into the healthy biology of nearly all Eukaryotes, even as they evolved into multicellular, increasingly complex organisms. Beneficial relationships between different species are referred to as mutualistic symbioses and are generally accepted as a driving force of evolution (1). In the case of mutualisms with animals, bacterial interactions can aid in physical growth as well as in development of the host's innate immune system (2). Responses to bacterial symbionts are accomplished in part through specific signaling programs between the two partners, or through host recognition of invading or neighboring bacteria. Hosts often detect these bacteria based on microbe-associated molecular patterns, or MAMPs. MAMPs are common to both mutualists and pathogens, so a properly functioning innate immune system is vitally important to the host. One important MAMP in both mutualistic and pathogenic relationships is the main constituent of the bacterial cell wall, peptidoglycan (PG). PG has not been found in Eukaryotes but is conserved in nearly all known bacterial species. For these reasons,

PG is an ideal signaling molecule for both microbes and hosts and has been an important target for antibacterial drugs.

One example of PG as a MAMP is found in the mutualism between *Vibrio fischeri* and the Hawaiian bobtail squid, *Euprymna scolopes* (3). Importantly, this symbiosis is readily tractable in lab, and the PG-specific host changes are easy to observe and measure over time. *V. fischeri* has the typical PG structure found in Gram-negative organisms, allowing us to use it as a model for PG biosynthesis in other Gram-negative species. Additionally, the squid-*Vibrio* mutualism is a specific two-partner system (4, 5), making the study of PG signaling in this partnership relatively straightforward. These studies can further inform our understanding of Gram-negative PG biosynthesis and evolution, as well as how bacterial cells respond to altered PG synthesis and structure.

VIBRIO-EUPRYMNA SYMBIOSIS AS A MODEL SYSTEM

As stated above, the squid-*Vibrio* symbiosis is an excellent model system for investigating host-microbe interactions. Most importantly, both partners can be harvested from the ocean, Hawaiian bobtail squid can be maintained and bred in the lab, and *V. fischeri* is easily culturable and genetically manipulated under lab conditions (4, 6). In an established symbiosis between these partners, *V. fischeri* emits bioluminescence from specialized host tissues within a light-emitting organ (2, 6-8). This light organ is embedded on the ventral side of the ink sac, directed downward in the mantle cavity of the squid.

When juvenile *E. scolopes* hatch, their light organs are devoid of symbiotic bacteria; *V. fischeri* is then transmitted horizontally from the surrounding seawater (4).

Therefore, aposymbiotic squid can be raised in the lab, and initiation of the symbiosis can be controlled experimentally (9). This initiation simply involves placing the squid in seawater that has been inoculated with symbiosis-competent *V. fischeri*. The squid are able to obtain symbiotic bacteria from the water column, because the light organ is essentially external, always in contact with the surrounding seawater (2, 7). This direct exposure of the light organ to the environment allows researchers to not only experimentally inoculate squid with *V. fischeri*, but also to treat the animals and light organ with small molecules added to the water. This feature has enabled the important discoveries of lipopolysaccharide (LPS) and PG as key molecules in the squid-*Vibrio* symbiosis (3, 10). Additionally, the simple anatomy of the squid mantle cavity, including placement of the light organ, enables experimental dissection, staining, and observation of the organ. Light organ tissue is transparent to allow bioluminescence from symbionts to pass through, so fluorescence-based staining techniques can be combined with epifluorescence, confocal, or similar microscopy to investigate various attributes of an intact organ (6, 11-13).

Another key feature of this symbiosis as a model system is that *V. fischeri* is genetically tractable and amenable to manipulation. Its genome is about the size of that from *Escherichia coli*, between four and five million base pairs, and has been fully sequenced and published (14-19). Genetic constructs can be introduced either by conjugative transfer from *E. coli* or by inducing transformability; stable plasmids have been developed as shuttle vectors, while unstable plasmids have been used to generate mutants via transposon mutagenesis or allelic exchange; reporter genes are available; and experimental gene induction has been developed (20). Plasmids

expressing red- or green-fluorescent proteins can be used to visualize bacteria and/or their gene expression *in situ* (21), which can be done in combination with the host staining and microscopy techniques previously mentioned (8, 10, 21).

For the reasons above, the squid-*Vibrio* symbiosis has been studied as a model experimental system than can be manipulated and observed in the lab. Studies of *E. scolopes*, *V. fischeri*, and their symbiosis have contributed to the understanding of host-microbe interactions, host development, and bacterial genetics and physiology.

LIGHT ORGAN COLONIZATION

E. scolopes eggs develop and hatch aposymbiotically, before rapidly acquiring symbiotic *V. fischeri* from the surrounding seawater (4). This colonization is due in large part to the specific anatomy of the light organ itself. As previously stated, the light organ is in direct contact with environmental seawater, which cycles through the mantle cavity. The light organs of juvenile *E. scolopes* have specialized infection-promoting structures, known as ciliated epithelial appendages (CEA; shown in pink in **Figure 1.1**) (22). These appendages are lined with cilia that beat the surrounding seawater, pushing potential symbionts towards open pores at their base (22) (**Figure 1.1**). Gram-negative bacteria, such as *V. fischeri*, then aggregate on the surface of the light organ in mucus secreted by cells of the CEA (8). Using the current produced by beating of ciliated epithelial cells (22) as well as chemotactic signals from the squid (23, 24), the bacteria use swimming motility to then travel into pores on the light organ surface, through ducts and antechambers, and finally colonize the light organ crypts (**Figure 1.1**). These crypts provide both the space and nutrients that *V. fischeri* requires to grow, proliferate, and

luminesce (8, 22). Although *V. fischeri* represents less than a percent of the bacteria in the seawater, no other bacterial species can effectively colonize the *E.* scolopes light organ (5).

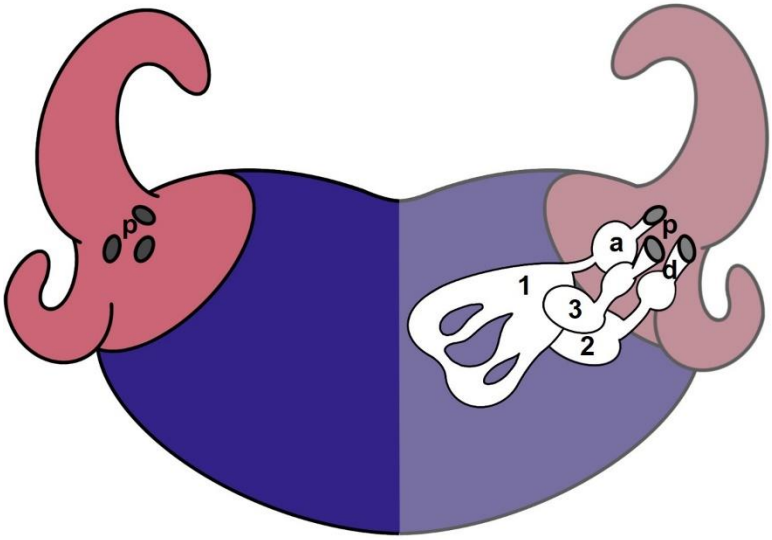

Figure 1.1. Organization of the juvenile *E. scolopes* light organ. Each lobe of the juvenile light organ has a set of ciliated epithelial appendages (CEA; pink). At the base of the appendages are three pores (**p**), which each lead to a duct (**d**), antechamber (**a**), and finally crypt. Crypts are numbered **1, 2, 3** according to the order in which they fully mature.

Upon successful colonization by *V. fischeri*, the squid light organ begins undergoing developmental changes. The first change is seen about two hours post-inoculation, with an increase in hemocyte levels within sinuses of the CEA (12). Soon after, epithelial cells of the CEA begin undergoing apoptosis, with final cell death starting around twelve hours post-infection (10, 11). As time progresses, levels of hemocyte trafficking and early-stage apoptosis continue increasing until reaching a maximum around 12 to 18 hours post-inoculation (10, 12).

In as few as fourteen hours post-inoculation, while many CEA cells are entering late-stage apoptosis, the appendages themselves begin narrowing, and a raised ridge along their border recedes. The CEA will continue to shrink and regress, fully disappearing within five-to-six days after colonization (11) (**Figure 1.2**).

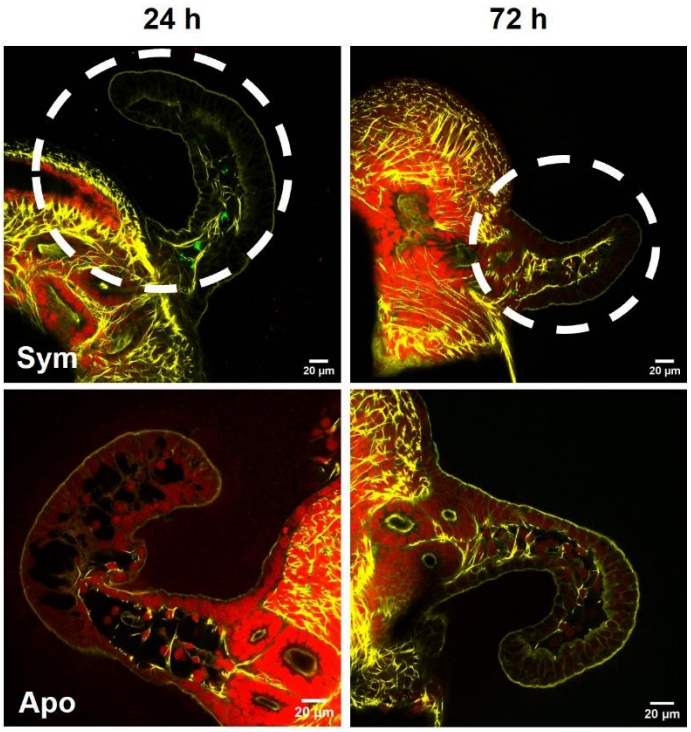

Figure 1.2. *E. scolopes* light organ morphogenesis. Fluorescence confocal microscopy images of one set of CEAs is shown. Over time, CEA of colonized squid regress (top, sym), while aposymbiotic squid (bottom, apo) do not experience regression. Confocal microscopy images courtesy of Liu Yang.

These developmental changes of the CEA are not experienced by juvenile *E. scolopes* that have not been colonized by *V. fischeri* or treated with specific signaling molecules (3, 10, 11, 25) (**Figure 1.2**). This phenomenon not only led to studies to determine the signaling molecules used by *V. fischeri* (3, 25), but also the finding that CEA are the first and only known host structure whose sole purpose is to facilitate infection (22).

SIGNALING MOLECULES IN SQUID-*VIBRIO*

To form lifelong, mutually beneficial relationships between microbes and their animal hosts, both partners must develop signals and receptors to properly communicate. These signals and their pathways lead to physical and transcriptional/translation changes within both partners, allowing them to form a productive partnership (9, 26-31). In the squid-*Vibrio* symbiosis, the most well-studied signals are the common MAMPs PG and LPS. Though not specific to *V. fischeri* or thought to be major factors underlying the specificity of the squid-*Vibrio* symbiosis, both PG and LPS trigger responses from the host. Moreover, as described below, *V. fischeri* has evolved to release unusual amounts of these MAMPs (25, 32, 33).

PG composes the bacterial cell wall and consists of linear glycan strands that are cross-linked by short peptides. Gram-positive bacteria have a thick outer layer of PG, while Gram-negative bacteria have a thinner layer of PG within the periplasm, internal to the outer membrane (34, 35). Within the context of this symbiosis, PG is recognized in different ways: as intact cell walls during the early stages of the symbiosis, or as distinct PG monomers at later stages. These monomers are referred to PG cytotoxin and tracheal cytotoxin (TCT), for their roles as signaling molecules in gonorrhea (36) and whooping cough (37), respectively.

LPS is the major structural component of the outer leaflet of Gram-negative outer membranes (38). Structurally, it is composed of the strongly conserved membrane-embedded Lipid A, a core oligosaccharide, and a species- or strain-specific O-antigen. Specifically, *E. scolopes* responds to the lipid A portion of LPS (10). In the context of this symbiosis, LPS can also be presented to *E. scolopes* as a main component of outer

membrane vesicles (OMVs) (32, 33, 39), which are portions of the outer membrane than have blebbed away from the cell, carrying periplasmic cargo. OMVs are released from most Gram-negative species, though their composition varies (40).

In *E. scolopes*, LPS induces apoptosis of the ciliated epithelial cells of the CEA (3, 10). This effect can be accomplished with LPS from several Gram-negative bacteria, when added to seawater (10). LPS induces apoptosis of host cells in many pathogenic associations as well, a phenomenon that has been extensively studied and reviewed (41-46). Although it triggers apoptosis of cells within the CEA, LPS alone does not trigger regression of the CEA or hemocyte trafficking into the CEA (3, 10)

PG triggers the earliest events in *E. scolopes* colonization: mucus secretion (47) and hemocyte trafficking into the sinuses of the CEA (3, 12). Receptors for both responses are seemingly located on the surface of the light organ, perhaps among the ciliated epithelial cells of the CEA. Currently, it is unknown whether these two events share receptors and/or signaling cascades. Once colonization has been established, PG continues to induce hemocyte trafficking into the crypts and CEA (3, 12) and induces the loss of PG recognition proteins within the host (48). PG also works in synergy with LPS to induce apoptosis of ciliated epithelial cells and leads to increased cell death. A PG monomer called TCT, which is composed of a disaccharide-tetrapeptide, can induce regression of the CEA and is also responsible for some induction of hemocyte trafficking (3).

As previously mentioned, these developmental morphogenic events of *E. scolopes* can be triggered via experimental treatment with LPS or PG fragments added to the seawater, as well as by intact symbionts (3, 8, 10, 12, 32, 33). Studies involving

the experimental addition of MAMPs have been integral to determining which molecules can trigger a specific developmental event, and this knowledge has in turn guided studies to determine which stages of colonization are actively selective for *V. fischeri*. For example, although PG from both Gram-negative and Gram-positive bacterial species can trigger mucus secretion from the CEA, only Gram-negative cells can aggregate within that mucus (8, 47). Similarly, although PG from numerous species induces hemocyte trafficking, *V. fischeri* appears to be the only species that can evade hemocyte binding and phagocytosis (3, 12, 49-51). Overall, these data indicate that, though the signals are not *V. fischeri*-specific, only *V. fischeri* is able to reach and proliferate within the crypts to produce enough of signal to elicit developmental responses from the squid. Moreover, as noted above, LPS is released from *V. fischeri* cells as membrane blebs, making it relatively abundant in cell-free extracts of cultures, perhaps enhancing its role in this symbiosis. As described below, PG fragments formed during cell-wall remodeling and PG recycling are likewise released in relatively high concentrations from *V. fischeri*.

PG BIOSYNTHESIS AND RECYCLING IN *V. FISCHERI*

The bacterial PG cell wall provides structural rigidity to the cell, while allowing for dynamic movement, and changes in cell size and shape. PG is made up of linear repeating strands of β-1,4 linked *N*-acetylglucosamine (NAG) and *N*-acetylmuramic acid (NAM), with short peptide chains covalently bound to most NAM molecules. In most Gram-negative bacteria, the mature peptide chain bound to NAM is L-ala, D-glu, *meso*-diaminopimelic acid (*m*DAP), and D-ala. Many of the peptides are crosslinked together,

to add stability to the structure (**Figure 1.3**). This net-like polymer, known as the sacculus, must be able to grow, expand, change shape, accommodate structures that span the inner and outer membranes, and separate into two daughter sacculi upon cellular division. To facilitate each of these functions, biosynthesis, breakdown, and recycling of PG are tightly controlled by the cell.

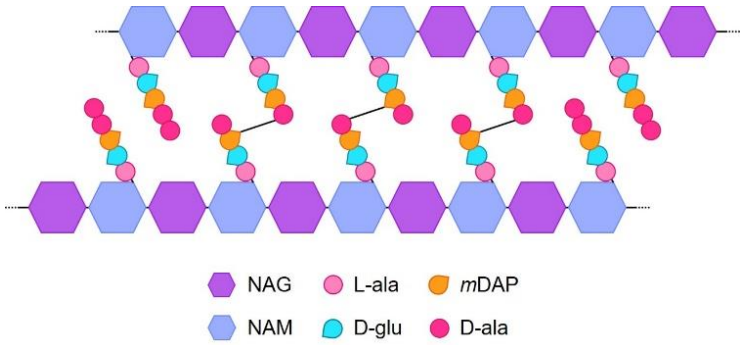

Figure 1.3. Diagram of peptidoglycan structure in *V. fischeri*.

PG biosynthesis has three phases: cytoplasmic, membrane-bound, and periplasmic (52). Synthesis begins in the cytoplasm. Here, UDP-NAG is produced from fructose-6-phosphate, UDP-NAM is formed from UDP-NAG, amino acids are racemized and dimerized as needed, and the peptide chain is bound to UDP-NAM by successive addition of the amino acids L-ala, D-glu, *m*DAP, and finally a D-ala dimer (53). The UDP-NAM-pentapeptide is then bound to the membrane-bound lipid carrier bactoprenol, to form lipid I (54). UDP-NAG is then added, forming lipid II, which is subsequently flipped from the cytoplasmic to the periplasmic side of the inner membrane (54). In the periplasm, transglycosylases polymerize PG's glycan strands, adding newly flipped monomers onto existing PG, and transpeptidases form crosslinks between the peptide

chains (55). The crosslinks of *V. fischeri* are one of the most common types seen: A1γ. These A1γ crosslinks are covalent bonds between the *m*DAP of one PG chain and D-ala at the fourth position of the adjacent chain (35). When these links are formed, the fifth position D-ala is removed from the chain (34).

In conjunction with *de novo* PG synthesis, the cells are also remodeling, breaking down, and recycling extant PG. To remove sections of PG, endopeptidases cleave crosslinks and lytic transglycosylases cleave bonds between NAM and NAG of adjacent monomers (55-57). Free PG monomers can then be shuttled into the cytoplasm via the AmpG permease (58) or cleaved by *N*-acetylmuramoyl-L-ala amidase (59) and the peptide chain shuttled into the cytoplasm through Opp (60). Once in the cytoplasm, recycled monomers and peptides are broken down further. Recycled NAG, NAM, and tripeptides (L-ala-D-glu-*m*DAP) then feed directly back into PG synthesis.

It is estimated that each generation about 50% of PG is recycled and fed back into PG synthesis (61). Most bacteria are efficient at recycling PG monomers, shuttling them into the cytoplasm for reuse. A few species, however, release a subset of monomers that are generated during PG recycling, with notably similar effects on their hosts. Two examples are the pathogens *Bordetella pertussis* (62), and *Neisseria gonorrhoeae* (36), which cause whooping cough and gonorrhea, respectively. A third example, discovered more recently than the pathogens, is *V. fischeri* (3). In all three, the same PG monomers are released from the cell, and in each case the released monomers are partly responsible for triggering the loss of ciliated cells in the host. Monomers released from *B. pertussis* cause the death and loss of ciliated epithelial cells in the airway. This is the origin of the name tracheal cytotoxin, as well as the cause

of the primary symptoms of whooping cough. The same molecule released from *N. gonorrhoeae* is called PG cytotoxin, and triggers cell death in ciliated cells of fallopian tubes. As described above, when released by *V. fischeri*, TCT triggers apoptosis and regression of the ciliated CEA.

B. pertussis has an insertion sequence element disrupting *ampG*, which encodes the permease involved in PG recycling. The resulting loss of AmpG function hinders the shuttling of PG monomers into the cytoplasm for recycling (63), accounting for the high level of TCT release from the cells. In *V. fischeri* and *N. gonorrhoeae*, high PG monomer release is largely due to the activity of lytic transglycosylases, which cleave bonds between adjacent disaccharides in the PG strands (25, 64), although in *N. gonorrhoeae ampG* also appears to have evolved a loss of efficiency (65, 66). While they can be studied via cell culture or organ donation of fallopian tubes, the cytopathic effects of PG monomer release of *B. pertussis* and *N. gonorrhoeae* of course cannot be experimentally studied in their human hosts. However, as detailed above, the squid-*Vibrio* symbiosis is a great model system that can be readily studied in experimental settings. Open questions that remain to be addressed are whether variation in PG monomer structure is possible, and how such variation would affect outcomes with the host.

VARIATIONS IN PG STRUCTURE

Overall, the structure of PG is highly conserved throughout the Bacterial Kingdom, though there are examples of variation in the peptide chain, as well as in the type and degree of crosslinking (34, 35, 67). The glycan strands of PG often have

covalent, reversible modifications, such as *N*-deacetylation and *O*-acetylation (68). Some temporary variations can also be seen in the peptide side chains as well, often due to media content (69-75), or endogenous factors such as production of non-canonical amino acids (76-78). The amount of PG cross-linking can also vary, both by genotype and growth phase (35).

Currently, known variations in *de novo* PG are found only in the peptide chain (34, 35, 67). Usually, this variation is seen at the third position. In most Gram-negative species such as *V. fischeri*, this is *m*DAP, while Gram-positive species usually have L-lys. Other known variations at this position include the diamino acids lanthionine or ornithine (34, 79-82), and even rarer cases of incorporation of monoamino acids (34, 35). In the Gram-negative species *Thermotoga maritima*, the peptide's third position can be either L-lys or D-lys (83), the latter being a residue only shared by the fourth position in a subset of PG in the Gram-positive *Butyribacterium rettgeri* (84). While variation at the third position is most common, there are also some known substitutions at the first, fourth, and fifth positions of the peptide chain, specifically with molecules similar in structure to alanine, such as glycine, serine, or lactate (35, 67). Only D-glu is known to be added at the second position of the PG peptide, though some species will modify the structure later (35).

Crosslinks between adjacent PG strands are a common source of variation, with differences in mode and composition of interpeptide bridges. Most bacteria have 3-4 crosslinks, meaning adjacent peptides are linked from the amino group of the third amino acid, to the carboxy group of the fourth amino acid on the adjacent PG strand. In Gram-negative species, this is usually a direct peptide bond formed from the *m*DAP or

L-lys of one chain, to the D-ala of the adjacent chain. Most Gram-positive bacteria, on the other hand, have an interpeptide bridge, consisting of one to seven additional amino acids. Some bacteria, specifically coryneform bacteria, have 2-4 linkages, which connect the α-carboxyl group of D-glu at position two, to the carboxyl group of the fourth position D-ala on the adjacent strand. These peptide bridges always contain a diamino acid but can have other amino acids in addition (35).

Previous studies have attempted to genetically alter bacteria to change the structure of their PG peptide (76, 85-87). Interestingly, though different bacterial species were studied, three of these studies found that *m*DAP auxotrophy was suppressed by replacing *m*DAP in the PG with lanthionine, which is naturally found in this position in *Fusobacterium nucleatum* (79, 80). Mutants of one study retained DAP in their PG, but a large proportion was a different stereoisomer (L,L-DAP, **Figure 1.4**), while wild type contained entirely *m*DAP (85). These studies influenced the goals and methods undertaken in the work reported in this dissertation.

A striking feature of PG peptide described above is the incorporation of D-amino acids (DAAs), rather than their proteinogenic L-amino acid enantiomeric counterparts. Although less common than L-amino acids, DAAs are not unique to PG. In the following sections, I explore the topics of DAAs in bacteria and the racemase enzymes that interconvert D- and L-forms, thus providing a biosynthetic side-track from standard protein synthesis.

D-AMINO ACIDS IN BACTERIA

Amino acids are ubiquitous in nature, with both D- and L-forms having important, specific roles in all domains of life and in varied environments. L-amino acids are essentially universal, as they are the building blocks of ribosomally-produced peptides and proteins. DAAs are less commonly found in nature but are also important. They play a fundamental role in bacteria, where D-ala, D-glu, and often *m*DAP, are constituents of the cell wall PG (88). Additionally, bacteria can also use DAAs as growth substrates (89-92), for the building of non-ribosomal peptides (93-96), and as regulators of PG biosynthesis, metabolism, and structure (77, 97-103). In particular, exogenous non-canonical DAAs (i.e., those not typically found in PG) can be readily incorporated into the mature periplasmic PG peptides during PG cross-linking and remodeling, which can affect growth rate and PG metabolism (77, 103, 104). Some bacteria can also scavenge DAAs from their environment to use as nutrient sources (90-92).

As detailed above, all bacterial PG contains at least one DAA, D-glu. Most bacteria also include D-ala, and many Gram-negatives have *m*DAP as well. Additionally, Gram-positives often use DAAs in their interpeptide bridges. The incorporation of DAAs in these PG structures makes them more resilient against proteases, which typically require specific L-L-peptide bonds (100). *Enterococci* have even evolved altered PG with an additional D-ser residue enabling them to resist inhibition by vancomycin (105). Additionally, non-canonical DAAs can be incorporated into PG peptides, which allow bacteria to cope with different environmental stresses (77). DAA residues can also be found in the teichoic acids of the Gram-positive cytoplasmic membrane (106, 107), and in poly-γ-glutamate, which is a non-ribosomal

peptide produced by *Bacillus* species. When incorporated into structural components of bacterial cells, it can be speculated that DAAs function to avoid cleavage by proteases, but more research is needed to elucidate all of their functions and mechanisms.

As noted above, many non-ribosomal polypeptides contain DAAs, and these include antimicrobials produced by bacteria, such as bacitracin (96, 99, 106-109). These polypeptides, as well as free DAAs themselves, can be secreted as signaling molecules between cells of the same species and even between organisms from different kingdoms (110-113). Within microbial communities, DAAs can also affect cell wall structure and synthesis and growth phase transitions (99). Some bacteria appear to use exogenous DAAs as chemotactic signals (114-116). There has been mixed evidence that DAAs may play a role in assembly and dissolution of bacterial biofilms, and experimental results depend upon the bacterial species, DAAs used, and the experimental setup (117-126).

Similarly, many DAAs have been found to inhibit bacterial growth through a variety of mechanisms, including enzyme inhibition and translation disruption through mischarging of tRNAs (100, 107, 109, 127-132). For example, D-glu inhibits glutamate dehydrogenase, interfering with synthesis of L-glu for use in proteins (133). D-met inhibits biosynthesis of PG (104, 134) and D-ala and D-his inhibit spore formation of various *Bacillus* species (135-139). Hypotheses for mechanisms of inhibition vary for each amino acid and bacterial species tested, but often include inhibition of PG synthesis and cross-linking, competition with L-isomers, and mischarging of tRNAs to ribosomal protein synthesis (100, 104, 128-131, 133).

BACTERIAL AMINO ACID RACEMASES

Bacterial DAAs can be synthesized two ways: racemization of L-forms, or stereospecific amination of α-ketoacids (107). This dissertation focuses on the former. Racemases are enzymes that interconvert amino acids between their L- and D- forms. Some of the first bacterial racemases discovered were those for alanine (140), glutamate (141), and DAP (142). We now know of many more racemases with specific amino acid substrates, as well as broad-spectrum racemases that can interconvert multiple amino acids, including both proteinogenic and non-proteinogenic L-form amino acids. Most racemases function as dimers, and racemases are found in both the cytoplasmic and periplasmic/extracellular spaces (143, 144). Racemases sort into two main categories based on their need for pyridoxal 5'-phosphate (PLP): PLP-independent, and PLP-dependent (143, 145-147).

The most well-characterized PLP-independent racemases are glutamate racemase and DAP epimerase (146). Lactic acid bacteria also have PLP-independent aspartate racemases to produce the D-asp needed for PG cross-bridges (143, 148). Other bacterial PLP-independent enzymes are proline, hydroxyproline, *O*-ureidoserine, and some lysine racemases (143, 149). Interestingly, two broad-spectrum racemases, YgeA from *E. coli* and RacX from *B. subtilis* are also PLP-independent (150), while all other known broad-spectrum amino acid racemases do require PLP. Known PLP-independent enzymes have two catalytically active cysteine residues in their active sites (143), apart from YgeA from *E. coli*, which has one cysteine and one threonine (150).

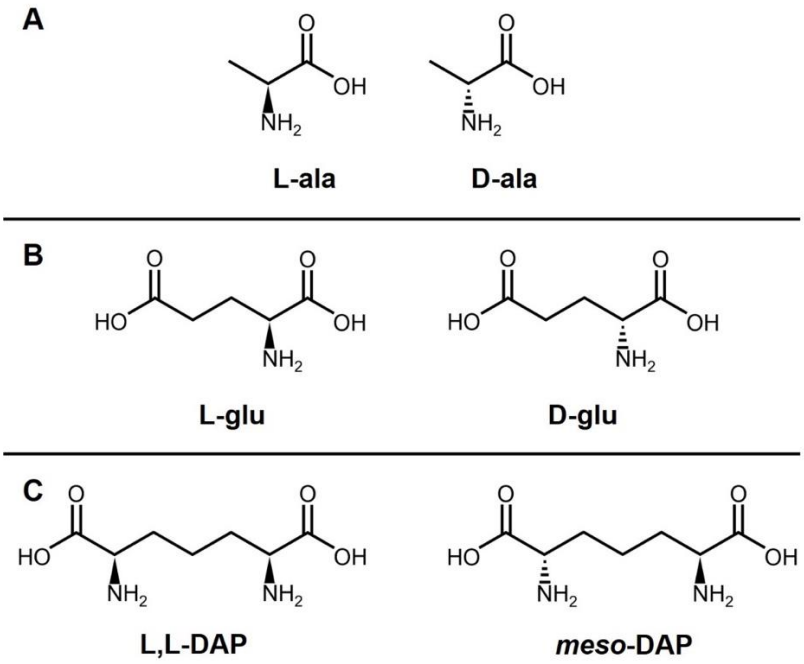

Figure 1.4. Enantiomeric structures of PG-specific DAAs. **A** Alanine, **B** Glutamate, **C** DAP

PLP-dependent enzymes include alanine, asparagine, and serine racemases, as well as most broad-spectrum amino acid racemases (**Table 1.1**) (144, 146, 150-157), and some lysine racemases (154, 155). Though PLP can bind and behave differently with the various PLP-dependent racemases, they all share a common conversed lysine within the PLP binding site (144). *V. fischeri* has three racemases characterized in publications, though others are likely. The published reports include: Alr (158), MurI (158), and RacD (87), which racemize alanine, glutamate, and aspartate, respectively. There are also a DAP epimerase and YgeA-like racemase predicted by genome annotation (14), and a broad-spectrum racemase that drew our interest and was relevant in the research described in this dissertation. Unlike the related bacterium *E. coli*, *V. fischeri* only has one annotated alanine racemase, Alr, which produces the D-ala

needed for PG biosynthesis and is essential to *V. fischeri* (158). Similarly, *V. fischeri* also has only one known glutamate racemase, MurI, that is essential for PG biosynthesis and bacterial growth (87, 158). Currently, neither Alr nor MurI of *V. fischeri* is known to racemize other amino acids. *V. fischeri*'s aspartate racemase, RacD, was implicated to have glutamate racemase activities; although induced by D-asp, its expression could compensate for the loss of *murI* (87). The putative DAP epimerase and broad-spectrum racemase YgeA (VF_A0624) have not yet been studied in *V. fischeri*.

Table 1.1. Examples of well-characterized bacterial broad-spectrum racemases.

Enzyme	Species	Localization	PLP-	Preferred Substrate	Other Substrates	Source
Amino Acid Racemase	*Aeromonas caviae*	Cytoplasm	Dependent	Lysine	Aromatics, Acidic	(159, 160)
BAR	*Pseudomonas putida* IFO 12996	Unknown	Dependent	Lysine	Basic, Aliphatic	(152, 161, 162)
ArgR	*Pseudomonas taetrolens*	Periplasm	Dependent	Lysine	Arginine	(153)
BsrV	*Vibrio cholerae*	Periplasm	Dependent	Methionine, Leucine	Aliphatic, Basic	(77, 156)
Alr	*P. putida* KT2440	Periplasm	Dependent	Lysine	Arginine, Methionine, Glutamine	(163, 164)
YgeA	*Escherichia coli*	Cytoplasm (Predicted, (165)	Independent	Homoserine	Hydrophobic	(150)
RacX	*Bacillus subtilis*	Cytoplasm, Predicted (165)	Independent	DAP, lysine, arginine	Basic amino acids	(150)

Like the RacD of *V. fischeri*, many racemases are initially predicted to be specific for one amino acid, but are later characterized as having more diverse substrates, often including secondary substrates similar to the primary substrate (e.g., an aspartate

racemase acting somewhat on glutamate) (152, 153, 159, 166, 167). Moreover, broad-spectrum racemases that efficiently interconvert D- and L-forms of many relatively unrelated amino acids are being discovered and characterized (77, 150, 156, 168). Likely, more of these broad-spectrum racemases exist but are currently unannotated or annotated incorrectly as specific amino acid racemases. With the diverse substrate ranges of bacterial broad-spectrum racemases, it's difficult to pinpoint their exact function. However, as interest in DAAs and broad-spectrum racemases increases, research will likely elucidate more of their functional roles soon.

Because amino acid racemases are ubiquitous and important in bacteria, they are considered attractive drug targets, at least when they are distinct from racemases in plants or animals. Specifically, arginine, glutamate, and aspartate racemases are currently believed to be specific to bacteria, lessening the worry of off-target effects on human racemases (147). DAP epimerase and alanine racemase are also strong candidates as they are rare in eukaryotes and not found in humans (107, 147). Most efforts have so far been focused on glutamate and alanine racemases. Studies have proposed many structural analogs to D-glu as possible inhibitors of bacterial glutamate racemases (169, 170). Many do appear to inhibit glutamate racemase and therefore seem promising, though as of yet there are no medically relevant glutamate racemase inhibiting drugs. Inhibition of alanine racemase has also focused on structural analogs (171). One of these, D-cycloserine (DCS) has been used successfully for treatment of *Mycobacterium tuberculosis* infections (172). Unfortunately, many bacterial racemase inhibitors have off-target affects due to their structural similarity to both the D- and L-forms of amino acids.

RATIONALE AND SCOPE OF THIS WORK

Because its structure is so conserved among Bacteria, PG is often used by hosts to recognize bacterial invaders or guests, whether pathogenic or mutualistic, so the host can react appropriately to infection. One example of this is the *E. scolopes*-*V. fischeri* mutualism, in which PG fragments shed from symbiotic *V. fischeri* cells trigger changes in light organ morphology, as described above. The goal of this dissertation work was to force evolution of PG structure or biosynthesis in *V. fischeri*, in order to gain insights into the constraints on PG evolution, how bacteria respond to environmental stress and inability to produce wild-type PG, and how PG structure and biosynthesis affect bacterial growth, antibiotic resistances, and host-microbe interactions.

Previously, our lab designed a selection for spontaneous suppressors of PG-specific DAA auxotrophic strains of *V. fischeri*. This dissertation focuses on studies using two PG-specific auxotrophies: D-glu and D-ala. Suppressor selection was achieved by attempting to grow these auxotrophic strains on media that had not been supplemented with the necessary amino acid. Two possible mechanisms of suppression were: novel biosynthetic pathways to wildtype PG structure, or novel PG structure. We use PG analysis via HPLC and mass spectrometry to determine PG structure, paired with whole genome sequencing to elucidate the genes responsible for suppression. Chapters 2 and 4 describe novel metabolic routes to production of D-glu and D-ala, respectively, while Chapter 3 describes a set of mutations that increase transport of D-glu, and lead cells to produce PG with a novel structure.

CHAPTER 2

A PROTOTROPHIC SUPPRESSOR OF A *VIBRIO FISCHERI* D-GLUTAMATE AUXOTROPH REVEALS A MEMBER OF THE PERIPLASMIC BROAD-SPECTRUM RACEMASE FAMILY, BSRF [1]

[1] Macey N. Coppinger, Kathrin Laramore, David L. Popham, and Eric V. Stabb. To be submitted to the *Journal of Bacteriology*.

ABSTRACT

Although bacterial PG is highly conserved, some natural variations in PG biosynthesis and structure have evolved. Understanding the mechanism and limits of such variation will inform our understanding of antibiotic resistance, innate immunity, and the evolution of bacteria. We have explored the constraints on PG evolution by blocking essential steps in PG biosynthesis in *Vibrio fischeri*, and then selecting mutants with restored prototrophy. Here, we attempted to select prototrophic suppressors of a D-glu auxotrophic *murI racD* mutant. No suppressors were isolated on unsupplemented lysogeny broth salts (LBS), despite plating $>10^{11}$ cells, nor were any suppressors generated through mutagenesis of ethyl methanesulfonate. A single suppressor was isolated on LBS supplemented with iso-D-gln, although the iso-D-gln subsequently appeared irrelevant. This suppressor has a genomic amplification, bounded by a novel junction that fuses *proB* to a gene encoding a putative broad-spectrum racemase of *V. fischeri*, *bsrF*. An engineered *bsrF* allele lacking the putative secretion signal (ΔSS-*bsrF*) also suppressed D-glu auxotrophy, resulting in PG that was indistinguishable from wild type. The ΔSS-*bsrF* allele similarly suppressed the D-ala auxotrophy of an *alr* mutant, and restored prototrophy to a *murI alr* double mutant auxotrophic for both D-ala and D-glu. The ΔSS-*bsrF* allele increased resistance to D-cycloserine but had no effect on sensitivity to PG-targeting antibiotics penicillin, ampicillin, or vancomycin. Our work helps define constraints on PG evolution and reveals a periplasmic broad-spectrum racemase in *V. fischeri* that can be co-opted for PG biosynthesis, with concomitant D-cycloserine resistance.

IMPORTANCE

DAAs are used and produced by organisms across all domains of life, but often their origins and roles are not well understood. In bacteria, D-ala and D-glu are structural components of the canonical PG cell wall and are generated by dedicated racemases Alr and MurI, respectively. The more recent discovery of additional bacterial racemases is broadening our view and deepening our understanding of DAA metabolism. Here, while exploring alternative PG biosynthetic pathways in *V. fischeri*, we unexpectedly shed light on an unusual racemase, BsrF. Our results illustrate a novel mechanism for the evolution of antibiotic resistance and provide a new avenue for exploring the roles of non-canonical racemases and DAAs in bacteria.

INTRODUCTION

Most Bacteria have a cell wall comprised of PG, which helps define cell shape and provides resilience against environmental stresses. As a highly conserved and uniquely bacterial structure, PG is a key MAMP recognized by bacteria-surveillance systems of plants and animals and is a prime target for medically relevant antibiotics. Although PG and its biosynthesis are strikingly similar across the Bacterial Kingdom, PG structural variation has evolved (35). Understanding the possible trajectories for and constraints on PG evolution will inform our understanding of host-microbe interactions and the emergence of resistance to PG-targeting antibiotics.

We became interested in PG in *V. fischeri* because of PG's role in the symbiosis between *V. fischeri* and the Hawaiian bobtail squid *E. scolopes* (173-175). Specifically, PG monomers released by *V. fischeri* trigger development of the host's symbiotic light

organ (3, 25, 48). However, studying PG in *V. fischeri* is broadly relevant, as PG structure and biosynthesis in *V. fischeri* parallel that in other Proteobacteria. For example, PG monomers released by *V. fischeri* are identical to TCT and PG cytotoxin released by *Bordetella pertussis* (62) and *Neisseria gonorrhea* (36), respectively. Therefore, we have used *V. fischeri* as a model for exploring how bacteria can evolve new PG biosynthetic pathways. Our approach has been to block wild-type PG biosynthesis and select for suppressor mutants capable of growing without a normally essential gene.

The *murI* gene contributes to PG biosynthesis and is considered essential in many bacteria (176, 177), including *V. fischeri* (158, 178). MurI is a cytoplasmic, coenzyme-independent glutamate racemase that interconverts L- and D-glu, producing the D-glu for the peptide moiety of PG (179). Another cytoplasmic enzyme, MurD, adds D-glu to the second position of the PG peptide chain, linking it to the L-ala in the first position; then MurE links the D-glu side chain acid to the amino group of DAP, creating gamma-D-glu (180). Glutamine has been found in the second position in a few bacteria, but in these cases D-glu appears to be initially added by MurD, then later modified to iso-D-gln (181). Given their respective roles in an essential and uniquely bacterial pathway, both MurI and MurD have been considered attractive antibacterial targets (169).

Previously, we generated a *murI* mutant in *V. fischeri* which, like *murI* mutants in other bacteria, could only be grown in media supplemented with D-glu (158). Subsequently, we selected prototrophic suppressors of this *murI* mutant that were able to grow without D-glu supplementation, leading to the discovery of a locus in *V. fischeri*

and some other Proteobacteria that enables the catabolism of D-aspartate, underpinned by the aspartate racemase RacD (87). Overexpression of RacD could compensate for the loss of *murI*, with PG still containing D-glu, suggesting that RacD has glutamate racemase activities that can compensate for the loss of *murI* (87).

Here, the goal was to select suppressors of a *murI racD* mutant that have restored prototrophy. Such suppressors may create a new pathway to wild-type PG, and/or evolve an altered PG structure. Aside from MurI and RacD, *V. fischeri* possesses a typical alanine racemase Alr, which provides the D-ala for PG. In other bacteria, Alr acts mostly on alanine and, to a lesser extent, serine (156). Due to its specificity for small, uncharged amino acids, it seemed unlikely that Alr would be involved in suppression of D-glu auxotrophy without compromising D-ala production, although such a scenario could not be ruled out. It is also worth noting that MurD has a high specificity for D-glu as the substrate added to the PG peptide, but it is not known whether altered substrate specificity could obviate the need for D-glu. Although this background knowledge provides some important context for our selection, it was impossible to predict how or even if D-glu auxotrophy of a *murI racD* double mutant could be suppressed.

RESULTS

Reversion of a *murI*::mini-Tn*5* allele by precise mini-transposon deletion. We first attempted to generate prototrophic suppressor mutants of RMJ13 (*murI*::mini-Tn*5* Δ*racD*) by growing the strain in LBS supplemented with D-glu, then plating the culture onto unsupplemented LBS. Mutants that grew independently of D-glu supplementation

arose at a rate of ~10^{-10}; however, whole genome sequencing of six prototrophs revealed that they were revertants at the *murI* locus. Instead of acquiring mutations at other sites to suppress D-glu auxotrophy, these strains had precisely lost the mini-Tn*5* transposon that had disrupted *murI*, reverting to a wild-type *murI* allele. The mini-Tn*5* used encodes resistance to erythromycin (Em), and we subsequently determined that an additional twenty-seven prototrophs selected in this manner were sensitive to Em, suggesting similar loss of the mini-Tn*5*. Thus, instead of suppressing auxotrophy, these strains had instead reverted to prototrophic Δ*racD* strains. Based on these data, precise deletion of this mini-transposon, which does not encode a transposase (182), occurs at a rate around 10^{-10} (**Table 2.1**).

Selection of a rare suppressor of D-glu auxotrophy. Further attempts to select suppressors in RMJ13 were performed with Em in the medium as a selective agent to maintain the transposon insertion in *murI*. However, after plating over 10^{11} cells onto LBS-Em, we did not recover any suppressor mutants. Next, we performed a series of experiments chemically mutagenizing RMJ13 with ethyl methanesulfonate (EMS) which primarily causes G:C to A:T transition substitutions in DNA (183, 184). We plated a total of over 10^8, $4x10^7$, and $1.4x10^7$ viable cells from treatments with approximately 90%, 99% and 99.9% EMS-mediated killing respectively, but still recovered no prototrophic suppressors of D-glu auxotrophy (**Table 2.1**).

Table 2.1. Selection for prototrophic suppressors in D-glu auxotroph RMJ13

RMJ13 Transposon Revertants (LBS without Em)			
	CFU Plated	**Revertants**	**Revertants/CFU**
LBS	1.8×10^{11}	27	1.4×10^{-10}
RMJ13 EMS Mutagenesis			
	Plated	**Suppressors**	**Suppressors/CFU**
90% killing	1×10^{8}	0	-[a]
99% killing	4×10^{7}	0	-
99.9% killing	1.4×10^{7}	0	-
Total CFU plated		**1.5×10^{8}**	
RMJ13 Suppressor Generation (LBS-Em)			
	Plated	**Suppressors**	**Suppressors/CFU**
None	1.08×10^{11}	0	-
Iso-D-gln	1.13×10^{10}	1	9×10^{-11}
Total Cells plated		**1.4×10^{11}**	

[a] "-" indicates below the limit of detection, i.e., no suppressors

We considered the possibility that supplements to LBS other than D-glu might allow us to select suppressors of D-glu auxotrophy. For example, knowing that D-glu is added to the PG side chain as iso-D-glu, we supplemented LBS-Em with iso-D-glutamine. From over 10^{10} cells plated to LBS-Em with iso-D-gln, we selected one suppressor mutant, named RMJ13S10 (**Table 2.1**). Unexpectedly, subsequent experiments revealed that RMJ13S10 grew well on LBS-Em and does not require iso-D-gln supplementation (**Figure 2.1**). Taken together, these results suggest that a rare mutation underpinned suppression of D-glu auxotrophy in RMJ13S10, enabling it to grow on unsupplemented LBS.

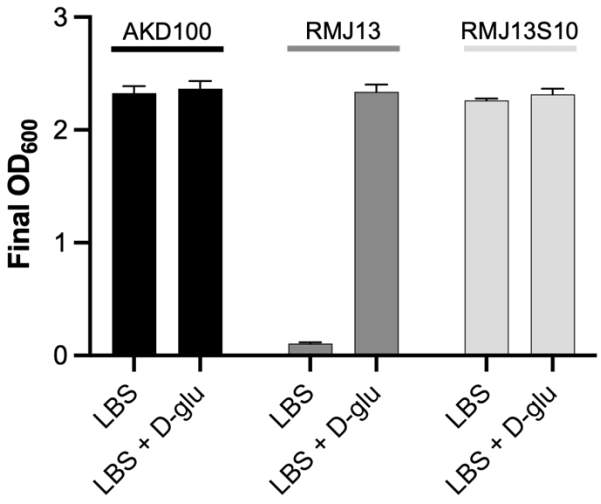

Figure 2.1. D-glu independent prototrophy of suppressor RMJ13S10. Shown are final OD_{600} readings for *V. fischeri* cultures grown with or without 400 μg/mL D-glu in LBS-Em. Strains include AKD100 (wild type ES114 marked with Em-resistance cassette at a neutral site), RMJ13 (*murI*::mini-Tn*5-erm* Δ*racD*), and RMJ13S10 (*murI*::mini-Tn*5-erm* Δ*racD proB-bsrF* fusion and amplification). Cultures were grown for 24 hours before reading final OD_{600}. Error bars indicate standard error of the mean (n=8). Data from one representative experiment of at least three are shown.

Mutation of *bsrF* suppresses D-glu auxotrophy. The genomic sequence of RMJ13S10 revealed an amplification of a 9.2-kb region in chromosome I spanning *bsrF* (VF_0735) to *proB* (VF_0740), including a novel fusion junction involving *proB* and *bsrF* (**Figure 2.2**). In contrast to the wild-type sequence (**Figure 2.2A**), the fusion disrupts the final five codons at the 3' end of *proB*, and the start codon of *bsrF*. Those six amino acids are then replaced by a single valine, linking the two proteins together to create a fusion with an N-terminal ProB domain and C-terminal BsrF domain (**Figure 2.2B**). Based on the relative number of sequencing reads, the 9.2-kb region appears to be amplified four to five times, relative to the surrounding regions. One would expect such a large amplification to be unstable and prone to reversion by homologous recombination under non-selective conditions. To test this genetic model, RMJ13S10

was grown in the absence of selective pressure (i.e., in LBS-Em supplemented with D-glu). By the fifth passage in non-selective culture, thirty to thirty-five percent of CFU had lost the ability to grow without D-glu supplementation (**Figure 2.2C**) and had lost the *proB-bsrF* fusion (**Figure 2.3D, E**).

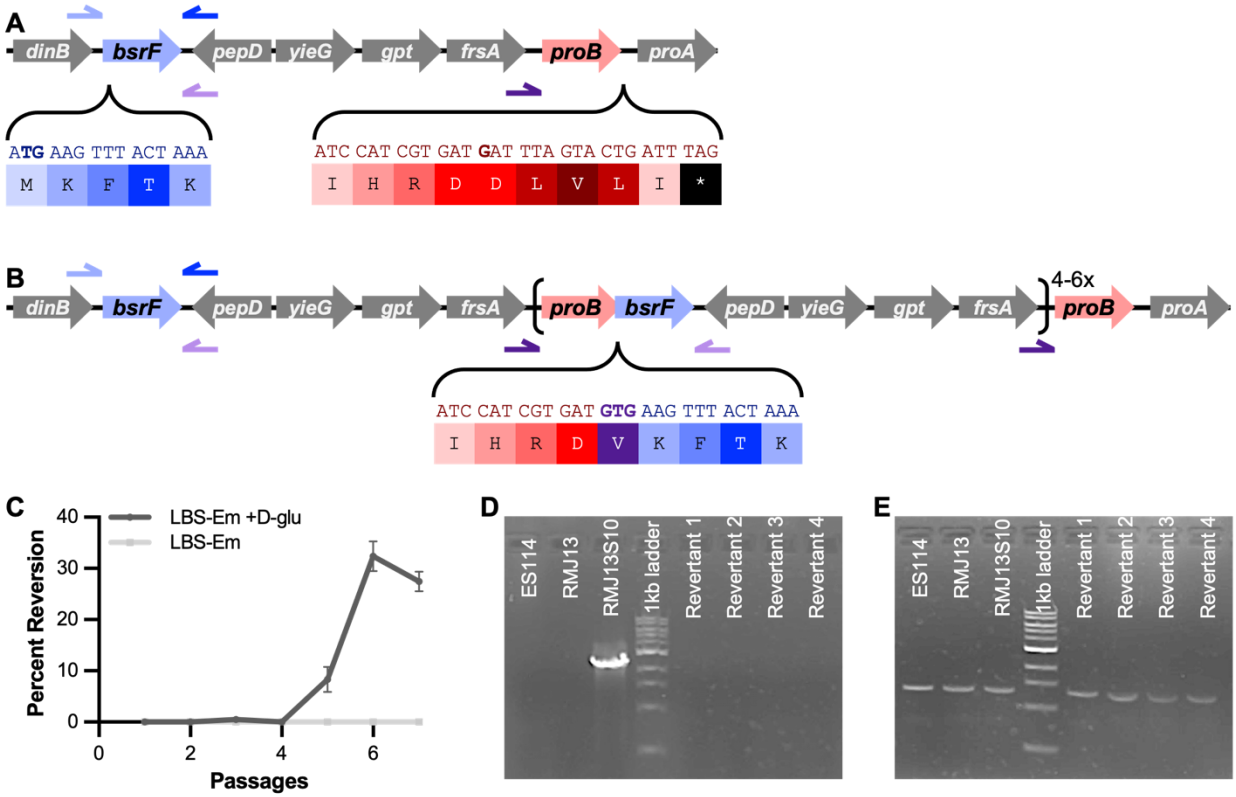

Figure 2.2. Genotype of RMJ13S10. (**A**) Schematic of wild-type *V. fischeri* ES114 genotype, in the region containing *dinB* to proA (VF_0734 to VF_0741). Insets highlight the N-terminal region of *bsrF* and the C-terminal region of *proB*. Bases in bold encode the newly created junction codon. (**B**) Schematic of the genetic fusion found in strain RMJ13S10. Brackets surround the amplified region. Inset highlights the new junction created by fusing *bsrF* to *proB*. In (**A**) and (**B**), blue arrows represent primers used to amplify wild-type *bsrF*, and purple arrows represent primers used to amplify the *proB-bsrF* fusion. (**C**) When grown without selective pressure, the RMJ13S10 culture begins reverting to D-glu auxotrophy after multiple passages (for each passage a stationary-phase culture was diluted 1:1000 into fresh medium and grown for 24 hours). (**D**) 0.8% agarose gel with PCR products amplifying the *proB-bsrF* genetic fusion, which is present in RMJ13S10, but absent in revertants to D-glu auxotrophy. (**E**) 0.8% agarose gel with PCR products amplifying wild-type *bsrF*.

The *bsrF* gene encodes a putative broad-spectrum racemase that shares 57% identity to the periplasmic BsrV characterized in *Vibrio cholerae* (77, 103, 156, 185-187). Bioinformatic analysis of the wild-type *V. fischeri* BsrF strongly suggested that the first 20 amino acids constitute a Type-II Sec-dependent secretion signal, followed immediately by a cleavage site (**Figure 2.3A**). This amino acid stretch resembles the basic N-hydrophobic-C pattern seen in many signal peptides recognized by the Sec translocon system, as well as the typical signal sequence motif of having small, uncharged residues in positions -1 and -3 relative to the cleavage site (188). Thus, *in silico* analysis is consistent with BsrF secretion to the periplasm, like that of its orthologue in *V. cholerae*. When the ProB-BsrF fusion sequence was analyzed, however, no such secretion signal was found, which is unsurprising considering the N-terminus of the fusion is ProB, a cytoplasmic protein.

We hypothesized that the ability of RMJ13S10 to suppress D-glu auxotrophy was due to fusion of the cytoplasmic ProB to the periplasmic BsrF, burying the latter's secretion signal within the protein. This hypothesis proposes that fusion to ProB blocks BsrF secretion, allowing its racemase activity to compensate for the lack of MurI and RacD in the cytoplasm, where *de novo* PG synthesis occurs. To test this hypothesis, we generated a mutant *bsrF* allele that lacks the putative secretion signal sequence (ΔSS-*bsrF*) (**Figure 2.3b**). The ΔSS-*bsrF* allele was then cloned into a shuttle vector (pVSV105) and introduced *in trans* into various *V. fischeri* strains. When placed in RMJ13, the ΔSS-*bsrF* allele on pMNC26 fully suppressed D-glu auxotrophy, while pKAL6 carrying wild-type *bsrF* and the parent vector pVSV105 did not (**Figure 2.3C**).

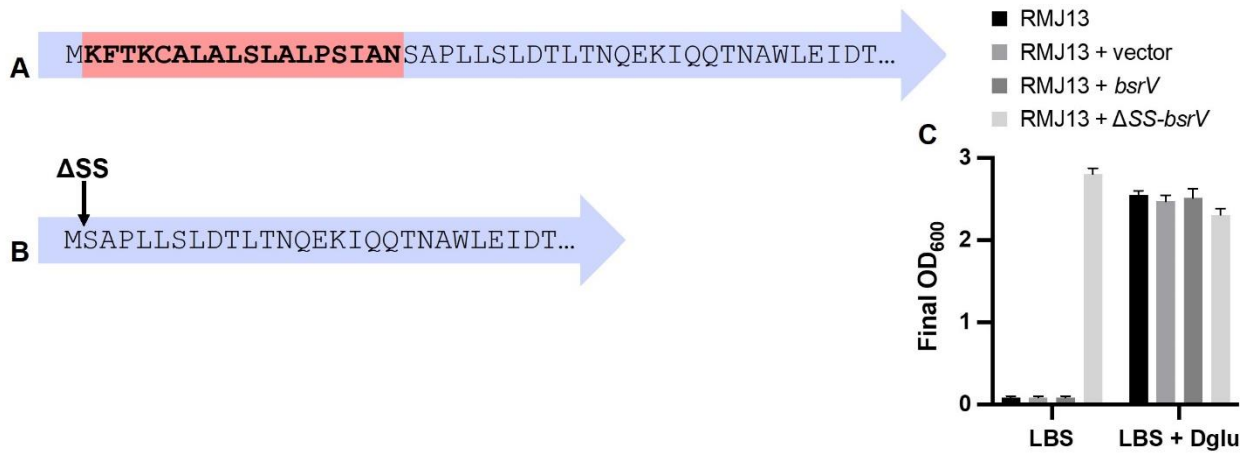

Figure 2.3 Removal of putative secretion signal sequence from BsrF. Schematic of N-terminus of BsrF, with **(A)** and without **(B)** the putative Sec-dependent signal sequence. **(A)** N-terminal amino acid sequence of BsrF; signal sequence that was removed in ΔSS-BsrF is highlighted in red. **(B)** N-terminal amino acid sequence of BsrF that has been altered to remove the signal sequence. New junction is marked with an arrow. **(C)** Removing the secretion signal from BsrF rescues RMJ13 (Δ*racD murI*::mini-Tn*5*-em) from D-glu auxotrophy. Shown are final OD_{600} readings for *V. fischeri* cultures grown with or without 2.7 mM D-glu. Strains include RMJ13 alone, or carrying plasmids pVSV105 (parent vector), pKAL6 (*bsrF*), or pMNC26 (ΔSS-*bsrF*)**.** Cultures were grown for 24h before reading final OD_{600}. Error bars indicate standard error of the mean (n=3). Data from one representative experiment is shown.

Expression of ΔSS-BsrF increases resistance to D-cycloserine. We hypothesized that the cytoplasmic BsrF in RMJ13S10 might confer different patterns of resistance to antibiotics that act upon the cell wall, PG synthesis, or DAA production. We found that this mutant's sensitivity to beta-lactams ampicillin and penicillin, as well as to vancomycin are similar to that of wild type (data not shown); however, RMJ13S10 had increased resistance to D-cycloserine (DCS) relative to an Em-resistant derivative of wild type (**Figure 2.4a**). To verify that the altered BsrF protein is responsible, we also tested strains with and without the plasmid carrying ΔSS-*bsrF*. As predicted, resistance to DCS increased when ΔSS-*bsrF* was expressed, while the shuttle vector alone or carrying wild-type *bsrF* had no effect (**Figure 2.4b**).

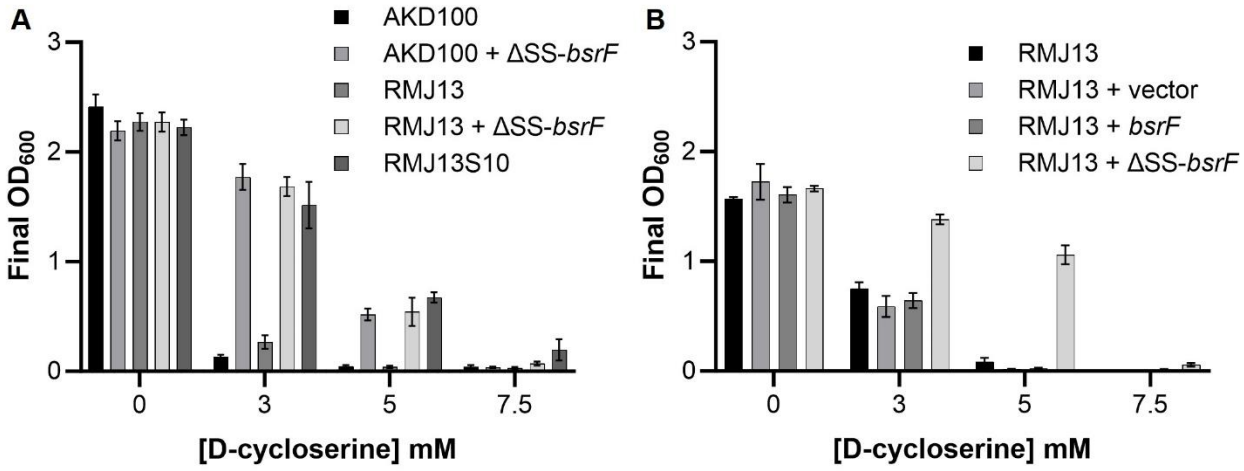

Figure 2.4. Removing the secretion signal from BsrF increases resistance to DCS (**A**) Expression of ΔSS-BsrF (encoded by plasmid pMNC26) increases resistance to DCS in both an Em-resistant derivative of wild type (AKD100) and the D-glu auxotroph (RMJ13). Similar rescue is seen in RMJ13S10, which has the original *proB-bsrF* fusion. (**B**) Expression of Δ*SS-bsrF* increases resistance of RMJ13 to DCS, while the empty vector (pVSV105) and WT *bsrF* (carried on pKAL6) do not. Shown are final OD_{600} readings for *V. fischeri* cultures grown with increasing concentrations of DCS. Cultures were grown for at least 20 hours before reading OD_{600}. Error bars indicate standard error of the mean (n=6). Data from one representative experiment of at least three is shown.

Expression of Δ*SS-bsrF* suppresses multiple auxotrophies. Because DCS interrupts cell wall synthesis by competitively inhibiting D-ala:D-ala ligase (DdlA) and Alr (189), and BsrV from *V. cholerae* has alanine racemase activity (156), we speculated that ΔSS-BsrF could be compensating for both the loss of D-glu racemase activity, and the inhibition of Alr. To test this hypothesis, we engineered a D-ala auxotrophic strain MC13 (Δ*bsrF* Δ*alr*), as well as a strain auxotrophic for both D-glu and D-ala, MC21 (Δ*bsrF* Δ*alr* Δ*murI*). While these strains require supplementation of D-ala or D-ala and D-glu, respectively, expression of Δ*SS-bsrF* allows each of them to grow in LBS without D-ala or D-glu supplementation (**Figure 2.5**).

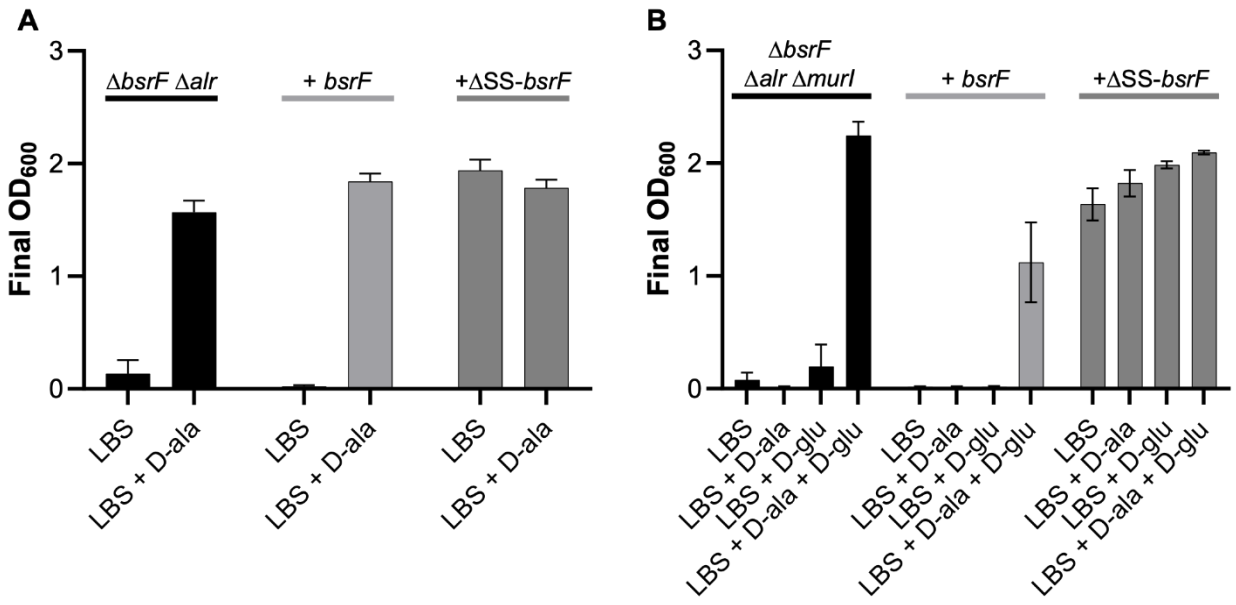

Figure 2.5. Expression of ΔSS-*bsrF* suppresses multiple auxotrophies. (**A**) Growth of MC13 (Δ*bsrF* Δ*alr*) alone, expressing *bsrF* (pKAL6), or ΔSS-*bsrF* (pMNC26). (**B**) Growth of MC21 (Δ*bsrF* Δ*alr* Δ*murI*) alone, expressing *bsrF,* or ΔSS-*bsrF*. Shown are final OD_{600} readings for *V. fischeri* cultures grown in unsupplemented LBS, and LBS supplemented with 100 µg/mL D-glu and/or D-ala. Cultures were grown for 20 hours before reading OD_{600}. Error bars indicate standard error of the mean (n=4). Data from one representative experiment of at least three are shown.

The *proB-bsrF* and ΔSS-*bsrF* alleles enable cells to produce PG indistinguishable from wild type. We speculated that RMJ13S10 and RMJ13 expressing ΔSS-*bsrF* would have altered PG structure because *V. cholerae*'s BsrV does not appear to produce the D-glu that would be needed for D-glu auxotrophs to restore wild-type PG (156). However, D-glu auxotrophs suppressed by the *proB-bsrF* fusion and ΔSS-*bsrF* have PG that is indistinguishable from that of wild-type *V. fischeri* (**Figure 2.6**). This was also seen in the strain auxotrophic for both D-ala and D-glu, when suppressed with ΔSS-*bsrF* (**Figure 2.6**).

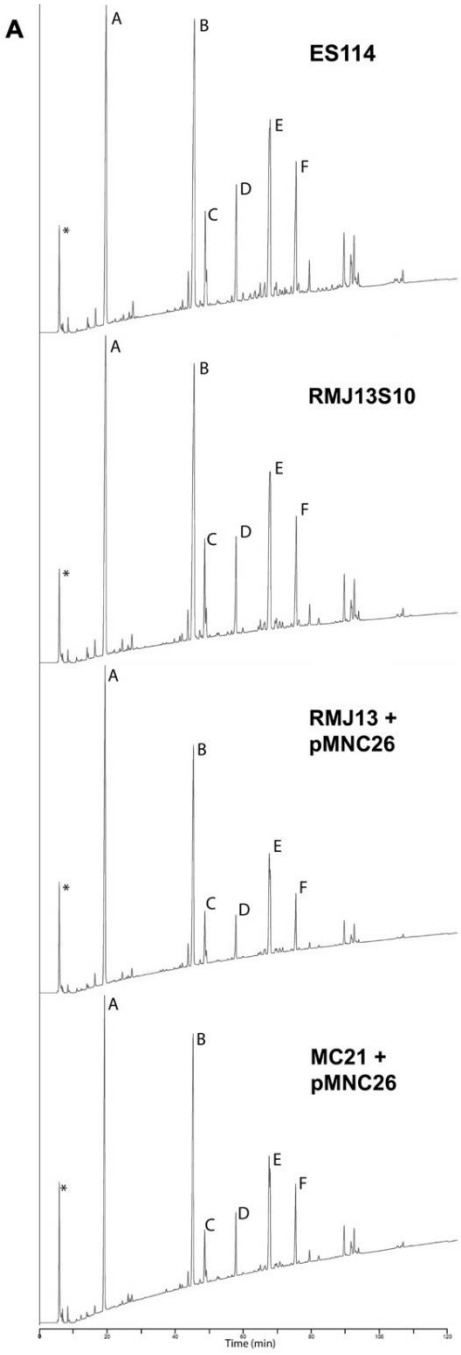

B

Peak	Structure
*	Buffer component
A	DS-TP (Disaccharride tetrapeptide)
B	DS-TP-TP-DS (crosslinked disaccharide-tetrapeptide dimer)
C	anhydroDS-TP (disaccharide tetrapeptide with anhydroNAM)
D	DS-TP-TP-DS-(TP-DS) (crosslinked disaccharide-tetrapeptide trimer)
E	anhydroDS-TP-TP-DS (Crosslinked disaccharide-tetrapeptide dimer with anhydroNAM)
F	Unknown, predicted disaccharide-tetrapeptide trimer with anhydroNAM

Figure 2.6. Cytoplasmic BsrF does not affect PG composition. (**A**) HPLC chromatograms of select PG samples. Strains were grown in LBS with Em and/or Cm as needed. PG sacculi were purified and digested with Mutanolysin, and muropeptides were separated by HPLC, detected by A 206-nm, and further analyzed as described previously (87). (**B**) Identification of labeled peaks in (**A**).
* indicates a buffer component peak, while lettered peaks correspond to PG fragments.

DISCUSSION

PG structure is largely structurally conserved throughout the Bacterial Kingdom, but both structural motifs of PG, the disaccharide strands and the peptide chains, do have some natural variation. The glycan strands can have covalent, reversible modifications, usually *N*-deacetylation or *O*-acetylation (68). The amino acids of the peptide chain can also vary to a small extent, based on exogenous factors (69-73, 75) or endogenous factors due to production of non-canonical amino acids (76-78). Currently, the only known permanent and heritable variations in PG structure are found in the peptide chain (35, 67). The most common of these variations is the amino acid at the third position, which is *meso*-diaminopimelate (DAP) or L-lys in most Bacteria. There are known exceptions that incorporate other diamino acids such as lanthionine and ornithine (34, 79-82), and even rarer cases of monoamino acids (34, 35) into the third position of the peptide chain. Though less common, variations can occur in the first, fourth, and fifth positions of the peptide chain, with structurally similar amino acids such as glycine, serine, and lactate replacing the canonical alanine residues (35, 67). Only D-glu is known to be added at the second position of the nascent PG peptide (35), although it may be later modified.

Our approach of selecting for suppressors of D-glu auxotrophy parallels similar successful attempts to experimentally evolve PG. Specifically, previous studies, including one in *V. fischeri*, found that selection of prototrophic suppressors of DAP auxotrophy resulted in DAP replacement by lanthionine (76, 86, 190), which is naturally found at this position in *Fusobacterium nucleatum* (79, 80). These results set the precedent and encouraged the current research; however, they focused on the peptide position that has the most natural variation. In contrast, incorporation of D-glu in the

second position of *de novo* PG synthesis is, to the best of our knowledge, invariant. Despite a concerted effort to isolate rare suppressor mutants of D-glu auxotrophy, we did not isolate any mutants that replaced D-glu with another moiety in the PG peptide. For whatever reason(s), D-glu may be a more difficult moiety to replace than DAP.

The lone suppressor mutant selected in this study contained a fusion of *bsrF*, encoding a putative broad-spectrum racemase, onto *proB*, which encodes an enzyme involved in proline and arginine biosynthesis. Further experiments suggested that the ProB moiety was significant only for preventing secretion of BsrF. Broad-spectrum racemases are being discovered and characterized in a number of bacteria (77, 150, 153, 156, 162, 164, 191), and many more are likely unannotated, or incorrectly annotated as specific amino acid racemases. However, as appreciation for the production and roles of DAAs in bacteria grows, so too does interest in exploring broad-spectrum racemases. Many questions remain as to why bacteria have broad-spectrum racemases, and how they are using the non-canonical DAAs that are produced.

The best studied homologue of BsrF is the periplasmic broad-spectrum racemase BsrV in *V. cholerae* (77, 103, 156, 185-187). BsrV can interconvert at least ten proteinogenic amino acids, as well as six non-proteinogenic amino acids, but in the context of this study it is notably unable to racemize glutamate (156). We found that *V. fischeri* BsrF lacking its putative secretion signal can suppress D-glu auxotrophy by compensating for the loss of MurI and RacD (**Figures 2.1, 2.4**), resulting in PG that is indistinguishable from that of wild type (**Figure 2.6**). Although it is possible that BsrF and ΔSS-BsrF have different substrate ranges, SWISS-MODEL predictions suggest that deletion of the signal sequence has little or no effect on other domains of the protein

(data not shown) (192-194). Thus, our results suggest that BsrF can act on glutamate, which would distinguish it from BsrV. Because BsrF is normally periplasmic, this racemization is unable to compensate for the loss of MurI in PG biosynthesis. When the secretion signal is removed, BsrF racemizes sufficient D-glu in the cytoplasm to allow production of wild-type PG. Similarly, the ΔSS-*bsrF* allele compensated for the loss of Alr, suggesting that alanine is also a substrate for BsrF, as it is for BsrV.

If the cytoplasmic BsrF generates other DAAs that are not usually produced there, they appear not to have been incorporated into the PG in significant quantity (**Figure 2.6**). In *V. cholerae*, activity of BsrV in the periplasm leads to alteration of the mature PG structure, including incorporation of D-met at the fifth peptide position (77, 99, 156), so future studies in this lab will be aimed at determining whether the same is true for BsrF. Although the *proB-bsrF* and ΔSS-*bsrF* alleles may lead to retention of racemase activity in the cytoplasm, a wild-type copy remained even in RMJ13S10, which could potentially support periplasmic function (**Figure 2.2**).

Our results suggest that broad-spectrum racemases might contribute to antimicrobial resistance, with implications for future development of antimicrobials that target PG and its biosynthesis. We measured antibiotic resistances of strains expressing wild-type BsrF or ΔSS-BsrF. We focused our studies on antibiotics that disrupt PG synthesis: beta-lactams, vancomycin, and DCS. In contrast to the others, which act on PG crosslinking and remodeling of the mature cell wall, DCS targets cytoplasmic enzymes involved in *de novo* PG synthesis; specifically, DCS inhibits both Alr and DdlA, the enzyme that produces D-ala:D-ala dipeptides for PG biosynthesis (172). Both the ΔSS-*bsrF* allele and the *proB-bsrF* allele in RMJ13S10 increase

resistance to DCS, so we speculate that the enzyme is producing D-ala. Currently, DCS is a second-line antibiotic used for treatment of infections by multidrug resistant *Mycobacterium tuberculosis* (195, 196). Although *M. tuberculosis* resistance to DCS is relatively rare, those strains that do arise tend to do so through mutation of alanine racemase (197). Though different mechanisms for resistance are employed in the two species, mutation of racemases increased resistance to DCS in both cases.

Though resistance to only one antimicrobial was discovered in this study, the observation that ΔSS-BsrF leads to increased resistance to DCS does lead to some concern about antibiotic resistance in pathogens that encode broad-spectrum racemases. Alanine and glutamate racemases have long been targets for antimicrobial drug discovery, due to their essential nature in many bacterial species (169, 171, 195, 198-202). Currently, DCS is the only widely used racemase-inhibiting antimicrobial drug, though the search for more continues. The current research adds to speculation that these racemase-targeting antibiotics could be rendered useless by alteration of broad-spectrum racemases (187). Although DCS inhibits Alr, the altered ΔSS-BsrF compensates well enough that *V. fischeri* becomes resistant to DCS at levels that would be medically relevant in the treatment of pathogens. Based on rescue of D-glu auxotrophy, the same possibility could arise against drugs targeting glutamate racemases, or the incorporation of D-glu into the growing PG peptide. A serine racemase can confer resistance to the PG-targeting antibiotic vancomycin (203), and the possibility that racemases could underlie additional examples of antimicrobial resistance is concerning, when considering that broad-spectrum racemases, and

racemases with low specificity, are being discovered in primary and opportunistic pathogens (77, 150, 164).

Finally, while unrelated to the goals of this study, the initial finding that the mini-Tn*5* disrupting *murI* could spontaneously and precisely delete was important. This phenomenon was also seen when performing similar studies with a mini-Tn*5* disruption in *alr* (data not shown). The mini-transposon used in these studies originated from pEVS170 (182), which has been used in many mutagenic analyses of *V. fischeri* (87, 158, 204-215) and other bacteria (216-220), and has been engineered to expand its utility (218). The reversion rate observed here of about 10^{-10} is sufficiently rare that for most purposes the transposon insertion can be considered stable; however, our results show that with strong selection and a sufficient population, reversion of Tn-disrupted loci can confound an experimental design. It is therefore important to maintain selection for Em, which is encoded on the mini transposon. This mini-Tn*5* lacks a transposase, so we hypothesize that reversion and loss of the mini-Tn*5* occurs through homologous recombination at the 9-bp direct repeats formed upon insertion.

MATERIALS AND METHODS

Bacterial strains and culture conditions. The strains used in this study are listed in **Table 2.2**. When added to LB medium (221) for selection of *Escherichia* coli, chloramphenicol (Cm) and kanamycin (Km) were used at concentrations 20 and 40 µg/mL, respectively. For selection of *E. coli* with Em, 150 µg/mL was added to BHI medium (Difco, Sparks, MD). When added to LBS (222) for selection of *V. fischeri*, Cm, Km, and Em were used at concentrations of 2, 100 and 5 µg/mL respectively. D-glu and

iso-D-gln were added to LBS at a final concentration of 400 µg/mL unless otherwise indicated. *Fischeri* minimal medium (FMM) (1 mM Tris [pH 7.5], 400 mM NaCl, 10mM KCl, 50mM $MgSO_4$, 10mM $CaCl_2$, 2 µM $FeSO_4$, 2mM glycerol-3-phosphate, 5mM ribose, 20mM NAG) was used for natural transformation of *V. fischeri*. In FMM, D-ala and D-glu were added at a final concentration of 25 µg/mL. Agar was added to a final concentration of 1.5% for solid media.

Molecular genetics and sequence analysis. Plasmids used in this study are listed in **Table 2.2**. Oligonucleotides used in this study are listed in **Table 2.3**, and were synthesized by Integrated DNA Technologies (Coraville, IA). DNA ligase and restriction enzymes were purchased from New England Biolabs (Beverly, MA). PCR was conducted with KOD DNA polymerase (Millipore Sigma, Burlington, MA). Plasmids used for cloning were prepared with the ZymoPURE Plasmid Miniprep kit (Zymo Research, Irvine CA). DNA was repurified after PCR and between cloning steps using the DNA Clean & Concentrator kit from Zymo Research. Cloned plasmids were Sanger sequenced at the University of Illinois-Chicago Genome Research Core facility. Genomic DNA from *V. fischeri* strains was extracted using the Invitrogen PureLink™ Genomic DNA Mini Kit (Thermo Fisher Scientific, Inc). DNA was then sonicated to generate fragments of approximately 500 bp, and gDNA libraries were prepared using the NEBNext Ultra II DNA library prep kit for Illumina (New England Biolabs), which includes end-repair, adaptor ligation, and addition of index primers. Sequencing was performed by the University of Georgia Genomics and Bioinformatics Core (Athens, GA) on an Illumina NextSeq500 instrument. All sequences were analyzed via Geneious

Prime version 2019.0.4 with default settings, and paired-end reads were compared to the reference genome of *V. fischeri* strain ES114.

Table 2.2. Strains and plasmids used in this study

Strain	Genotype	Source
E. coli		
DH5α	φ80d*lacZ*ΔM15 Δ(*lacZYA-argF*)U169 *deoR supE44 hsdR17 recA1 endA1 gyrA96 thi-1 relA1*	(223)
DH5αλ*pir*	DH5α lysogenized with λpir	(216)
CC118λ*pir*	Δ**(***ara-leu***)** *araD* Δ*lac74 galE galK phoA20 thi-1 rpsE rpsB argE*(Am) *recA* λ*pir*	(222)
V. fischeri		
AKD100	ES114 with a mini-Tn*7*-Em	(224)
ES114	Wild type isolate from *E. scolopes*	(5)
KL3	Δ*bsrF*	This study
MC9	Δ*bsrF* Δ*alr*::Em	This study
MC13	Δ*bsrF* Δ*alr*::FRT	This study
MC19	Δ*bsrF* Δ*alr*::FRT Δ*murI*::Em	This study
MC21	Δ*bsrF* Δ*alr*::FRT Δ*murI*::FRT	This study
RMJ13	*murI*::miniTn*5*-Em Δ*racD* (VF_1547)	(87)
RMJ13S10	*murI*::miniTn*5*-Em Δ*racD*; new amplification junction including *bsrF* (VF_0375) to *proB* (VF_0740) [TCCATCGTGATG::TGAAGTTTACTA]	This study
Plasmid [b]	**Relevant Characteristics**	**Source**
pCR-Blunt II-TOPO	*oriV*$_{ColE1}$, km^R	Thermo Fisher
pEVS104	Conjugative helper plasmid; *oriV*$_{R6K}$ *oriT*$_{RP4}$ km^R	(222)
pEVS118	*oriV*$_{R6K}$, *oriT*$_{RP4}$, cm^R	(216)
pKAL4	*bsrF* from ES114 cloned into pCR-Blunt II-TOPO	This study
pKAL6	*bsrF* from ES114 cloned into pVSV105	This study
pKV494	pJET + FRT-Em^R	(225)
pKV496	pEVS79-Km^R+ flp$^+$	(225)
plostfoX	tfoX$^+$, Cm^R	(226)
pMNC26	Δ*SS-bsrF* allele cloned into pVSV105	This study
pRMJ13	Δ*bsrF* allele in pCR-Blunt II-TOPO	This study
pRMJ14	pRMJ13 ligated to pEVS118	This study
pVSV105	*oriV*$_{R6K}$, *oriV*$_{pES213}$, *oriT*$_{RP4}$, *cm*^{R}, *lacZα*	(21)

[a] Drug resistance abbreviation used: Em, erythromycin; cm, chloramphenicol, km, kanamycin

[b] Alleles cloned in this study are from *V. fischeri* strain ES114. Replication origins (*oriV*) on each vector are listed as R6K and/or ColE1. Plasmids based on pES213 are stable in *V. fischeri* and do not require antibiotic selection for maintenance (21).

Table 3 Oligonucleotides used in this study

Primer *	Sequence	Source
Frt-F	CCA TAC TTA GTG CGG CCG CCT A	(225)
Frt-R	CCA TGG CCT TCT AGG CCT ATC CC	(225)
KAL1	CAT GCT AGC GGT TAA AAA AAC GAC GAT ATA TAA TTC CC	This study
KAL2	CAT GCT AGC GTA CCT AAT TAT TCT TAC TTA AAT TGG TGC	This study
MNC22	GGT TAA AAA AAC GAC GAT ATA TAA TTC CC	This study
MNC23	GTA CCT AAT TAT TCT TAC TTA AAT TGG TGC	This study
MNC37	CAT CCT AGG ACT AGT GTT CTG ATT TGC TTG CTA AAA GTA GTG TCA G	This study
MNC38	CAT CCT AGG CTT ACT TAA ATT GGT GCA ACC CGA CG	This study
MNC43	CCG TGT TCC CTG CCA ACA ATG	This study
MNC44	taggcggccgcactaagtatgg CAT AAC TGA AAC CAC AGA CTC	This study
MNC45	CCG TGT TCC CTG CCA ACA ATG	This study
MNC46	ggataggcctagaaggccatgg TAG GAT CAT TAG CAA TAC GCA CTT	This study
MNC50	CAT CCT AGG AAA CGG TTG TTT ATG TCA GCT CCA CTT CTT TC	This study
MNC51	GGG CTC GTA TTT CTT CTA CTA TGG GC	This study
MNC52	taggcggccgcactaagtatgg CAT GAT TCA GCC TTA TTA TTC ATC A	This study
MNC53	ggataggcctagaaggccatgg AAT GAG AGT CTT CTT GAA TTC ATT	This study
MNC54	CTC TAT ACT CGA GAC ACC GCT ATC	This study
RJ14	GGG TCA TCA TGC AGT AGC GA	This study
RJ28	AAT GTC GAC CAT AAA CAA CCG TTT TTA TAT AAT AAT TAT TTC G	This study
RJ29	ATT GTC GAC TAG ACG TCG GGT TGC ACC AAT TTA	This study
RJ30	TAA AAA CCG TTT TCA TAA AGG AGA TTC TTG	This study

* All oligonucleotides are shown in the 5'-to-3' direction. Underlined regions are restriction-enzyme recognition sites. Lowercase bases represent the tail sequences used for splicing fragments via SOE PCR.

Plasmid construction. Plasmids were generated and maintained in *E. coli* DH5α with the exception of pVSV105 and its derivatives which were maintained in DH5αλpir, and pEVS104 which was maintained in CC118*λpir* (222). When relevant, plasmids were conjugated into *V. fischeri* via triparental mating with helper plasmid pEVS104. Complementation plasmid pKAL6 was constructed by amplifying *bsrF* from ES114 with primers KAL1 and KAL2. This PCR product was cloned into pCR-Blunt II TOPO (Thermo Fisher, Waltham, MA), yielding pKAL4. pKAL4 was then digested with NheI, and the *bsrF*-containing NheI fragment was ligated into XbaI-cut pVSV105 (222)

producing pKAL6. Plasmid pMNC26 containing the ΔSS-*bsrF* allele was produced by amplifying *bsrF* from pKAL6 with primers MNC23 and MNC50, which amplifies the gene while looping out 54 base pairs of the putative secretion signal sequence. This product was then digested with AvrII and ligated into pVSV105 that had been cut with XbaI and SmaI, yielding pMNC26. To generate a *bsrF*-deletion construct, the ~2-kb region upstream of *bsrF* was PCR amplified from ES114 using primers RJ14 and RJ28, and the ~1.5-kb region downstream of *bsrF* was amplified with primers RJ29 and RJ30. The upstream and downstream fragments were digested with SalI, ligated together, gel purified, and cloned into pCR-Blunt II TOPO (Invitrogen, Thermo Fisher Scientific, Waltham, MA), to produce pRMJ13. To generate pRMJ14, pRMJ13 was digested with KpnI, and ligated to KpnI-cut pEVS118 (21).

Construction of mutant strains. Strain KL3 was made via plasmid-mediated allelic exchange, with plasmid pRMJ14. Briefly, a Δ*bsrF* allele on plasmid pRMJ14 (described below) was mobilized into ES114 via triparental mating. The resulting Δ*bsrF* strain KL3 was verified by PCR with primers MNC22 and MNC23. Additional mutant strains were generated via TfoX-mediated transformation (226). For each, an Em resistance cassette flanked by Frt-recombinase recognition sites was amplified from pKV494 using primers Frt-F and Frt-R. Strain MC9 was made by deleting *alr* from KL3. Briefly, a ~500-bp fragment upstream of *alr* was amplified from ES114 using primers MNC51 and MNC52, and the ~500-bp region downstream of *alr* was amplified with primers MNC53 and MNC54. Fragments were then spliced to either side of the Em cassette by overlap extension PCR (SOE-PCR) (225). This fragment was PCR amplified, then naturally

transformed into KL3 carrying the TfoX-overexpressing plasmid plosTfoX (226). Strain MC9 was selected on media containing Em and D-ala. The Em cassette was removed by expressing *flp* recombinase on pKV496 leaving an FLP recombinase recognition site scar in its place, and the plasmid was cured (225). The Δ*alr* allele of the resulting strain, MC13, was verified by PCR with primers MNC51 and MNC54. Strain MC19 was then generated by deleting *murI* from MC13. The ~500-bp fragment upstream of *murI* was amplified from ES114 using primers MNC43 and MNC44, and the ~500-bp region downstream of *murI* was amplified with primers MNC45 and MNC46. Fragments were spliced together with Em and amplified as above, then naturally transformed into MC13 carrying the TfoX-overexpressing plasmid plosTfoX. Strain MC19 was selected on media containing Em, D-ala and D-glu. The Em cassette was again removed by introducing pKV492, screening for loss of the Em marker, and curing the plasmid. The resulting strain, MC21, was verified as Δ*murI* by PCR amplification with primers MNC43 and MNC46.

Selection for spontaneous revertants and suppressor of D-glu auxotrophy. Strain RMJ13 was grown in LBS containing 400 µg/mL D-glu (with or without Em, as described above), to an OD_{600} of 1. 100 µL of culture were plated to LBS without D-glu (in the case of revertants), or LBS containing Em and iso-D-gln (in the case of RMJ13S10). Cultures were dilution plated non-selectively in parallel on LBS plates supplemented with D-glu, to determine the number of CFU plated and resulting mutation frequency. Plates were incubated at 28°C, and colonies counted at 24 hours and 48 hours. Colonies were streak purified on media containing Em, then frozen at -80ºC in LBS with 20% glycerol.

Mutagenesis of RMJ13 with ethyl methanesulfonate (EMS). Strain RMJ13 was grown overnight in 50 mL LBS-Em with 400 µg/mL D-glu. The next morning, strain was subcultured at a 1:500 dilution into 20 mL LBS-Em with D-glu. At an OD_{600} between 0.5-0.8, cells were harvested by centrifugation at 9400 x *g* at room temperature for 5 minutes, then washed twice with 1 M NaCl and centrifugation as before. Pellet was resuspended in 8 mL of FMM and split into 4x-2 mL aliquots. Cultures were incubated shaking at 200 rpm and 28°C for 1 hour. One tube was left untreated; others were dosed with 50uL EMS at 0, 20, or 40 Minutes of incubation (EMS exposure times 60, 40, and 20 minutes, respectively). Cells were harvested by centrifugation as above and washed three times with 1 M NaCl; EMS waste was treated with 10 N NaOH before disposal. Pellets were resuspended in 1 mL of FMM, and incubated shaking at 200 rpm at 28°C. After 5 minutes, 1 mL of FMM was added to each tube, and left to incubate for 10 more minutes. Cells were then plated to LBS-Em without D-glu, for selection of mutants able to overcome D-glu auxotrophy. Cultures were dilution-plated non-selectively in parallel on LBS-Em supplemented with D-glu, to determine the number of CFU plated, and percent-killing by EMS. Plates were incubated at 28°C. Colonies were counted at 24 hours; selective plates were incubated for up to 72 hours.

***In silico* analyses.** Potential secretion signal sequences in BsrF and the ProB-BsrF fusion were predicted using the SignalP-5.0 server from DTU health (https://services.healthtech.dtu.dk/service.php?SignalP-5.0) (188), and a probability graph was constructed, with calculated likelihood that the sequences were standard Sec

signal peptides, TAT signal peptides, lipoprotein Sec signal peptides, or cleavage sites. Protein similarity scores were analyzed via NCBI services (National Center for Biotechnology Information (NCBI)[Internet]. Bethesda (MD): National Library of Medicine (US), National Center for Biotechnology Information; [2023] – [cited 2017 Apr 06]. Available from: https://www.ncbi.nlm.nih.gov/) and SnapGene® software (from Dotmatics; available at snapgene.com).

Analysis of PG amino acid and muropeptide content. Cells were grown overnight in LBS with any necessary antibiotics and amino acids, chilled on ice for 10min, and centrifuged at 4°C and 17,600 x *g* for 15 minutes. Pellets were washed by resuspension in 400 mL 1 M NaCl and centrifuged as above. Pellets were resuspended in 10 mL water that had been chilled on ice, then dripped into 50mL of boiling 4% SDS. The solution was then boiled for 30 min with continuous stirring and allowed to cool to room temperature, at which point they were centrifuged at 120,000 x *g* for 60 min, resuspended in room temperature water and washed three to four more times by centrifugation and resuspension as above. Before resuspension, the supernatant was assayed for SDS using methylene blue and chloroform (227) and washed repeatedly until no SDS was detected. When SDS was undetectable, the pellet was resuspended in 1 mL of water, with Tris-HCl (pH 7.5) added to a final concentration of 100 mM and $MgSO_4$ added to a concentration of 20 mM, then treated with 10 µg DNase I and 50 µg RNase A for 30 minutes at 37°C. Samples were then treated with 100 µg of Trypsin, $CaCl_2$ was added to a final concentration of 10 mM, and samples were incubated overnight at 37°C. Samples were then centrifuged at 15,880 x *g* for 10 minutes and

pellets resuspended in 1% SDS. The solution was incubated in a 95°C hot water bath for twenty minutes, diluted into warm water, and then centrifuged at 120,000 x *g* for 60 minutes at room temperature. The pellet was then washed with warm water and centrifuged as above, until SDS-free. Subsequent pellets were then resuspended in 12.5 mM $NaPO_4$ (pH 5.5) and digested with 125 units of Mutanolysin at 37°C overnight. Insoluble material was removed by centrifugation at 15,880 x *g* for 15 minutes. The muropeptide-containing supernatant was transferred to a new tube, lyophilized until dry, and stored at -20°C until analysis. Amino acid (228) and muropeptide analyses (229) were performed using HPLC as previously described. Peaks from these analyses were then analyzed by tandem mass spectrometry to further verify the muropeptide structure.

ACKNOWLEDGEMENTS

We thank Doreen Nguyen for technical assistance, and Richard Helm at Virginia Tech for performing and analyzing mass spectrometry. This research was supported by NSF grant IOS-1557964 awarded to EVS and DLP.

CHAPTER 3

MUTANT *GLTS* ALLELES ENABLE A *VIBRIO FISCHERI* D-GLUTAMATE AUXOTROPH TO GROW WITH LOWER REQUIREMENTS FOR EXOGENOUS D-GLUTAMATE [2]

[2] Macey N. Coppinger, Richard F. Helm, David L. Popham, Liu Yang, Edward G. Ruby, and Eric V. Stabb. To be submitted to *Microbiology Spectrum*.

ABSTRACT

D-glu is a key component of PG and is essential for growth in most bacteria. To assess constraints on bacterial requirements for D-glu and on PG evolution, we sought to artificially evolve PG biosynthesis, leading to either replacement of D-glu in the peptide chain, or alternative pathways to D-glu incorporation into PG. We previously found that suppression of D-glu auxotrophy in a *murI racD* mutant of *Vibrio fischeri* grown on LBS medium was rare but could be accomplished by mutation of *bsrF*, with restoration of wild-type PG structure. Here, we selected nine prototrophic suppressors of the same D-glu auxotroph from 10^{10} CFU plated on LBS-Em supplemented with ~2.7 mM D-gln. Each suppressor had a mutation in *gltS*, which encodes a putative sodium:glutamate symporter. Increased copy numbers of these *gltS* alleles enabled growth on unsupplemented LBS and resulted in PG that contains D-glu. Preliminary results suggest that D-gln supplementation had inadvertently added ~0.10 mM D-glu and that LBS itself contains ~1.4 µM D-glu. The mutations in *gltS* enabled growth with similarly low D-glu concentrations, but also increased sensitivity to homocysteic acid, suggesting more promiscuous or permissive transport. Surprisingly, we also discovered that expression of mutant *gltS* in the auxotroph leads to a subset of PG containing lysine in the peptide chain; however, this *V. fischeri* mutant still colonized the host squid and triggered PG-induced morphogenesis. Our results shed light on glutamate transport, highlight tradeoffs in GltS structure and function, and reveal an unusual PG modification.

IMPORTANCE

D-glu is an important building block in the PG component of the bacterial cell wall, and its endogenous production is considered essential in most bacteria, even in most rich complex media. In *Vibrio fischeri*, overexpression of mutant GltS symporters allow D-glu auxotrophic strains to grow on LBS medium without exogenous D-glu, though with the fitness tradeoff of increased sensitivity to homocysteic acid. Our finding that LBS contains sufficient D-glu to support robust growth highlights the understudied importance of DAA transport and the ubiquity of DAAs. Moreover, the discovery of lysine in the PG peptide is an unusual and as-yet unexplained PG modification.

INTRODUCTION

DAAs play important roles in biology and are widespread in the biosphere. Although less abundant than proteinogenic L-amino acids and often overlooked, DAAs can be formed enzymatically or abiotically from their enantiomeric L-amino acid counterparts, and they serve nutritional and other functional roles for bacteria. D-ala and D-glu play well-known roles for bacteria as highly conserved components of the PG cell wall. In this context, the presence of DAAs in the PG side chain may render PG more resistant to proteases, which typically target L-L peptide bonds (100). The unusual and bacteria-specific structure of PG also make it a MAMP recognized by bacteria-surveillance systems of plants and animals, with the peptide chain being an important recognition determinant (230-232). PG and fragments of it play important roles in symbiont recognition in the mutualism between the Hawaiian bobtail squid, *E. scolopes* and *V. fischeri* (3), which prompted our interest in PG structure and biosynthesis in this

bacterium. We have used *V*. *fischeri* as a model for exploring the experimentally forced evolution of new PG biosynthetic pathways, providing insight into how PG can evolve as well as the constraints on that evolution. Our strategy has been to block PG biosynthesis and select for suppressor mutants that can grow without a gene normally considered essential. In this and an earlier study (Chapter 2), we focused on the D-glu moiety of PG.

D-glu is a critical component of the PG for many bacteria and is supplied for PG biosynthesis by the activity of glutamate racemase(s), usually encoded by a *murI* (*racE*) gene (176, 233, 234). In general, “essential” in these experimental contexts means the gene is required to grow on a rich medium such as lysogeny broth (LB) medium, which provides a complex source of nutrients that can obviate the need for many endogenous biosynthetic pathways. In some bacteria, *murI* mutants can be obtained on media supplemented with D-glu (158, 235, 236), though in *Escherichia coli* recovery of a *murI* mutant required both addition of D-glu to LB and secondary mutations in *gltS*, which encodes a glutamate transporter (237, 238).

As in many other bacteria, *murI* was categorized as an essential gene in *V. fischeri*, in this case based on an InSeq analysis (178). A *murI*::Tn mutant was subsequently recovered on LBS supplemented with ~2.7 mM D-glu (158). Previously, we found that growth on unsupplemented LBS could be restored to a *V. fischeri murI* mutant by the overexpression of RacD (87), an aspartate racemase, or by removal of a secretion signal sequence of the broad-spectrum racemase BsrF (Chapter 2). No other suppressors of D-glu auxotrophy in the *murI racD* mutant were recovered on LBS,

despite plating >10^{10} cells (Chapter 2). Here we set out to select prototrophic suppressors of the *murI racD* mutant on LBS supplemented with ~2.7 mM D-glutamine.

RESULTS

Mutations in *gltS* allow a D-glu auxotroph to grow with very low concentrations of D-glu. We attempted to select for mutants of RMJ13 (Δ*racD murI*::mini-Tn*5*-Em) able to grow without D-glu supplementation by plating cells on LBS containing erythromycin (LBS-Em) further supplemented with D-gln. After plating over 10^{10} CFU total, we isolated nine mutants, RMJ13M1 through RMJ13M9, yielding a recovery rate of $7x10^{-10}$. At least seven of these nine mutants arose independently, while two may be siblings, as described below. With one exception, these strains require exogenous supplementation in LBS-Em to grow **(Figure 3.1A)**. Unlike the others, mutant RMJ13M3 displayed an inconsistent requirement for supplementation, and sometimes grew on unsupplemented LBS-Em. While working with RMJ13M3, we isolated a derivative, RMJ13M3.1, which consistently grew on unsupplemented LBS-Em (**Figure 3.1B**).

Sequencing revealed that RMJ13M1 through RMJ13M9 each contain mutations in *gltS* (VF_A0507), which encodes a putative sodium:glutamate symporter (14, 15). For most strains, these *gltS* alleles were revealed by whole-genome sequencing, while RMJ13M7 and RMJ13M9 *gltS* alleles were targeted for cloning and Sanger sequencing.

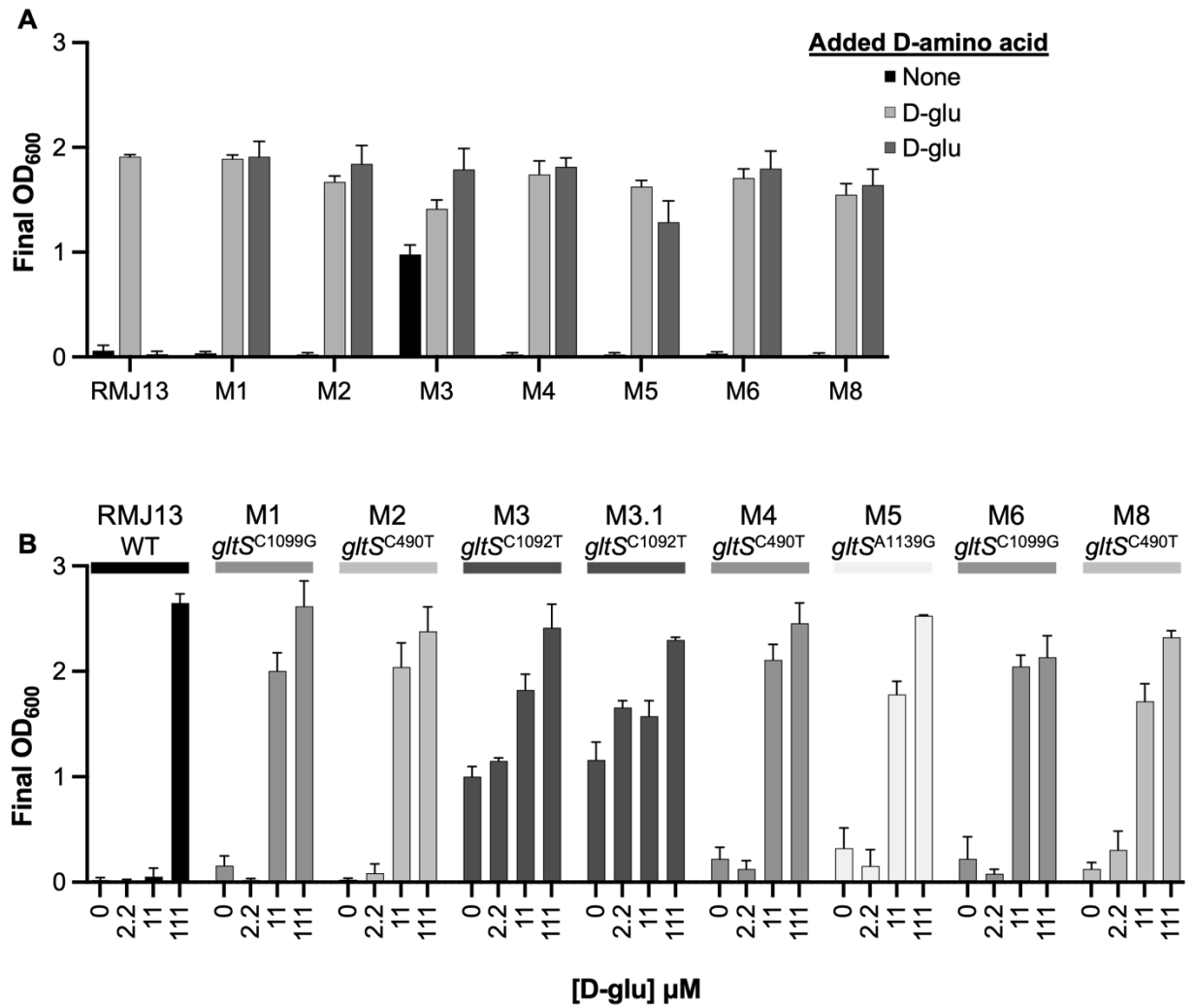

Figure 3.1. RMJ13 and suppressor mutants grow with varied supplementation. (**A**) Final OD_{600} of RMJ13 (*murI*::mini-Tn*5* Δ*racD*) and its derivatives RMJ13M1 through RMJ13M8 (denoted here as M1 through M8) grown in LBS-Em supplemented with D-gln or D-glu. (**B**) D-glu requirements for *gltS* mutants were assessed by growing strains in LBS-Em containing increasing concentrations of D-glu. Cultures were grown for 24 hours before reading OD_{600}. Error bars indicate standard error of the mean (n=4). Data from one representative experiment of at least three are shown.

Four different mutant *gltS* alleles were recovered: C490T, C1092T, C1099G, and A1139G, each of which leads to an amino acid replacement (**Table 3.1**). Mutations C490T and C1099G were isolated from multiple independent cultures, while C1092T and A1139G each occurred once. Although some of these strains also have additional

mutations in their genomes, the one commonality was mutation of *gltS* (**Table 3.1**). Mutant RMJ13M7 has the same *gltS* allele as RMJ13M6 and was isolated from the same culture. Mutant RMJ13M9 was isolated from the same culture as RMJ13M8 and has the same *gltS* allele. Thus, RMJ13M7 and RMJ13M9 could be siblings to RMJ13M6 and RMJ13M8 respectively and are not further analyzed in this study.

Table 3.1 RMJ13 derivative strains and mutations.

RMJ13 Mutant	*gltS* Allele	GltS amino acid replacement	Other Mutations
RMJ13.M1	*gltS*^{C1099G}	G3667R	None
RMJ13.M2	*gltS*^{C490T}	A164T	VF_0468^{A699G} *gacS*^{G644C}
RMJ13.M3	*gltS*^{C1092T} Duplication	M364I	Amplification junction [ACTTAACTTGAT::GATGTTGTTTTA]
RMJ13.M3.1	*gltS*^{C1092T} ~10x amplification	M364I	VF_2147^{G778A} Amplification junction [ACTTAACTTGAT::GATGTTGTTTTA]
RMJ13.M4	*gltS*^{C490T}	A164T	*gacS*^{G644C}
RMJ13.M5	*gltS*^{A1139G}	F380S	None
RMJ13.M6	*gltS*^{C1099G}	G3667R	VF_0468^{A699G}
RMJ13.M7	*gltS*^{C1099G}	G3667R	Unknown
RMJ13.M8	*gltS*^{C490T} Duplication	A164T	Duplication junction [TGTGCTGATAAA::AGGTGAAAAGGG]
RMJ13.M9	*gltS*^{C490T}	A164T	Unknown

Since recovering these suppressor mutants, we subsequently discovered that our D-gln stocks contain low amounts of D-glu. Though it was made to contain ~273 mM D-gln, the stock was measured to actually have ~10.5 mM D-gln and ~1.5 mM D-glu, likely due to degradation and spontaneous deamidation of D-gln (202) (**Table 3.2**). This finding led us to believe that mutant GltS symporters are less likely to be promiscuously transporting D-gln, but more likely have increased efficiency of D-glu transport. To verify, we grew RMJ13 as well as eight of the derivative mutants on LBS-

Em with varying concentrations of exogenous D-glu. While the parental auxotroph requires 111 μM exogenous D-glu in LBS-Em medium, most of the derivative strains require about ten-fold less (**Figure 3.1B**). Suppressor strains RMJ13M3 and RMJ13M3.1 do not require any D-glu supplementation in LBS-Em.

Table 3.2 Average DAA concentrations in various media and solutions, as measured by solid phase extraction and mass spectrometry [a]

	Concentration (μM)			
	L-glu	**D-glu**	**L-gln**	**D-gln**
LBS	93.57 ± 9.28	1.41 ± .07	-	-
YEBS	185.33 ± 45.15	1.70 ± 0.21	0.73 ± .05	-
TBS	60.06 ± 0.37	-	0.68 ± 0.03	-
D-glu stock	1105 ± 0.7	89,400 ± 654	-	-
D-gln stock	9.2 ± 0.89	1488 ± 27	-	10,447 ± 118

"-" indicates that amino acid was not detected
[a] Experiment was performed once. Results are shows as average +/- SD (n=3)

Increased copy number amplifies phenotypes of mutant *gltS* alleles. Based on Illumina sequencing depth, RMJ13M3 and RMJ13M3.1, and RMJ13M8, with *gltS* alleles C490T (RMJ13M3 and RMJ13M3.1) and C1092T (RMJ13M8), appear to have amplifications of large regions of chromosome II that include *gltS*. Strains RMJ13M3 and RMJ13M3.1 share amplification junctions, with an amplified region of about 60 kb that includes the mutant allele of *gltS*. As noted above, RMJ13M3 has an inconsistent requirement for supplementation, which we believe is due to spontaneous amplification and resolution of the chromosomal duplication, leading to varied *gltS* copy number and amount of GltS expressed in the cells. RMJ13M3.1, however, was isolated on LBS-Em

without supplementation, and consistently grows without additional supplementation, and based on sequencing depth has more copies of the amplified region (**Table 3.1**). Based on the sequencing depth and identification of a novel chromosomal junction, RMJ13M8 also has a duplication, in this case of about 83 kb. These data led us to hypothesize that increased copy number of mutant *gltS* alleles leads to increased D-glu transport, thereby decreasing the amount of exogenous D-glu needed to support growth of these auxotrophic strains.

To test this hypothesis, we cloned wild-type *gltS* as well as two of the mutant *gltS* alleles (C490T and C1092T) into shuttle vector pVSV105 and moved them into RMJ13. Based on previous work (21), it was estimated that *V. fischeri* holds 10-15 copies of pVSV105 per cell on average. *In trans* expression of mutant *gltS* alleles on this shuttle vector enabled growth of RMJ13 on LBS-Em without supplementation, while the wild-type *gltS* and the parental shuttle did not (**Figure 3.2A**). These results, in combination with data of the mutant strains, is consistent with our hypothesis that overexpression of these mutant forms of GltS improves cells' ability to suppress D-glu auxotrophy by enabling them to access external D-glu at lower concentrations.

LBS contains trace amounts of some DAAs. When expressing many copies of mutant *gltS*, a D-glu auxotroph can grow on LBS-Em without exogenous supplementation. The nutrient-rich components of LBS, tryptone and yeast extract, are known to contain L-amino acids, but to our knowledge the presence of DAAs has not been reported or quantified. Based on our results, we predicted that LBS does contain DAAs, though likely in concentrations that are not easily measured or utilized by

bacteria. We analyzed LBS, as well as less-complex media derivatives tryptone broth saline (TBS) and yeast extract broth saline (YEBS) via solid phase extraction and mass spectrometry, and results of one trial are listed in **Table 3.2**. Importantly, these data indicate that LBS contains ~1.4 µM (0.2 µg/mL) D-glu, mostly supplied by yeast extract (**Table 3.2**). When grown in defined FMM expression of *gltS*^{C490T} or *gltS*^{C1092T} can support growth in similarly low concentrations of D-glu, although the strains do still require D-glu (**Figure 3.2B**).

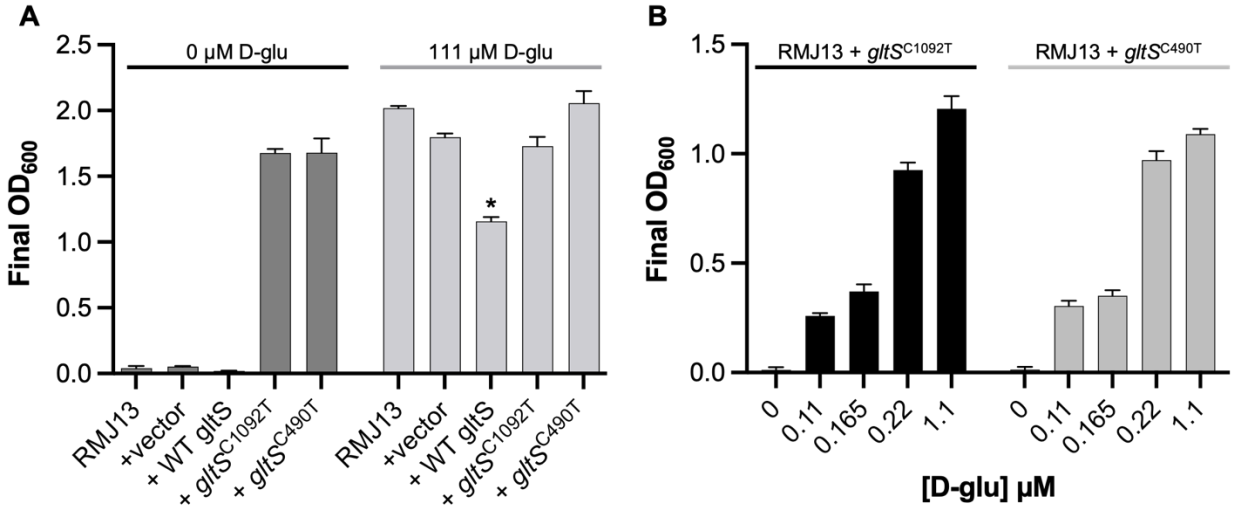

Figure 3.2. Mutant *gltS* alleles lower D-glu requirement of D-glu auxotroph. (**A**) Final OD_{600} readings for *V. fischeri* cultures grown for 24 hours in LBS-Em with or without D-glu. Strains included RMJ13 alone or carrying vector pVSV105 (vector), pMNC15 (*gltS*), pMNC16 (*gltS*^{C1092T}), or pMNC17 (*gltS*^{C490T}). (**B**) Final OD_{600} readings for *V. fischeri* cultures grown for 24 hours in FMM with varying amounts of D-glu as indicated. Error bars indicate standard error of the mean (n=3). Data from one representative experiment of at least three are shown.
* RMJ13 expressing WT *gltS* grows to a significantly lower final OD_{600} than all other strains ($P < 0.05$)

Expression of mutant GltS increases sensitivity to homocysteic acid and D-glu. In *Escherichia coli*, GltS acts as a relatively low-affinity transporter for homocysteic acid

(HCA), a metabolite shown to inhibit growth (239, 240). Mutations in *gltS* can influence sensitivity of *E. coli* to HCA (241). The effect of *gltS* alleles on the sensitivity of *V. fischeri* to HCA was tested by shuttling wild-type and mutant *gltS* alleles carried on pVSV105 into the wild-type strain ES114. The mutant alleles conferred increased sensitivity to HCA, while the *gltS* and the parental shuttle vector did not (**Figure 3.3**).

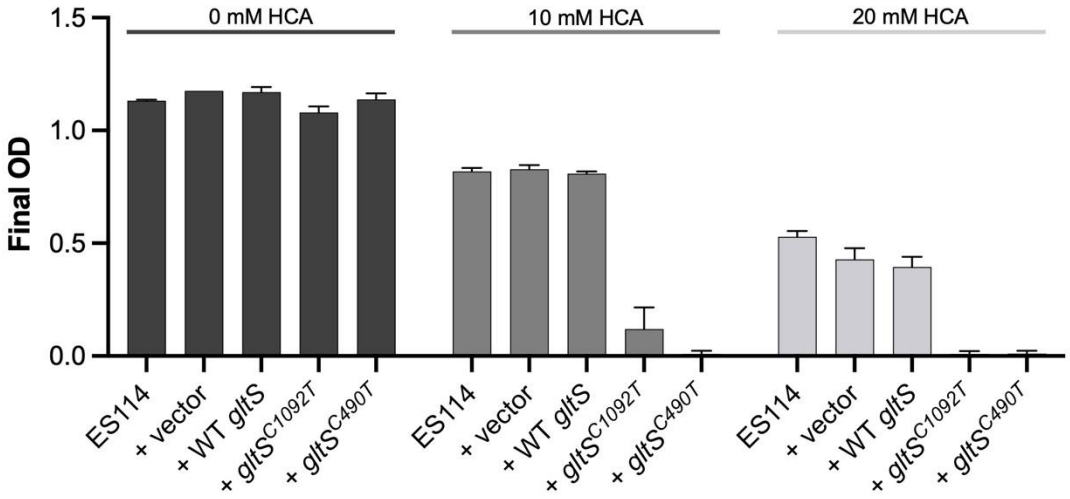

Figure 3.3. Expressing mutant *gltS* increases sensitivity to HCA. Shown are final OD_{600} readings for *V. fischeri* cultures grown with increasing concentrations of HCA. Strains include ES114 alone, or carrying pVSV105 (vector), pMNC15 (*gltS*), pMNC16 (*gltS*^{C1092T}), or pMNC17 (*gltS*^{C490T}). Cultures were grown for 24 hours before reading OD_{600}. Error bars indicate standard error of the mean (n=4). Data from one representative experiment of at least three is shown.

Expression of mutant GltS alters PG structure. The wild-type PG structure in *V. fischeri*, and most Gram-negative bacteria, is composed of linear repeating strands of β-1,4 linked *N*-acetylglucosamine (NAG) and *N*-acetylmuramic acid (NAM), with short peptide chains covalently bound to most NAM molecules. The mature peptide chain bound to NAM is L-ala, D-glu, *meso*-diaminopimelic acid (mDAP), and D-ala. We hypothesized that RMJ13 expressing mutant *gltS* alleles would have PG structure, as

the mutant GltS symporters appear to enable growth on small amounts of D-glu, rather than supporting D-glu-independent growth. HPLC and mass spectrometry indicated that RMJ13 expressing *gltS*^{C490T} mostly contains PG indistinguishable from wild type, with D-glu in its peptides (**Figure 3.4**). However, LC-MS also showed another relatively minor peak corresponding to a molecule about 128 Da larger than wild-type monomers (**Figure 3.4B**). Further analysis revealed that a subset of PG in this strain is composed of a NAG-NAM-tetrapeptide moiety with an additional lysine bound to the fourth position D-ala.

***In silico* analysis of mutant GltS.** According to the BLAST alignment tool (242-244), GltS from *V. fischeri* shares 48% identity and 64% similarity with GltS from *E. coli* B (EcGltS). Like EcGltS, GltS from *V. fischeri* is predicted to be an integral membrane protein in the cytoplasmic membrane (245-248), They are also both predicted to consist of two domains, each with five transmembrane helices and a pore loop that's likely involved in substrate specificity (192-194, 246, 247, 249) (**Figure 3.5**). The four mutant *gltS* alleles in our suppressor strains each have an amino acid substitution: A164T, M364I, G367R, and F380S, respectively (**Figure 3.5**). Based on the SWISS-MODEL predictions, one substitution, A164T, is found within a transmembrane helical region, while the other three are predicted to be clustered in the cytoplasmic region of a pore loop (**Figure 3.5**) (192-194).

A

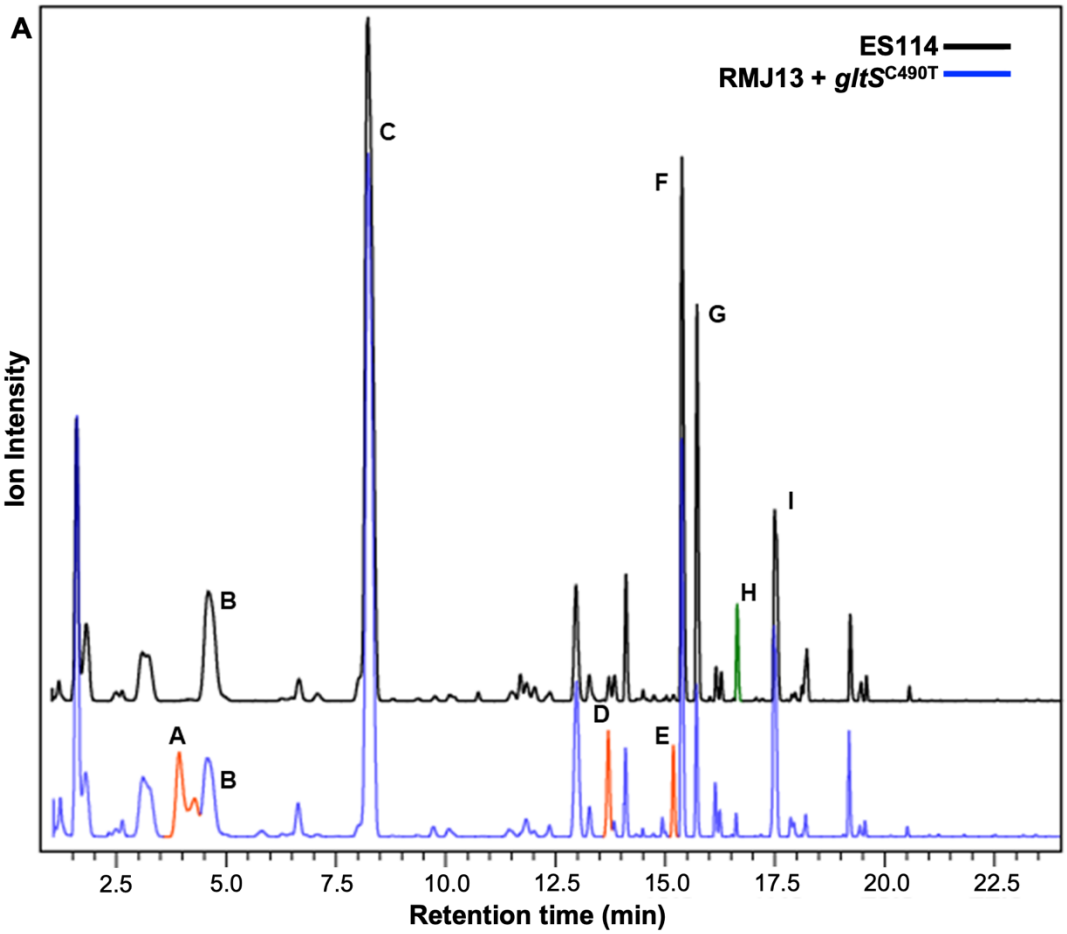

B

Peak	Structure	Abbr	Note
A	NAG-NAM-L-Ala-D-Glu-mDAP-Lys	M4 (Lys)	Only present in mutant
B	NAG-NAM-L-Ala-D-Glu-mDAP	M3	Present in both strains
C	NAG-NAM-L-Ala-D-Glu-mDAP-D-Ala	M4	Present in both strains
D	NAG-anhydroNAM-L-Ala-D-Glu-mDAP	anhM3	Higher in mutant
E*	M4 dimer - NAG	$(M4)_2$ - NAG	Trace in WT
F*	M4 dimer	$(M4)_2$	Present in both strains
G	anhydroM4 monomer	anhM4	Higher WT
H*	M4 trimer	$(M4)_3$	Higher WT
I*	M4-anhydroM4 dimer	M4-anhM4	Present in both strains

* Crosslink not determined

Figure 3.4. Muropeptide profiles of V. fischeri strains. (**A**) Representative LC spectra of comparative muropeptide analysis of ES114 (black) and RMJ13 expressing gltS^{C490T} (carried on pMNC17, blue), in which the amount of purified and injected PG was normalized to height of peak C. (**B**) Identification of peaks labeled in **A**.

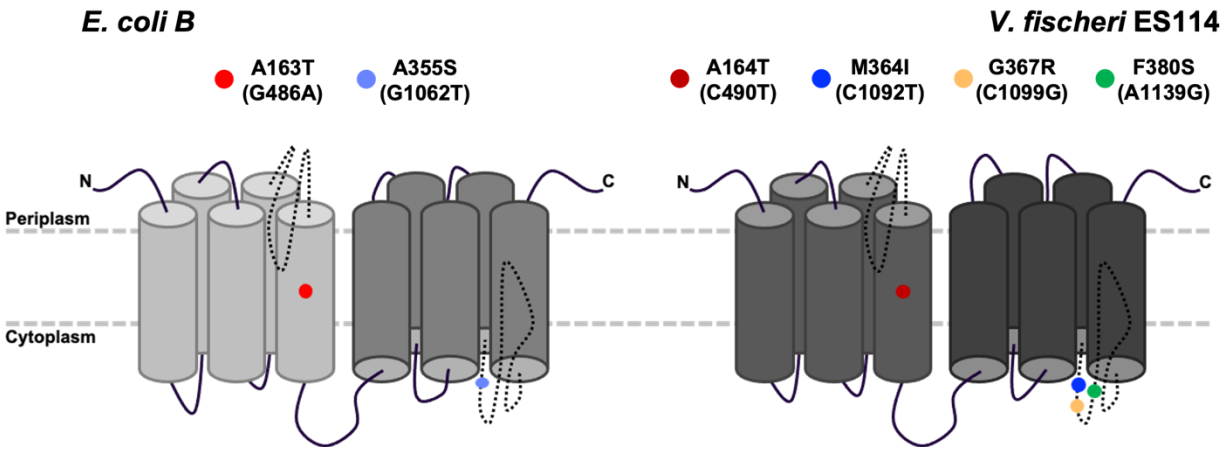

Figure 3.5. Diagrams of predicted GltS protein structures of (left) *E. coli* and (right) *V. fischeri*. (**Left**) Structure of GltS of *E. coli* B strain WM335, which has two amino acid substitutions compared to the wild type. Both replacements (shown as colored dots) exist within the same strain. Diagram is based on SWISS-MODEL predictions and previous publications (192-194, 246, 247, 249). (**Right**) Structure of GltS from *V. fischeri*, showing amino acid replacements corresponding to mutations in RMJ13 suppressor strains. All amino acid replacements are shown on one structure, although only one exists per strain. Amino acid locations and overall structures are approximate, based on SWISS-MODEL predictions (192-194).

RMJ13 colonizes *E. scolopes*, dependent upon exogenous D-glu. Due to the importance of PG as a signaling molecule in the squid-*Vibrio* symbiosis, we sought to determine whether RMJ13 with the empty vector (pVSV105), as well as RMJ13 expressing *gltS*^{C490T} (pMNC17) were able to colonize hatchling *E. scolopes*. Hatchling squid were inoculated overnight in filtered sea water (FSW) containing *V. fischeri*, with both RMJ13 strains also getting supplementation with D-glu. Squid were then transferred into fresh FSW; half of each RMJ13-inoculated group were transferred to FSW with D-glu, while the others were placed in FSW without D-glu, to determine if removal of D-glu from FSW interrupted colonization by D-glu auxotrophs. Viability of the symbionts was measured by both average CFU per light organ and luminescence (**Figure 3.6**).

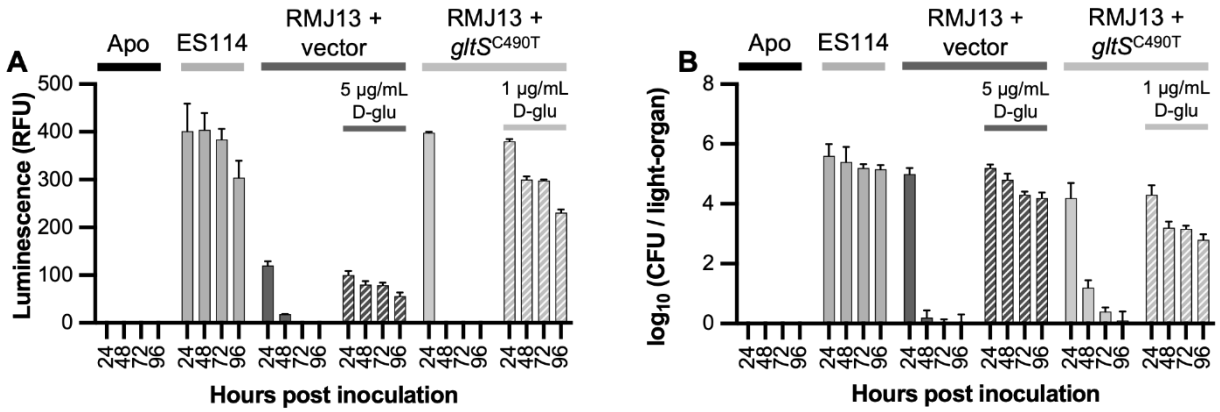

Figure 3.6. D-glu auxotrophic *V. fischeri* appear to transiently colonize *E. scolopes*, dependent upon D-glu. (**A**) Symbiont population levels (average CFU per light organ) over time for wild type (ES114) and RMJ13 carrying pVSV105 (vector) or pMNC17 (*gltS*^{C490T}), with and without persistent exogenous D-glu supplementation. "Apo" indicated uninoculated, aposymbiotic squid as negative controls. (**B**) Squid luminescence over time, with the same strains, conditions, and treatments as in panel **A**. Error bars indicate standard error of the mean (n=13). This experiment was performed once.

Both RMJ13 carrying the empty vector (pVSV105) and RMJ13 expressing *gltS*^{C490T} (pMNC17) were able to colonize the squid when D-glu was present, but luminescence of squid infected with either strain rapidly decreased after D-glu removal (**Figure 3.6A**). Additionally, the average CFU per light organ of squid infected with each RMJ13 strain decreased rapidly after removal of D-glu, aligning with the luminescence data (**Figure 3.6B**). These results appear to be due to the rapid lysis of D-glu auxotrophic strains when D-glu is removed from the seawater (**Figure 3.7**).

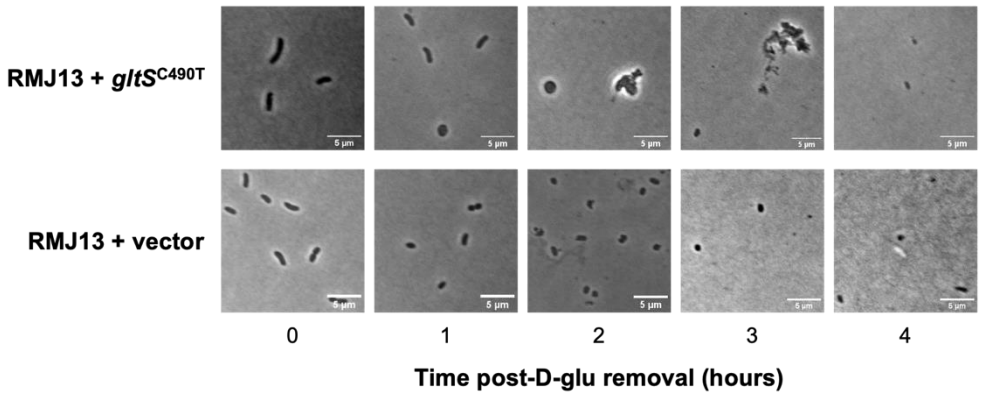

Figure 3.7. *V. fischeri* D-glu auxotroph lyses without D-glu. Within four hours of being placed in FSW without D-glu, auxotrophic cells begin to lyse. Expression of *gltS*^{C1092T} (top) does not have a growth advantage over RMJ13 carrying the vector alone (bottom) in these conditions.

DISCUSSION

While L-amino acids have been known to be vitally important building blocks of proteins in all life forms, there has been growing appreciation and study of DAAs more recently. Though they are less commonly found in nature, they do have fundamental roles in most organisms and ecosystems. For example, DAAs are constituents of the PG peptide in bacterial cells walls (250). In most Gram-negative bacteria, PG includes D-glu, *m*DAP, and D-ala. In *V. fischeri*, each of these is primarily produced for PG biosynthesis by a specific enzyme. D-ala is produced by Alr (158), *m*DAP is likely produced by a putative DAP epimerase encoded by the *dapE* gene (14, 15). The D-glu needed for PG biosynthesis is mainly produced by MurI (158); however, RacD (87) and BsrF (Chapter 2) can also provide D-glu for PG, though they do not appear to contribute to PG biosynthesis under normal growth conditions.

Previously, our lab has attempted to alter *V. fischeri*'s PG biosynthesis by creating strains auxotrophic for PG-specific DAAs and then selecting for prototrophic

suppressors (87, 190) (Chapter 2). Most recently, we found that removal of a putative secretion signal from the broad-spectrum racemase BsrF allowed the enzyme to produce sufficient D-glu to suppress auxotrophy. Although ultimately the suppressor mutant did not require it, we were only able to generate the mutant when supplementing LBS with iso-D-glutamine. Similarly, in the present study, we attempted to use exogenous D-gln to isolate suppressors of D-glu auxotrophy. In total ten suppressors were generated, with eight of them consistently requiring supplementation to grow in LBS-Em (**Figure 3.1**). All ten of these suppressors have mutations in *gltS*, which encodes a putative sodium:glutamate symporter (14, 15) (**Table 3.1**). Four mutant *gltS* alleles were isolated, two of which arose independently in multiple cultures.

Other mutations deviating from wild type were also discovered in the suppressor mutants, including VF_0468^{A699G} and *gacS*^{G644C} which were recovered independently from two mutants each (**Table 3.1**). GacS is a sensor kinase and part of the GacS/GacA two-component regulatory system, which has a broad regulon and is widespread among many Proteobacteria, including *V. fischeri* (14, 15, 251, 252). VF_0468 appears to encode an orthologue of LspA, a prolipoprotein signal peptidase II that in other bacteria plays a role in cell envelope and PG synthesis. Given that neither of these mutations was isolated absent a *gltS* mutation, it is uncertain whether they were primary mutations that contribute to survival in D-glu limiting conditions, or secondary mutations that arose to compensate for negative effects associated with the *gltS* mutations themselves. VF_0468 was categorized as an essential gene (178) and the VF_0468^{A699G} allele may be of interest for future studies, but here we chose to focus on the only gene consistently mutating in the suppressors, *gltS*.

A well-studied homologue of *V. fischeri*'s GltS is that of *E. coli* (EcGltS) (238, 240, 246, 247, 253-257). Specifically, a D-glu auxotroph of *E. coli* could not be generated without concomitant mutations in *gltS* (237, 238). Interestingly, the two mutations in *gltS* that allowed for generation of a D-glu auxotrophic strain of *E. coli* corresponded to two of the mutant alleles generated in this study. The first of these, codon 163 in EcGltS and 164 in *V. fischeri* (allele $gltS^{C490T}$), substitutes a threonine residue for alanine within the fifth transmembrane helix of the protein (**Figure 3.5**) (238). The second allele, $gltS^{C1092T}$ in the present study, is located at codon 355 in EcGltS and 364 in *V. fischeri* (238) (**Figure 3.5**). Although neither the wild-type (methionine in *V. fischeri* and alanine in *E. coli*) nor mutated amino acids (isoleucine and serine) are similar to each other, it is intriguing that corresponding codons were again found to increase GltS activity when mutated. Three of the *gltS* mutations in this study are in the cytoplasmic stretch of a predicted pore-loop (**Figure 3.5**) (192-194). Pore loops have been found to be selectivity filters of transport proteins (258-262). We speculate that these amino acid replacements in the GltS symporters of this study render them more permissive and/or promiscuous to the uptake of D-glu and HCA.

Because suppressors were selected on LBS-Em supplemented with D-gln, we initially hypothesized that mutant GltS symporters were enabling mutants to access D-gln in the media, with D-gln either directly incorporated into PG or being metabolized to D-glu to build PG. When we determined that overexpression of mutant GltS supported growth of a D-glu auxotroph in unsupplemented LBS however (**Figure 3.2B**), we instead speculated that, contrary to our prior assumptions, the components of rich media contained low amounts of D-glu that are sufficient to support growth when

glutamate transport is increased. Preliminary results support this possibility, as we found about 1.5 μM D-glu in unsupplemented LBS (**Table 3.2**), which is enough D-glu to support growth of the D-glu auxotroph expressing either GltS mutant in chemically defined FMM (**Figure 3.2B**). Moreover, based on estimates of 3.5-million PG monomers per cell in *E. coli* (263), even this low concentration of D-glu is theoretically enough to achieve a turbid culture of more than 10^8 cells per mL.

We now hypothesize that our *gltS* mutants, and their amplification, were enriched under selective pressure to access small amounts of D-glu. The small but significant amount of D-glu in LBS may be due to spontaneous racemization of L-glu within the medium, which could be catalyzed by the high-heat treatment of autoclaving (264-266). Additionally, our stock solution of D-gln appears to contain enough D-glu that, when added into LBS, sufficient D-glu is added for the original suppressor mutants to grow, even with mutant *gltS* alleles in single copy, though the concentration is much too low to sustain growth of the D-glu auxotroph (**Figure 3.1B** and **Table 3.2**). Spontaneous deamidation of glutamine has been previously studied (267-272), finding that glutamine is relatively unstable, degrading to ammonia and glutamate. Though these studies have mainly focused on the L-form, it seems likely that similar reactions could occur with D-gln at standard lab conditions. This would account for both lower-than-expected amount of D-gln and the relative concentration of D-glu in our D-gln stock. More samples will be analyzed to look further into this phenomenon. If our data are correct, LBS, and thereby LB and other rich complex media, contain trace amounts of some DAAs, including D-glu. This knowledge could lend itself to selecting for strains or proteins with increased capacity to transport DAAs.

An important drawback to the increased efficiency of mutant GltS proteins in both *V. fischeri* and *E. coli* is the increased sensitivity to toxic glutamate analogs, such as homocysteic acid (HCA) (**Figure 3.3**) and even D-glu itself (239-241, 257, 273, 274). HCA inhibits bacterial growth by competitively binding to MurD (275), the enzyme that adds D-glu to the growing PG peptide (53). D-glu was found to inhibit enzymes of ammonia assimilation of *Bacillus megaterium*, leading to altered growth phenotypes (273, 274). These data illustrate a fitness trade-off: although the strains can scavenge trace amounts of D-glu from their surroundings to build wild-type PG, they become more sensitive to toxic HCA. This adds appeal to the use of glutamate analogs as antimicrobial drugs against bacteria with sufficient glutamate transport activity.

An important yet unresolved finding in this project is the PG structure: preliminary data show that RMJ13 expressing *gltS*^{C490T} has a subset of PG peptides with lysine in the fifth amino acid position. Based upon its specificity for glutamate homologs, we do not believe that GltS itself is responsible for this variation. Following an assumption that the PG specifically contains the D-form, we hypothesize that lysine is added to the mature periplasmic PG peptides due to the activity of BsrF. The most well-characterized homologue of BsrF is *V. cholerae*'s BsrV, which is regulated by the alternative sigma factor RpoS, a stress-associated regulator (78). In *V. cholerae*, it is speculated that BsrV produces non-canonical DAAs for addition to mature PG as a way to promote resistance to various environmental threats and stressors. In the current study, BsrF may be producing D-lys in the periplasm, which subsequently is added to mature peptides to combat cell wall stress induced by dwindling D-glu supplies.

Despite its altered PG peptides, RMJ13 expressing *gltS*^{C490T} is able to colonize *E. scolopes* to the same level as the wild type, so long as there is D-glu in the seawater (**Figure 3.6**). In this context, the expression of *gltS*^{C490T} does not provide any apparent advantages over the empty vector. As seen in **Figure 3.7**, cells lyse within 4 hours of D-glu removal, due to insufficient PG biosynthesis. More work can be done to elucidate whether the altered PG peptide itself has any effect on squid colonization. As shown in **Figure 3.4**, only a small subset of the PG has this extra lysine, while a majority has the wild-type structure, so the wild-type PG signal the squid receives is still present and presumably predominant. The best way to observe specific effects of the altered peptide would be to isolate the altered-monomer peak from HPLC or LC-MS experiments and inoculate juveniles directly with the molecule. Such experiments would inform our understanding of the structure-function relationship between PG and symbiotic signaling.

MATERIALS AND METHODS

Bacterial strains and culture conditions. The strains used in this study are listed in **Table 3.3**. When added to LB medium (221) for selection of *E. coli*, chloramphenicol (Cm) and kanamycin (Km) were used at concentrations of 20 and 40 µg/mL, respectively. When added to LBS for selection of *V. fischeri*, Cm and Em were used at concentrations of 2 and 5 µg/mL respectively. Agar was added to a final concentration of 1.5% for solid media. Tryptone broth solution (TBS) (20 mM Tris-hydrochloride (Tris) (pH 7.5), 10 g/L tryptone, and 20 g/L NaCl) and yeast extract broth solution (YEBS) (20 mM Tris (pH 7.5), 5 g/L yeast extract, and 20 g/L NaCl) were autoclaved before use.

Stock solutions of D-glu (99+% powder, Sigma Aldrich, St. Louis, MO) and D-gln (99+% powder, Thermo Fisher Scientific Inc, Waltham, MA) were prepared at a concentration of 40 mg/mL in DI-water. HCl was added to 250 mM to dissolve D-glu. D-gln was incubated at 37°C shaking until completely dissolved. Stock solutions were filter-sterilized with VWR sterile syringe filters (25 mm 0.22 µm; VWR, Radnor, PA) attached to BD Luer-Lok tip syringes (Becton, Dickinson and Company, Franklin Lakes, NJ), and were stored at room temperature. Homocysteic acid was dissolved in water to create a stock solution of 250 mM (45.8 mg/mL), filter sterilized, and stored at 4°C.

Table 3.3. Strains used in this study.

Strain	Genotype	Source
E. coli		
DH5α	φ80d*lacZ*ΔM15 Δ(*lacZYA-argF*)U169 *deoR supE44 hsdR17 recA1 endA1 gyrA96 thi-1 relA1*	(223)
DH5α*λpir*	DH5α lysogenized with λpir	(216)
CC118*λpir*	Δ**(***ara-leu***)** *araD* Δ*lac74 galE galK phoA20 thi-1 rpsE rpsB argE*(Am) *recA λpir*	(222)
V. fischeri		
AKD100	ES114 with a miniTn*7*-Em	(224)
ES114	Wild type isolate from *E. scolopes*	(5)
RMJ13	*murI*::miniTn*5*-Em Δ*racD*	(87)
RMJ13.M1	*murI*::miniTn*5*-Em Δ*racD* *gltS*^{C1099G}	This study
RMJ13.M2	*murI*::miniTn*5*-Em Δ*racD* *gltS*^{C490T} *gacS*^{G644C}	This study
RMJ13.M3	*murI*::miniTn*5*-Em Δ*racD* *gltS*^{C1092T}; new duplication junction including VF_A0495 to VF_A0526 [ACTTAACTTGAT::GATGTTGTTTTA]	This study
RMJ13.M3.1	*murI*::miniTn*5*-Em Δ*racD* *gltS*^{C1092T} VF_2147^{G778A} amplification junction including VF_A0495 to VF_A0526 [ACTTAACTTGAT::GATGTTGTTTTA]	This study
RMJ13.M4	*murI*::miniTn*5*-Em Δ*racD* *gltS*^{C490T} *gacS*^{G644C}	This study
RMJ13.M5	*murI*::miniTn*5*-Em Δ*racD* *gltS*^{C1139G}	This study
RMJ13.M6	*murI*::miniTn*5*-Em Δ*racD* *gltS*^{C1099G} VF_0648^{A699G}	This study
RMJ13.M8	*murI*::miniTn*5*-Em Δ*racD* *gltS*^{C490T} new duplication junction including VF_A0498 to VF_A0571 [TGTGCTGATAAA::AGGTGAAAAGGG]	This study

[a] Drug resistance abbreviation used: Em, erythromycin resistance

Table 3.4 Plasmids and oligonucleotides used in this study

Plasmid [a]	Relevant Characteristics	Source
pCR-Blunt II-TOPO	*oriV*$_{ColE1}$, *kanR*	Thermo Fisher
pEVS104	Conjugative helper plasmid; *oriV*$_{R6K}$ *oriT*$_{RP4}$ *kanR*	(222)
pMNC11	*gltS* from ES114 cloned into pCR-Blunt II-TOPO	This study
pMNC12	*gltS* from RMJ13.M3 cloned into pCR-Blunt II-TOPO	This study
pMNC13	*gltS* from RMJ13.M2 cloned into pCR-Blunt II-TOPO	This study
pMNC15	*gltS* from ES114 cloned into pVSV105	This study
pMNC16	*gltS* from RMJ13.M3 cloned into pVSV105	This study
pMNC17	*gltS* from RMJ13.M2 cloned into pVSV105	This study
pVSV105	*oriV*$_{R6K}$, *oriV*$_{pES213}$, *oriT*$_{RP4}$, *cmR*, *lacZα*	(21)

Primer *	Sequence	Source
MNC28	CAT CCT AGG ACT AGT GAT ATT TCA ACT TAG GAG TAC TAT G	This study
MNC29	CAT CCT AGG TAT GAG AGG TAG GGC TTT TTT CTT A	This study

[a] Alleles cloned in this study are from *V. fischeri* strain ES114. Replication origins (*oriV*) on each vector are listed as RR6Kγ, ColE1, and/or pES213. Plasmids based on pES213 are stable in *V. fischeri* and do not require antibiotic selection for maintenance (21).
* Oligonucleotides are shown in the 5'-to-3' direction. Underlined regions are restriction-enzyme recognition sites.

Plasmid construction. Plasmids used in this study are listed in **Table 3.4**. Plasmids were generated in *E. coli,* then conjugated into *V. fischeri* using helper plasmid pEVS104 in strain CC118*λpir* (222). Complementation plasmids pMNC15, pMNC16, and pMNC17 were produced by PCR amplifying *gltS* from ES114, RMJ13M3.1, and RMJ13M2, respectively, using primers MNC28 and MNC29. These PCR products were then cloned into pCR-Blunt II TOPO (Thermo Fisher Scientific Inc), yielding pMNC11, pMNC12, and pMNC13 respectively. These plasmids were then digested with AvrII, and the *gltS*-containing fragments were ligated into XbaI-cut pVSV105 , producing pMNC15, pMNC16, and pMNC17, respectively.

Molecular genetics and sequence analysis. Oligonucleotides used for PCR and cloning are listed in **Table 3.4**, and were synthesized by Integrated DNA Technologies (Coraville, IA). DNA ligase and restriction enzymes were purchased from New England Biolabs (Beverly, MA). PCR was conducted with Phusion DNA polymerase, (New England Biolabs). Plasmids used for cloning were prepared with the ZymoPURE Plasmid Miniprep kit (Zymo Research, Irvine, CA). DNA was cleaned after PCR and between cloning steps using the DNA Clean & Concentrator kit from Zymo Research. Cloned plasmids were Sanger sequenced at the University of Illinois-Chicago Genome Research Core facility and analyzed via Geneious Prime version 2019.0.4. Genomic DNA from *V. fischeri* strains was extracted using the Invitrogen PureLink™ Genomic DNA Mini Kit (Thermo Fisher Scientific Inc). For whole-genome sequencing, DNA was sonicated to approximately 500-bp fragments, then DNA libraries were prepared using the NAGNext Ultra II DNA library prep kit for Illumina (New England Biolabs), including end-repair, adaptor ligation, and addition of index primers. Libraries were sequenced at the University of Georgia Genomics and Bioinformatics Core (Athens, GA). All sequences were analyzed via Geneious Prime with default settings, compared to *V. fischeri* wild-type strain ES114. Paired-end reads were mapped to the reference, then single-nucleotide polymorphisms were identified with a minimum variant frequency of 0.8.

***In silico* analyses.** Protein similarity scores of GltS from *V. fischeri* and *E. coli* were analyzed via NCBI services (National Center for Biotechnology Information (NCBI)[Internet]. Bethesda (MD): National Library of Medicine (US), National Center for

Biotechnology Information; [2023] – [cited 2017 Apr 06]. Available from: https://www.ncbi.nlm.nih.gov/) and SnapGene® software (from Dotmatics; available at snapgene.com).

Selection of spontaneous mutants of D-glu auxotrophy. Strain RMJ13 was grown in LBS-Em containing 400 µg/mL D-glu, to an OD_{600} of 1. 100 µL of culture were plated to LBS-Em supplemented with 400 µg/mL D-gln. Cultures were plated in parallel on D-glu plates to determine mutation frequency. Plates were incubated at 28°C, and colonies counted at 24 and 48 hours. Colonies were streak purified on media containing Em and D-gln, then stocked in LBS with 20% glycerol and stored at -80°C.

Analysis of amino acid content in media and amino acid solutions. Media samples and amino acid stock solutions were analyzed at the University of Illinois Chicago Mass Spectrometry Core. Amino acids were diluted into 4 mg/mL working solutions, and along with samples of LBS, TBS, and YEBS, were filter sterilized with VWR sterile syringe filters (25 mm 0.22 µm; VWR) attached to BD Luer-Lok tip syringes (Becton, Dickinson and Company) before submission. Three 1-mL samples of each solution were submitted to the Mass Spectrometry Core in the Research Resources Center of the University of Illinois Chicago for analysis of L-/D-glu and L-/D-gln concentrations. LCMS-grade analytes were purchased from Sigma-Aldrich (Burlington, MA), and dissolved in water to get stock solutions of 1 mg/mL. They were diluted in LCMS-grade 50% MeOH in water to create spiking standards to prepare standard curves. Stable Isotope Labeled Amino Acid Mix Solution (Millipore Sigma, Burlington, MA) was diluted

with 50% MeOH to create a 1 µg/mL working solution, used as the internal standard. Solid phase extraction was done using Oasis MCX Cartridge. LC-MS analyses were performed on an AB SCIEX 6500 QTRAP coupled with Agilent 1290 UPLC system, with an Agilent Poroshell 120 Chiral-T, 2.7 µm, 2.1 x 100 mm column. Data analysis was conducted by Sciex MultiQant software (Version 3.0.3, AB Sciex Pte, Ltd., Birmingham, MA).

PG isolation of intact PG sacculi. Cells were grown overnight in LBS with any necessary antibiotics and amino acids, chilled on ice for 10 minutes, and centrifuged at 4°C and 17,600 x *g* for 15 minutes. In response to precipitation at later steps, pellets of *gltS* mutant strains, and strains carrying pMNC16 or pMNC17 were washed by resuspension in 400 mL of 1 M NaCl and centrifuged as above. Pellets were resuspended in 10 mL cold water, then dripped into 50 mL of boiling 4% SDS. Solution was then boiled for 30 minutes with continuous stirring, then allowed to cool to room temperature. Samples were then centrifuged at 120,000 x *g* for 60 minutes, resuspended in room temperature water and washed three to four more times as above. Before resuspension, the supernatant was assayed for SDS using methylene blue and chloroform (227), and centrifuged as above until no SDS was detected in the supernatant. When SDS was undetectable, the pellet was resuspended in 1 mL of water, with Tris-HCl (pH 7.5) added to a final concentration of 100 mM and $MgSO_4$ added to a concentration of 20 mM, then treated with 10 µg DNase I and 50 µg RNase A for 2 hours at 37°C. Samples were then treated with 100 µg of Trypsin, $CaCl_2$ was added to a final concentration of 10 mM and incubated overnight at 37°C. Samples

were then centrifuged at 15,880 x *g* for 10 minutes and pellets resuspended in 1% SDS. The solution incubated in a 95°C hot water bath for 20 minutes, diluted into with warm water, and then centrifuged at 120,000 x *g* for 60 minutes at room temperature. The pellet was then washed with warm water and spun as above, until SDS-free. Pellet resuspended in 1 mL water and was stored at -80°C until analysis, or further processed as below.

PG processing for amino acid and muropeptide analysis. Intact PG sacculi were resuspended in 12.5 mM $NaPO_4$ (pH 5.5) and digested with 125 units of Mutanolysin overnight at 37°C. Insoluble material was then removed from the samples by centrifugation at 15,880 x *g* for 15 minutes at room temperature. The supernatant containing muropeptides was transferred to a new tube, lyophilized until dry, then stored at -20°C until analysis. Amino acid (228) and muropeptide analyses (229) were performed using HPLC as previously described. Peaks from these analyses can then be run through LC-MS to further characterize the muropeptide structure.

LC-MS analysis of PG samples and data analytics. Muropeptide and sacculi structural analyses were performed on a Shimadzu LCMS9030 QToF instrument interface with a LC-40B X3 UPLC, a SIL-40C X3 autosampler (10°C) and a CTO-40C column oven (40°C). Gradient separations utilized a BEH C18 column (2.1 mm × 50 mm, 1.7-µm particle size; Waters) with solvent A (0.1% formic acid in water) and solvent B (0.1% formic acid in MeOH) at a constant flow rate of 0.4 ml min^{-1}. Experiments were performed and analyzed as previously described (276).

Squid colonization assay. *V. fischeri* ES114 was cultured overnight at 28°C in LBS medium, and RMJ13 strains carrying pVSV105 or pMNC17 were grown in LBS with 50 µg/mL of D-glu, 5 µg/mL Em for retention of the mini-Tn*5* and 2 µg/mL chloramphenicol for plasmid retention. Overnight cultures were diluted 100-fold into Seawater Tryptone (SWT) liquid medium with D-glu and antibiotics as necessary and allowed to grow until mid-exponential phase at 28°C, then diluted to a final inoculum concentration of ~5000 CFU/mL in 100 mL of filter-sterilized ocean water (FSW). Inoculum of RMJ13 carrying pVSV105 was supplemented with 5 µg/mL D-glu, while inoculum was RMJ13 carrying pMNC17 received 1 µg/mL D-glu (strains were given different concentrations based on their needs for growth). Newly hatched *E. scolopes* were introduced into this mixture and inoculated overnight under a 12/12 day-night cycle. After about 16 hours, squid were transferred into individual vials: ES114-inoculated squid into FSW; half of each RMJ13 strain was transferred into FSW, and the other half into FSW with D-glu. At 24 hours post-inoculation and every 24 hours following, luminescence was measured using a TD 20/20 luminometer (Turner Designs, Sunnyvale, CA), after which the squid were either transferred to fresh FSW with D-glu as needed, or frozen at -80°C in 700 µL of FSW until ready for use. Most squid were individually homogenized, then dilution plated to LBS agar medium, and the number of CFU/mL was determined.

Microscopy of D-glu auxotrophic bacteria. RMJ13 carrying the empty vector (pVSV105) or *gltS*^{C490T} (pMNC17) were initially grown in LBS containing Em and Cm, and the RMJ13 carrying pVSV105 was supplemented with 50 µg/mL D-glu. When cultures reached an OD_{600} of ~0.6, cells were harvested by centrifugation at 7000 x *g* for

one minute at room temperature, washed with FSW, and then resuspended in FSW without D-glu supplementation. Every hour, aliquots were taken from the cultures, and fixed with ice-cold 70% ethanol in water, then incubated on ice for one hour. Cells were centrifuged at 10,000 x *g* at room temperature for one minute, then resuspended in FSW. A 1.5% agarose pad was made in FSW with SeaKem LE agarose (Lonza Biosciences, Morristown, NJ). 1 µL aliquot of cell sample was loaded onto a coverslip, and the agarose pad placed on top. Images were captured by an inverted Zeiss LSM 980 microscope equipped with a Plan Apochromat 1.4NA 100x oil Phase 3 objective at the Caltech Biological Imaging Facility. Images were processed and visualized in ImageJ.

ACKNOWLEDGEMENTS

This research was supported by NSF grant IOS-1557964 awarded to EVS and DLP. We thank the Mass Spectrometry Core in the Research Resources Center of the University of Illinois Chicago for doing small molecule analysis, and the Caltech Biological Imaging center where we performed the microscopy imaging.

CHAPTER 4

TRANSIENT INFECTION OF *EUPRYMNA SCOLOPES* WITH AN ENGINEERED D-ALANINE AUXOTROPH OF *VIBRIO FISCHERI* [3]

[3] Macey N. Coppinger†, Liu Yang†, Kathrin Laramore, David L. Popham, Edward G. Ruby, and Eric V. Stabb. For submission to *Applied and Environmental Microbiology*

† these authors contributed equally

ABSTRACT

The symbiosis between *Vibrio fischeri* and the Hawaiian bobtail squid, *E. scolopes*, is a tractable and well-studied model of bacteria-animal mutualism. Here, we developed a method to transiently colonize *E. scolopes* using a D-ala auxotroph, controlling the persistence of viable infection by supplying or withholding D-ala. We generated alanine racemase (*alr*) mutants of *V. fischeri* that lack avenues for suppression and reversion to prototrophy. To prevent reversion of an *alr*::mini-Tn*5* allele, we generated an unmarked *alr* deletion. The Δ*alr* mutant surprisingly did not require D-ala to grow in minimal medium, a phenomenon requiring *metC*. Likewise, overexpression of *metC* suppresses D-ala auxotrophy in rich medium. To block potential mechanisms of suppression, we combined the Δ*alr* mutation with deletions of *metC* and/or *bsrF*, which encodes a broad-spectrum racemase, and investigated the suppression rates of four D-ala auxotrophic strains. We then focused on Δ*alr* Δ*bsrF* mutant MC13, which has a suppression rate of $<10^{-9}$. When D-ala was removed from a log phase culture of MC13, cells rounded and lysed within forty minutes. Transient colonization of *E. scolopes* was achieved by inoculating squid in seawater containing MC13 and D-ala, and then transferring the squid into water lacking D-ala, which resulted in complete loss of viable symbionts within hours. Interestingly, the number and morphology of MC13 cells in crypt 3 of the light organ differed from that of the other crypts. Our study highlights a new approach for inducing transient colonization and provides insight into the biogeography of the *E. scolopes* light organ.

IMPORTANCE

The importance of this study is multi-faceted, providing a valuable methodological tool and insight into the biology governing the symbiosis between *Vibrio fischeri* and *Euprymna scolopes*. First, the study sheds light on the critical role of D-ala for bacterial growth, and the underpinnings of D-ala synthesis. Our observations that *metC* obviates the need for D-ala supplementation of an *alr* mutant in minimal medium and MetC-dependent growth correlates with D-ala in PG corroborate and extend previous findings in *Escherichia coli* regarding the role of MetC in D-ala provisioning. Our isolation of robust D-ala auxotrophs led us to a novel method for studying the squid-*Vibrio* symbiosis, allowing for transient colonization without the use of antibiotics, and revealed intriguing differences in the growth parameters in distinct light organ crypts. This work and the methodology developed will contribute to our understanding of the persistence and dynamics of *V. fischeri* within its host.

INTRODUCTION

The light organ symbiosis between *V. fischeri* and the Hawaiian bobtail squid, *E. scolopes* has been a useful model for understanding the initiation and persistence of beneficial bacterial infections (30, 173-175). *E. scolopes* hatchlings are aposymbiotic, but rapidly acquire *V. fischeri* from their environment (4). *V. fischeri* symbionts live within a specialized bilobed light organ of *E. scolopes*, where they grow and bioluminesce (2, 7, 8). The animal is thought to use the bioluminescence in a counter-illuminating behavior (277, 278) for nocturnal camouflage. As they are inactive during the day, a large portion of the symbionts are vented from the light organ each dawn, thus

increasing *V. fischeri* populations in the environment (279). The light organ is ventral to the ink sac, and is external, constantly in contact with the surrounding seawater (2, 6, 7). Each lobe of the hatchling light organ has a pair of ciliated epithelial appendages (CEAs) that serves to promote infection with *V. fischeri* (280). At the base of each pair of CEAs are three pores, each of which leads to a duct, antechamber, and epithelium-lined crypt. The three crypts are anatomically distinct, with crypt one maturing earliest, and crypt three the latest. Additionally, symbionts of crypt three appear to have slower growth-rates, are less likely to be vented, and do not interact in the same ways with epithelial cells as do the bacteria in crypts one and two (9, 21, 281-283).

In many symbioses, studies that initiate and terminate infections have been useful for understanding host-symbiont dynamics, and for determining whether host responses to infection are reversible. Transient colonization of *E. scolopes* by *V. fischeri* has previously been accomplished by curing infected animals with antibiotics. Chloramphenicol (Cm) was the first used to clear infection early in the symbiosis (284, 285). However, Cm alone proved insufficient for curing a fully established infection, which was achieved by using a combination of Cm and gentamicin (Gm) (49). These studies showed that some developmental programs within *E. scolopes*, including symbiont-induced regression of CEAs, are irreversibly triggered by transient infection (284), while others, like the behavior of host macrophage-like cells, require persistent presence of *V. fischeri* (49).

While using antibiotics to cure infections has proven useful, it may have drawbacks. Antibiotics must diffuse into host tissues, potentially causing a concentration gradient and uneven exposure. Especially with high drug concentrations, host tissues

themselves can be affected by antibiotics, though this has not yet been observed with the Cm and Gm most often used in *V. fischeri-E. scolopes* symbiosis. Perhaps most importantly, broad-spectrum antibiotics, such as Cm and Gm may also have off-target effects on bacterial symbionts in other organs, such as the gut or accessory nidamental gland (ANG) (286-288). For example, treatment of *E. scolopes* eggs with Cm resulted in fungal infections, presumably by interfering with the bacterial communities transferred to eggs from the ANG, underscoring the possibility of undesirable side effects (286).

An alternative and complementary approach to using antibiotics to generate transient infections is to colonize animals with bacterial mutants that require metabolic supplementation, then subsequently remove the necessary supplement. For example, bacteria that are auxotrophic for D-ala, D-glu, and meso-diaminopimelic acid (DAP) colonized hosts while being supplemented with these compounds but were cured from the host when these amino acids were no longer provided (235, 289-291). These three amino acids are specific components of the bacterial PG, and are not typically found in animals, making it unlikely that hosts could support growth of auxotrophic strains without external supplementation. However, some auxotrophs can give rise to suppressor mutants that have developed alternative pathways to PG biosynthesis, so mutation of multiple genes or pathways may be required to generate robust auxotrophy (289, 290). These studies led to the goal of developing D-ala auxotrophy of *V. fischeri* to accomplish transient colonization within the *E. scolopes* light organ.

Previously, we reported that an *alr*::mini-Tn*5*-erm mutant was auxotrophic and unable to colonize *E. scolopes* without D-ala supplementation (182). However, we recently discovered that, despite lack of an encoded transposase gene, this mini-

transposon can precisely delete from a *murI* disruption, leading to reversion to the wild-type allele (Chapter 2). We also discovered that exceptionally rare mutations of the gene encoding BsrF, a broad-spectrum racemase, could compensate for lack of Alr (Chapter 2). In this study, we sought to determine whether D-ala auxotrophic strains of *V. fischeri* could be generated that would not give rise to revertants or suppressors, whether such strains could be used to transiently colonize *E. scolopes*, and if so, what could be learned about the symbiosis from such transient colonization.

RESULTS

To prevent reversion in the *alr*::mini-Tn*5*-erm mutant by precise deletion of the transposon, we generated a Δ*alr* mutant (MC6). This Δ*alr* mutant is auxotrophic for D-ala in LBS medium (**Figure 4.1**). Surprisingly, we discovered that the Δ*alr* mutant could grow in a defined minimal medium without D-ala supplementation (**Figure 4.2A**). Kang et al. (292) previously showed that upregulation of *metC*, which encodes cystathionine-β-lyase and contributes to L-met biosynthesis, could restore prototrophic growth to a D-ala auxotrophic *alr dadX* mutant in *E. coli*. We similarly found that expression of *metC* from a multicopy plasmid in *V. fischeri* can compensate for loss of *alr*, enabling growth on unsupplemented LBS (**Figure 4.2B**). Moreover, growth of the Δ*alr* strain in defined minimal medium without D-ala is dependent on *metC* (**Figure 4.2A**). Although deletion of *metC* also creates L-met auxotrophy in this minimal medium, we observed that addition of L-met to the growth medium of strains with intact *metC* abolishes growth without D-ala supplementation (**Figure 4.2A**). This pattern was also noted in *E. coli*, in which the *met* operon is known to be repressed by the presence of L-met (292). We

hypothesize that, as in *E. coli*, MetC is available to racemize alanine while L-met levels are low, but *metC* is repressed when the cell has sufficient L-met, such as during growth in rich media like LBS (**Figure 4.3**).

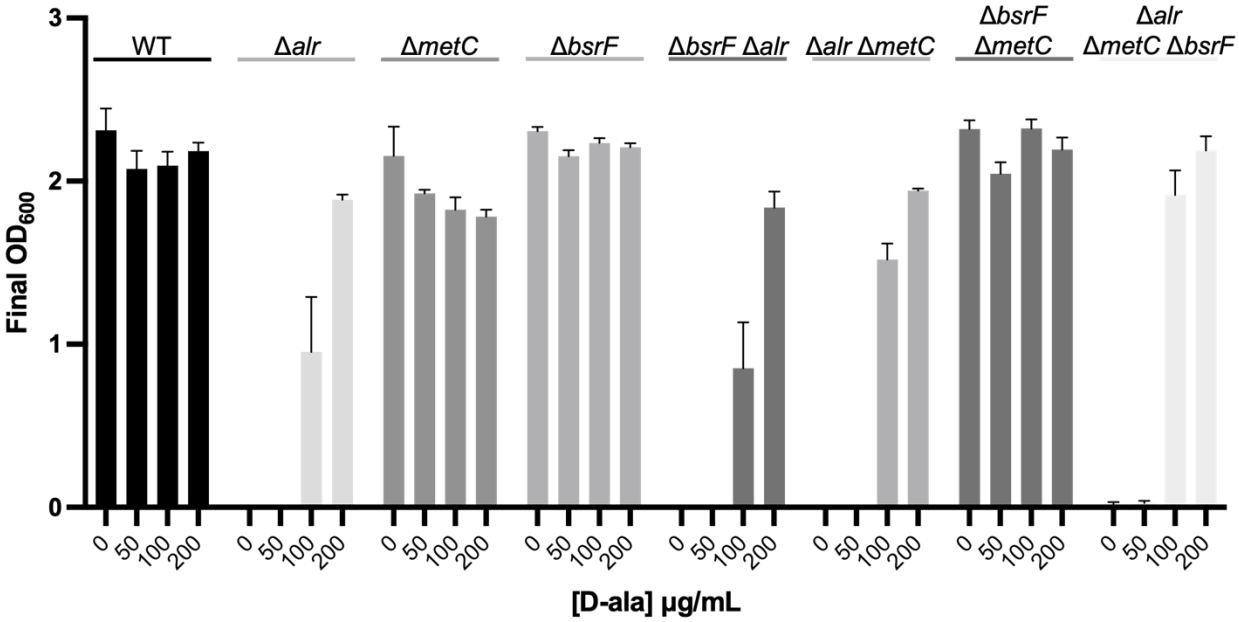

Figure 4.1: Generation and recovery of D-ala auxotrophy. Shown are final OD_{600} readings for *V. fischeri* cultures grown in LBS. Cultures were grown for 24 hours before reading final OD_{600}. Error bars indicate standard error of the mean (n=4). Data from one representative experiment of at least three is shown. From left to right, strains included are ES114, MC6, MC5, KL3, MC13, MC24, MC12, and MC27)

Much like over-expressing *metC*, removing the putative secretion signal of BsrF can compensate for the loss of Alr, obviating the need for D-ala supplementation in LBS (Chapter 2). Therefore, to block known possible avenues to D-ala synthesis, we deleted *alr*, *metC*, and *bsrF* singly and in each possible combination (**Table 4.1**). The four Δ*alr* mutants MC6 (Δ*alr*), MC13 (Δ*alr* Δ*bsrF*), MC24 (Δ*alr* Δ*metC*), and MC27 (Δ*alr* Δ*metC* Δ*bsrF*), require exogenous D-ala to grow in LBS broth (**Figure 4.1**). All D-ala

auxotrophs, regardless of additional mutations beyond deletion of *alr*, required the same concentration of exogenous D-ala, 100 µg/mL, to restore growth in LBS (**Figure 4.1**).

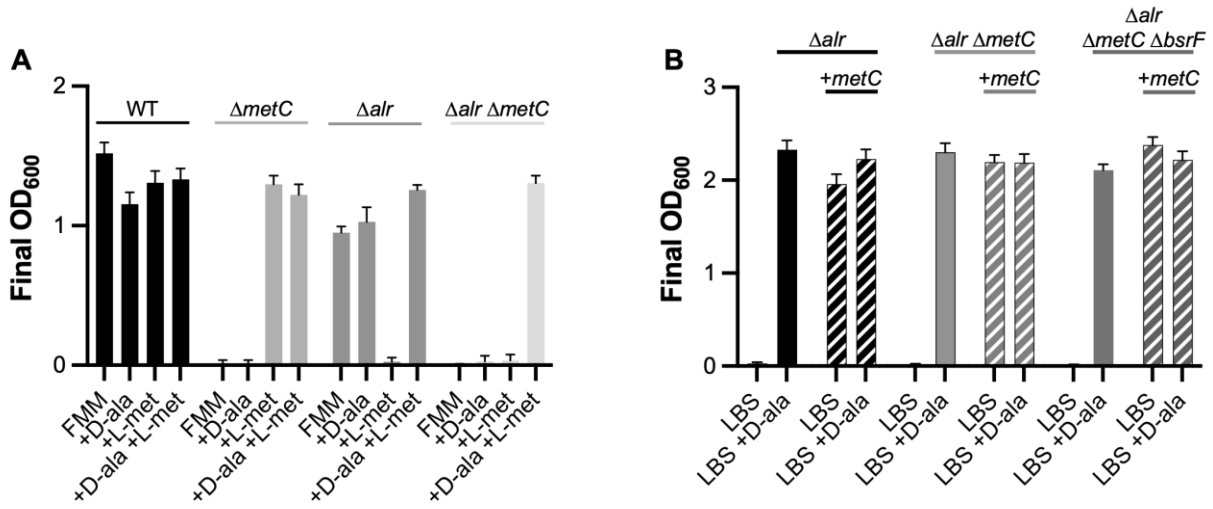

Figure 4.2: Expression of *metC* in an *alr* mutant can enable growth without D-ala. (**A**) Intact *metC* in an *alr* mutant enables growth in FMM without D-ala supplementation. (**B**) *alr* mutants can be rescued from D-ala auxotrophy in LBS by expression of *metC* on the multicopy plasmid pMNC6. L-met was added to 50 µg/mL in FMM. D-ala was supplemented at 50 µg/mL in FMM or 200 µg/mL in LBS. Strains include ES114 (WT), MC5 (Δ*metC*), MC6 (Δ*alr*), MC24 (Δ*alr* Δ*metC*), and MC27 (Δ*alr* Δ*metC* Δ*bsrF*). Strains were grown for 24 hours at 28°C shaking before reading final OD_{600}. Error bars indicate standard error of the mean (n=3). Data from one representative experiment of three is shown.

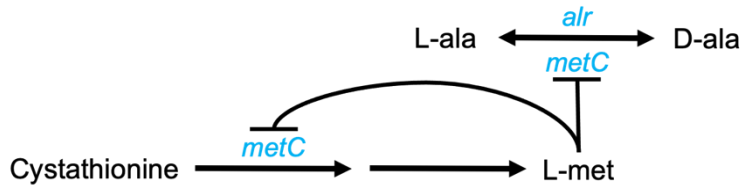

Figure 4.3: MetC is involved in L-met and D-ala synthesis. When derepressed, MetC is available to produce D-ala. Part of the *met* operon, production of MetC is repressed by sufficient levels of L-met in the cell. Genes (shown in blue) encode the proteins involved in these pathways.

While alanine is MetC's preferred substrate for racemization, MetC of *E. coli* can racemize other amino acids as well, including serine and aminobutyrate (157). To test whether MetC in this case was indeed restoring growth by producing the D-ala that is incorporated into PG, we analyzed PG amino acid content of the wild type (ES114) and the D-ala auxotroph MC27 (Δ*alr* Δ*metC* *bsrF*) expressing *metC* from a multicopy plasmid. Both samples have the expected Ala:DAP:Glu ratio of 2:1:1 that is typical in Gram-negative sacculi (data not shown), and they have identical HPLC chromatograms (**Figure 4.4**), further supporting the hypothesis that MetC is racemizing alanine to provide the D-ala needed for PG synthesis.

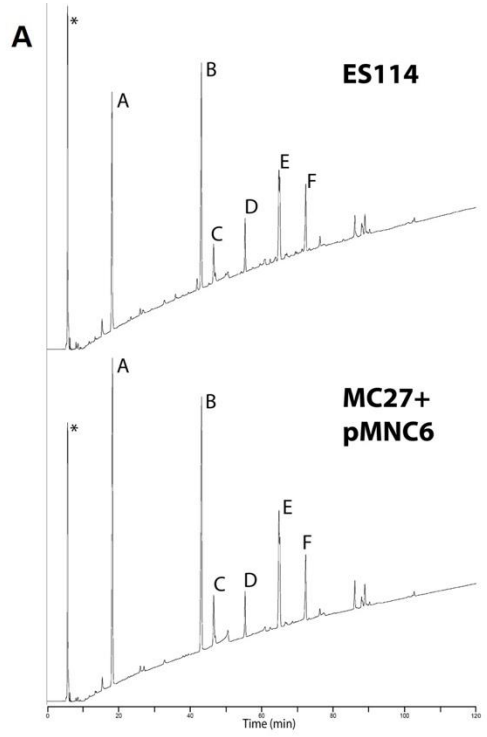

B

Peak	Structure
*	Buffer component
A	DS-TP (Disaccharide tetrapeptide)
B	DS-TP-TP-DS (crosslinked disaccharide-tetrapeptide dimer)
C	anhydroDS-TP (disaccharide tetrapeptide with anhydroNAM)
D	DS-TP-TP-DS-(TP-DS) (crosslinked disaccharide-tetrapeptide trimer)
E	anhydroDS-TP-TP-DS (Crosslinked disaccharide-tetrapeptide dimer with anhydroNAM)
F	Unknown, predicted disaccharide-tetrapeptide trimer with anhydroNAM

Figure 4.4: Expression of *metC* leads to wild-type PG structure. (**A**) HPLC chromatograms of the wild-type parent (ES114; top) and a D-ala auxotroph overexpressing *metC* (bottom; MC27 + pMNC6). ES114 was grown in LBS, while MC27 with pMNC6 was grown in LBS-Cm. (**B**) Identification of labeled peaks in **Figure 4.3A**. * indicates a buffer component peak, while lettered peaks correspond to PG fragments.

Table 4.1. Strains used in this study

Strain	Genotype	Source
E. coli		
DH5α	φ80d*lacZ*ΔM15 Δ(*lacZYA-argF*)U169 *deoR supE44 hsdR17 recA1 endA1 gyrA96 thi-1 relA1*	(223)
DH5α*λpir*	DH5α lysogenized with λpir	(216)
CC118*λpir*	Δ**(***ara-leu***)** *araD* Δ*lac74 galE galK phoA20 thi-1 rpsE rpsB argE*(Am) *recA λpir*	(222)
V. fischeri		
AKD100	ES114 with a mini-Tn*7*-Em	(224)
ES114	Wild type isolate from *E. scolopes*	(5)
KL3	Δ*bsrF*	Chapter 2
MC2	Δ*metC*::FRT- Em^R	This study
MC3	Δ*alr*::FRT- Em^R	This study
MC5	Δ*metC*::FRT	This study
MC6	Δ*alr*::FRT	This study
MC8	Δ*bsrF* Δ*metC*::FRT- Em^R	This study
MC12	Δ*bsrF* Δ*metC*::FRT	This study
MC13	Δ*bsrF* Δ*alr*::FRT	Chapter 2
MC23	Δ*alr*::FRT Δ*metC*::FRT- Em^R	This study
MC24	Δ*alr*::FRT Δ*metC*::FRT	This study
MC26	Δ*bsrF* Δ*alr*::FRT Δ*metC*::FRT- Em^R	This study
MC27	Δ*bsrF* Δ*alr*::FRT Δ*metC*::FRT	This study

[a] Drug resistance abbreviation used: Em, erythromycin

To evaluate the possibility of D-ala prototrophy arising in suppressors of *alr* mutants during host colonization, we grew these strains in LBS containing D-ala, then spread the cultures to plates without D-ala. The cultures were plated in parallel to LBS with D-ala, to determine the number of cells plated and frequency of suppression. For the Δ*alr* mutant, MC6, ten suppressors were generated after plating about 10^{10} cells, for a suppression rate of $1x10^{-9}$ (**Table 4.2**). We hypothesized that these suppressors had mutations affecting expression of *metC* and/or secretion of *bsrF*. If so, the frequency of suppression should be lower than 10^{-9} in a Δ*alr* background also lacking *metC* or *bsrF*, so we therefore compared the suppression rate of the Δ*alr* mutant to those of mutants with additional mutations in *metC* and/or *bsrF*. For D-ala auxotrophs MC13 (Δ*alr* Δ*bsrF*), MC24 (Δ*alr* Δ*metC*), and MC27 (Δ*alr* Δ*bsrF* Δ*metC*), no prototrophic suppressor mutants

were isolated, after plating between $4.5x10^9$ and $2x10^{10}$ cells (**Table 4.2**), consistent with the possibility that suppressors of D-ala auxotrophy in the Δ*alr* mutant likely involved *metC* or *bsrF*. D-ser has been previously found in place of D-ala in some PG (35), and we considered the possibility that if D-ser were present within the squid light organ but not in LBS, it could lead to a higher frequency of suppression in the symbiosis than we had observed in culture. However, after plating > 10^9 cells of MC13 (Δ*alr* Δ*bsrF*) and MC27 (Δ*alr* Δ*bsrF* Δ*metC*) on LBS supplemented with D-ser, we also failed to isolate suppressors (**Table 4.2**). Taken together, our data indicate that for MC13, MC24, and MC27 under the conditions tested, suppression of D-ala auxotrophy appears to occur at a frequency of $<10^{-9}$. For reference, juvenile *E. scolopes* are colonized by approximately 10^5 to 10^6 *V. fischeri* cells.

Table 4.2 Selection of prototrophic suppressors of D-ala auxotrophy

D-ala suppressor generation						
	Genotype	**CFU plated LBS**	**CFU plated LBS + D-ser**	**Total CFU plated**	**Suppressors**	**Suppressors per CFU**
MC6	Δ*alr*	10^{10}	-	10^{10}	10	1×10^{-9}
MC13	Δ*alr* Δ*bsrF*	$6 * 10^9$	$3 * 10^9$	$9 * 10^9$	0	N/A
MC24	Δ*alr* Δ*metC*	$4.5 * 10^9$	-	$4.5 * 10^9$	0	N/A
MC27	Δ*alr* Δ*metC* Δ*bsrF*	10^{10}	10^{10}	$2 * 10^{10}$	0	N/A

[a] "-" indicates that cells were not plated on LBS + D-ser

As illustrated above, deleting *metC* eliminates a potential avenue to D-ala prototrophy, but it isn't clear that the Δ*metC* allele is necessary from a practical standpoint, and the added need for L-met to support growth could complicate symbiotic studies (**Figure 4.2A**). Graf and Ruby showed that a methionine auxotroph of *V. fischeri* colonized the light organ at 23% of the population-level achieved by the parent strain at 45 hours post-inoculation (293), suggesting that the host can supply the symbiont with

L-met, though perhaps in insufficient quantity to attain full colonization. Although it is possible that provisioning of L-met is spatially or temporally uneven, it seems likely that there is sufficient L-met available for initial colonists, and *metC* may not be highly expressed in this context. We observed growth of an *alr* mutant in minimal medium without D-ala supplementation, specifically in the absence of L-met (**Figure 4.2A**), likely due to repression of the *met* operon by L-met as seen in *E. coli* (292). Taken together with the fact that intact *metC* did not allow an *alr* mutant to initiate colonization of *E. scolopes* (158), we speculate that initial symbiont growth in the light organ is more like growth in LBS than our defined minimal medium, at least in respect to D-ala metabolism. We decided that the likelihood of MetC giving rise to growth without *alr* or exogenous D-ala was relatively low and proceeded to examine MC13 (Δ*alr* Δ*bsrF*) as a potential tool for initiating and then terminating squid-*Vibrio* symbiosis.

We first tested the effect of removing D-ala from pre-grown MC13 (Δ*alr* Δ*bsrF*). The synthesis of PG is essential for maintaining structural integrity and cell morphology (294), and its inhibition, as seen with the use of beta-lactam antibiotics, results in cell lysis due to accumulated internal pressure (295). We used these observations as a starting point for investigating the response of D-ala auxotrophic *V. fischeri* to a loss of exogenous D-ala. Microscopic observations revealed that depriving MC13 of D-ala led to cells assuming a more rounded form, before ultimately rupturing within a span of 40 minutes after D-ala removal (**Figure 4.5**). Such rapid cellular disruption and lethality resulting from D-ala deprivation suggested the potential utility of MC13 as a transient colonizer of *E. scolopes*.

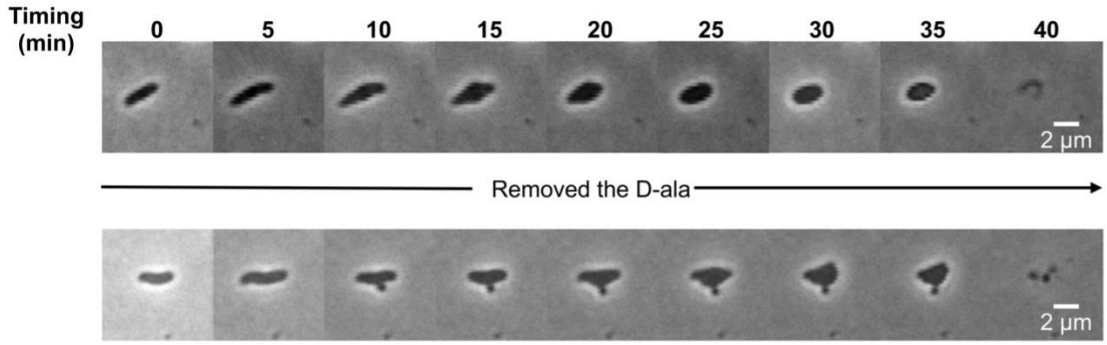

Figure 4.5: D-ala auxotrophic *V. fischeri* requires D-ala to maintain cell morphology. Displayed is a time-lapse montage depicting two MC13 (Δ*alr* Δ*bsrF*) cells undergoing morphological degradation and eventual rupture when placed on an agarose pad containing unsupplemented LBS. Images were sequentially acquired every 5 minutes over a 40-minute period**.**

We inoculated juvenile *E. scolopes* overnight with strain MC13, adding 50 µg/mL of D-ala into the FSW. After overnight inoculation, colonized squid were placed into FSW without D-ala, and maintained for an additional eight hours, to ensure thorough clearance of D-ala auxotrophic CFU within the light organ. The viability of the symbionts within the light organ crypts was evaluated by measuring both luminescence and CFUs (**Figure 4.6A**). Removal of D-ala resulted in an absence of detectable symbionts, yet confocal microscopy illuminated the ongoing presence of intact MC13 cells in crypt three (**Figure 4.6C**), even though they were not recoverable as CFU (**Figure 4.6B**). Crypt one was largely uncolonized, with the few remaining symbionts exhibiting morphological alterations. Interestingly, the symbionts in crypt three retained their typical bent-rod shape (**Figure 4.6C**). In conjunction with previous studies highlighting antibiotic resistance in crypt three symbionts, our results hint at a potential alteration in metabolic states or an as-yet unidentified interaction of nutrient metabolism with the host under nutrient-limited conditions.

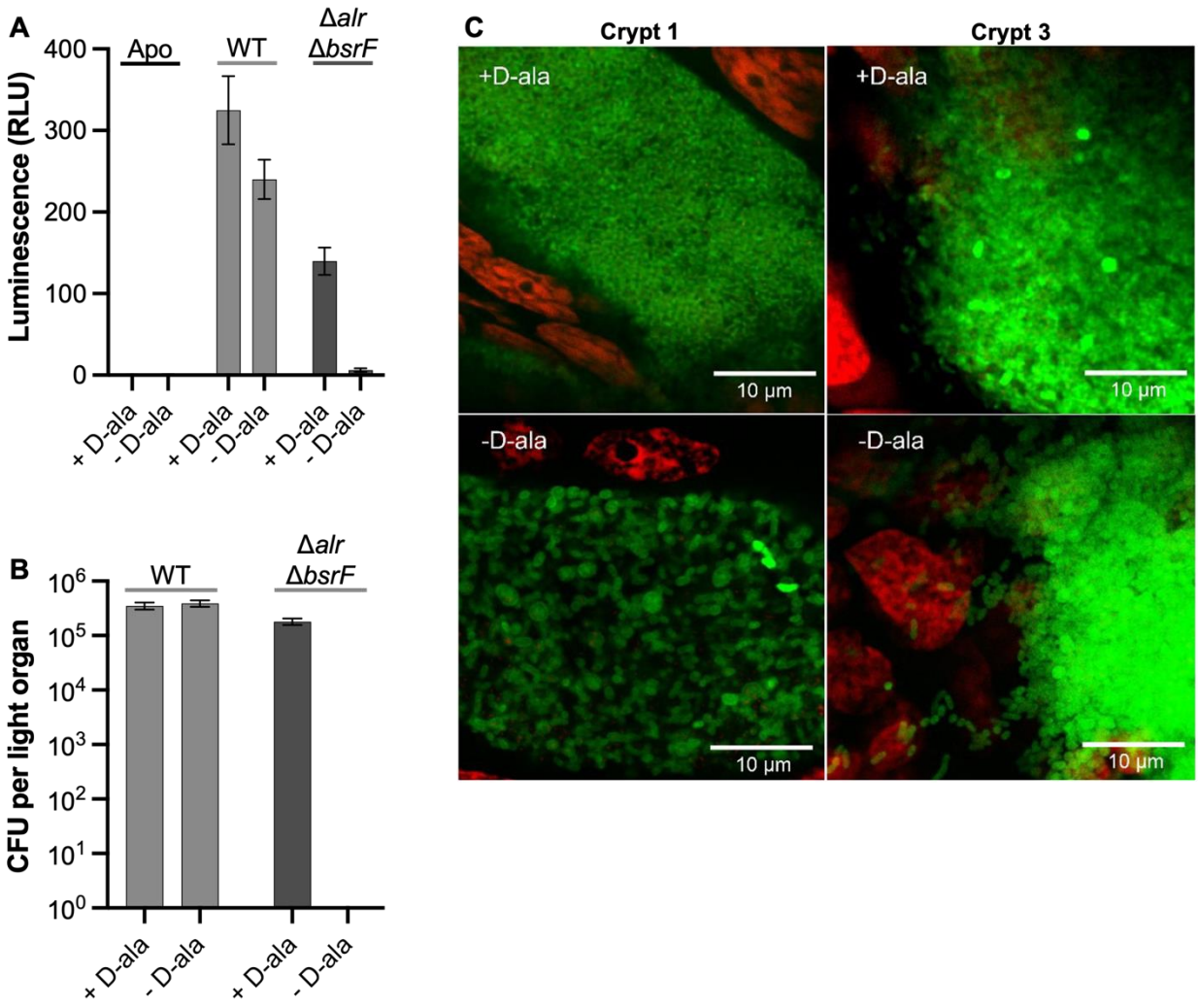

Figure 4.6: *V. fischeri* colonization of *E. scolopes* requires D-ala. **(A)** Efficiency of light organ colonization as observed by luminescence of squid 24 hours after inoculation. **(B)**. Symbiont population levels (average CFU per light organ) 24 hours post inoculation. **(C)** Representative confocal micrographs illustrate the crypts of the light organ colonized for 24 hours by GFP-labeled D-ala auxotrophic strain (carrying pVSV102) Host nuclei were stained with TO-PRO-3 (red). Strains in this this study include ES114 (wild type) and MC13 (Δ*alr* Δ*bsrF*). Error bars indicate standard error of the mean (n=16). Experiment was performed once.

DISCUSSION

PG structure is largely conserved across bacteria, due in large part to its structural stability and the DAAs that allow it to escape digestion by proteases (100). In

most Gram-negative bacteria, the stem peptide consists of L-ala, D-glu, *meso*-DAP, and D-ala (296). In contrast, Gram-positive bacteria usually have L-lys in the third position (35). Notably, the presence of D-ala at the fourth position of the PG peptide is universally conserved, emphasizing its pivotal role in bacterial cell wall synthesis, as evidenced by the present study.

Alanine racemases can produce the D-ala necessary for PG biosynthesis and are nearly ubiquitous in bacteria. In many species the primary alanine racemase, often encoded by *alr*, is considered essential for bacterial growth (158, 297-302). However, some bacteria have a secondary source of D-ala as well, which can compensate for the loss of Alr activity (299, 303, 304) Deletion of these alanine racemase-encoding genes leads to D-ala auxotrophy. A study in *E. coli* found that D-ala auxotrophy of an *alr dadX* mutant could be suppressed by overexpression of *metC*, which encodes cystathionine-β-lyase (292), although the PG structure was not analyzed and D-ala production and incorporation was assumed. Later research verified that this suppression was due to alanine racemase activity of MetC (157, 234). In our study of D-ala auxotrophy and suppression, we also sought to determine if MetC of *V. fischeri* could play a similar role. We confirmed that in *V. fischeri*, MetC can compensate for D-ala auxotrophy in defined medium (**Figure 4.2A**), and by overexpression in rich medium (**Figure 4.2B**). As in *E. coli*, this suppression appears to be due to alanine racemase activity, as evidenced by the presence of D-ala in the PG of a D-ala auxotroph overexpressing *metC*, giving it wild-type PG structure (**Figure 4.3**).

Previously, we identified BsrF, a broad-spectrum racemase that can compensate for the lack of Alr when relegated to the cytoplasmic space of *V. fischeri* (Chapter 2). To

elucidate any remaining potential avenues of D-ala production, we engineered four D-ala auxotrophs, and attempted to isolate suppressor mutants of each. Our selection approach parallels previous attempts to evolve PG biosynthesis (76, 86, 87, 190) ; (Chapter 2). Three such studies found that *m*DAP auxotrophy could be suppressed by incorporation of lanthionine at the third position of the PG peptide (76, 86, 190). Two other studies from this lab found that the aspartate racemase RacD (87) and ΔSS-BsrF (Chapter 2) could compensate for the loss of glutamate racemase activity by MurI. The latter two studies found suppressors to have wild-type PG structure, implicating the racemases as having glutamate racemase activity. Based on these previous studies, as well as the current work, it appears that D-glu and D-ala may be more difficult moieties to replace in PG than *m*DAP.

The present study provides compelling motivation for generating antibiotic drugs that target bacterial amino acid racemases, especially alanine racemases. One such drug, D-cycloserine (DCS) is currently used to treat multi-drug resistant *Mycobacterium tuberculosis* (195, 196). DCS is a structural analog of D-ala and inhibits both Alr and the D-ala dimerizing enzyme, DdlA (172). Our previous work showed that rare mutations of *bsrF* could increase tolerance to DCS, but the current research shows that by removing *bsrF* as well, cells struggle to overcome this loss of *alr*. Overall, enzymes involved in synthesis and incorporation of D-ala into PG are attractive targets for next-generation antibiotic development.

Previous studies have used PG-specific DAA auxotrophs as transient colonizers of cell cultures (305) and eukaryotes (289, 290), and even as vaccines against bacterial pathogens (291, 306, 307). Currently, transient colonization of *E. scolopes* is

accomplished by use of antibiotics (49, 284, 285). Here, we employed the use of *V. fischeri* strains auxotrophic for a PG-specific DAAs instead, with the assumption that the eukaryotic host was unlikely to provide DAAs.

Upon supplying D-ala in the seawater, the MC13 D-ala auxotroph was able to colonize hatchling *E. scolopes* squid (**Figure 4.5**). When D-ala is subsequently removed from the water, the auxotrophic bacteria rapidly begin to lose cell morphology before finally lysing (**Figure 4.4**), resulting in transient colonization of the squid (**Figure 4.4**). Understanding the dynamics of host-microbe interactions is especially crucial during the early, stress-susceptible stages of life, as organisms enter the environment and acquire their microbiomes. The deployment of auxotrophic strains unveils a complementary methodology to specifically target the growth dynamics of one species without perturbing the equilibrium of an entire microbial community, such as those found in the adult *E.* scolopes gut and ANG. This approach could therefore prove useful for long-term studies of the effects of cleared colonization of the light organ.

Studies of transient bacterial infections can inform our understanding of host-microbe dynamics, and specifically this research can aid in understanding the intricacies of symbiont-induced host maturation. For example, this method provided additional information about the specific biogeographies of the three crypt spaces within the *E. scolopes* light organ. Previous studies have shown that crypt three is the last to form and has distinct chemical and morphological differences from crypts one and two (9, 21, 281-283). The present research underscores this, as we observed the symbionts of crypt three to outlast those in crypts one and two after removal of D-ala from the seawater (**Figure 4.6**).

Unfortunately, we were unable to determine how long these cells persisted within the symbiosis, as it appeared that D-ala at the concentration used may be toxic to the hatchling squid over longer term experiments. While normally juvenile *E. scolopes* can be raised for at least four days, the squid in this study did not live for more than twenty-four hours after placement into water containing D-ala. Further work will need to be completed to determine if there is a lower dose of D-ala that can sustain growth of D-ala auxotrophs in seawater without harming the squid. These studies will help us to determine the extent of and mechanisms behind prolonged symbiont retention in crypt three. Currently, we speculate that either crypt three receives D-ala from the squid host, or that symbionts of crypt three simply grow slowly enough that lysis is delayed as compared to those in crypts one and two. Understanding the factors that contribute to this variability in crypt development and symbiont colonization could shed light on the selective pressures and adaptive strategies employed by both hosts and symbionts and strengthens previous hypotheses that the less-mature crypt three acts as a sanctuary, potentially safeguarding the symbionts from stress, i.e., antibiotic resistance (282, 283), or nutrient limitation.

MATERIALS AND METHODS

Bacterial strains and culture conditions. The strains in this study are listed in **Table 4.1**. When added to LB medium (221) for selection of E. coli, Cm and Kanamycin (Km) were used at concentrations of 20 and 40 µg/mL, respectively. For selection of *E. coli* with Em, 150 µg/mL was added to BHI medium (Difco, Sparks, MD). When added to LBS (308) for selection of V. fischeri, Cm, Em, and Km were used at concentrations of

2, 5, and 100 µg/mL, respectively. In LBS, D-ala was added at a final concentration of 400 µg/mL for auxotrophic strains unless otherwise indicated. FMM (1 mM Tris [pH 7.5], 400 mM NaCl, 10mM KCl, 50mM $MgSO_4$, 10mM $CaCl_2$, 2 µM $FeSO_4$, 2mM glycerol-3-phosphate, 5mM ribose, 20mM NAG) was used to pre-grow cells for natural transformation of *V. fischeri*. In FMM, D-ala was added at a final concentration of 100 µg/mL. Agar was added to a final concentration of 1.5% for solid media.

Molecular genetics and sequence analysis. Plasmids and oligonucleotides used in this study are listed in **Table 4.3**. and were synthesized by Integrated DNA Technologies (Coraville, IA). DNA ligase and restriction enzymes were purchased from New England Biolabs (Beverly, MA). PCR for chromosomal deletion by transformation was conducted with KOD DNA polymerase (Millipore Sigma, Burlington, MA). PCR for plasmid cloning was conducted with Phusion DNA polymerase (New England Biolabs). Plasmids used for cloning were prepared with the ZymoPURE Plasmid Miniprep kit (Zymo Research, Irvine CA). DNA was repurified after PCR and between cloning steps using the DNA Clean & Concentrator kit from Zymo Research. Plasmid inserts were Sanger sequenced at the University of Michigan Advanced Genomics core facility (Ann Arbor, MI). gDNA from *V. fischeri* strain ES114 was extracted using the Invitrogen PureLink™ Genomic DNA Mini Kit (Thermo Fisher Scientific, Inc) and used as a template for PCR.

Table 4.3 Plasmids and primers used in this study

Plasmid	Relevant Characteristics	Source
pCR-Blunt II-TOPO	*ori*V_{ColE1}, *km*^{R}	Thermo Fisher
pEVS104	Conjugative helper plasmid; *oriV*$_{R6K}$ *oriT*$_{RP4}$ *km*^{R}	(222)
pEVS118	*ori*VR6K *ori*TRP4, *cm*^{R}	(216)
pKAL4	*bsrF* from ES114 cloned into pCR-Blunt II-TOPO	Chapter 2
pKAL6	*bsrF* from ES114 cloned into pVSV105	Chapter 2
pKV494	pJET + FRT-Em^R	(225)
pKV496	pEVS79-Kn^R+ *flp*$^+$	(225)
plostfoX	tfoX$^+$, Cm^R	(226)
pMNC4	*metC* from ES114 cloned into pCR-Blunt II-TOPO	This study
pMNC6	*metC* from ES114 cloned into pVSV105	This study
pMNC26	Δ*SS-bsrF* cloned from pKAL6 into pVSV105	Chapter 2
pVSV102	*Km*^{R}, *gfp*	(21)

Primer *	Sequence	Source
Frt-F	CCATACTTAGTGCGGCCGCCTA	(225)
Frt-R	CCATGGCCTTCTAGGCCTATCCC	(225)
MNC7	CAT GCT AGC ACT AGT GAA TGG ATT CAT ATG	This study
MNC8	CAT GCT AGC CGC CTT TAA TTT ATT GTT AAG	This study
MNC39	GAT CTA AGA CAA AAA CTG CAA TAA GG	This study
MNC40	taggcggccgcactaagtatgg CAT ATG AAT CCA TTC AAT AAA AAG	This study
MNC41	ggataggcctagaaggccatgg TAACAATAAATTAAAGGCGATATT	This study
MNC42	CATCAATCTGGATAAGACGAACGC	This study
MNC51	GGGCTCGTATTTCTTCTACTATGGGC	Chapter 2
MNC52	taggcggccgcactaagtatggCATGATTCAGCCTTATTATTCATCA	Chapter 2
MNC53	ggataggcctagaaggccatggAATGAGAGTCTTCTTGAATTCATT	Chapter 2
MNC54	CTCTATACTCGAGACACCGCTATC	Chapter 2

[a] Alleles cloned in this study are from *V. fischeri* strain ES114. Replication origins (*oriV*) on each vector are listed as R6K and/or ColE1. Plasmids based on pES213 are stable in *V. fischeri* and do not require antibiotic selection for maintenance(21).
* All oligonucleotides are shown in the 5'-to-3' direction. Lowercase bases represent the tail sequences used for splicing fragments via SOE PCR.

Plasmid construction. Plasmids were maintained in *E. coli* DH5α with the exception of pVSV105 and its derivatives which were maintained in DH5αλpir, and pEVS104 which was maintained in CC118*λpir* (222). When relevant, plasmids were conjugated into *V. fischeri* via triparental mating with helper plasmid pEVS104. Complementation plasmid pMNC6 was constructed by amplifying *metC* from ES114 with primers MNC7 and

MNC8. This PCR product was cloned into pCR-Blunt II TOPO (Thermo Fisher, Waltham, MA), yielding pMNC4. pMNC4 was then digested with NheI, and the *metC*-containing fragment was ligated into XbaI-cut pVSV105 (222), producing pMNC6.

Construction of mutant strains. For all mutant strains engineered in this study, chromosomal deletions in ES114 were created via overlap extension PCR (SOE-PCR), by generating mutant alleles, which were introduced by TfoX-mediated transformation (226). An Em-resistance cassette flanked by Frt-recombinase recognition sites was amplified with KOD DNA polymerase from plasmid pKV494 using primers Frt-F and Frt-R (225). Deletions of *metC* and *alr* were made by splicing fragments from upstream and downstream of the genes to the Em resistance cassette by SOE-PCR (225). Briefly, a ~500-bp fragment upstream of *metC* was amplified from ES114 using primers MNC39 and MNC40, and the ~500-bp region downstream of *metC* was amplified using primers MNC41 and MNC42. The ~500-bp region upstream of *alr* was amplified from ES114 using primers MNC51 and MNC52, and the ~500-bp region downstream of *alr* was amplified using primers MNC53 and MNC54. These pairs of flanking sequences were fused to the Em-Frt cassette by SOE-PCR, and the resulting deletion-allele fragments were then transformed into *V. fischeri* strains harboring the TfoX-overexpressing plasmid plosTfoX (226). Strains were then selected on LBS containing Em (and D-ala, for Δ*alr* strains). The Em cassette was removed from each mutant via *flp* recombinase expression on pKV496 to leave a FLP recognition-site scar, and finally the FLP-expressing plasmid was cured (225). The Δ*metC* allele was then verified in resulting strains by PCR amplification with primers MNC39 and MNC41, and the Δ*alr* allele was

checked with primers MNC51 and MNC54. Strain MC2 was generated by replacing *metC* in ES114 with the Δ*metC*-Em deletion fragment. Removal of the Em cassette generated strain MC5. Strain MC3 was generated by replacing *alr* in ES114 with the Δ*alr*-Em deletion fragment. Removal of the Em cassette generated strain MC6. Strain MC8 was generated from KL3 (Chapter 2) by replacing *metC* with the Δ*metC*-Em deletion fragment. Removal of the Em cassette generated strain MC12. Strain MC23 was generated from MC6 by replacing *metC* with the Δ*metC*-Em deletion fragment. Removal of the Em cassette generated strain MC24. Strain MC26 was generated from MC13 (Chapter 2) by replacing *metC* with the Δ*metC*-Em deletion fragment. Removal of the Em cassette generated strain MC27.

Selection of spontaneous suppressors of D-ala auxotrophy. D-ala auxotrophs (MC6, MC13, MC24, and MC27) were grown in LBS containing 400 µg/mL D-ala to an OD_{600} of 1. 100 µL of culture was plated to LBS without D-ala. Cultures were dilution-plated in parallel on LBS with D-ala, to determine the number of CFU plated, thereby enabling calculation of mutation frequency. Plates were incubated at 28°C, and colonies counted at 24h and 48h. Suppressor colonies were streak-purified, then grown in LBS without D-ala supplementation, and stocked at -80°C in 20% glycerol.

Analysis of PG amino acid and muropeptide content. Cells were grown overnight in LBS (or LBS-Cm), chilled on ice for 10min, and centrifuged at 4°C and 17,600 x *g* for 15 minutes. Pellets were resuspended in 10 mL water that had been chilled on ice, then dripped into 50mL of boiling 4% SDS. The solution was boiled for 30 min with

continuous stirring and allowed to cool to room temperature, at which point they were centrifuged at 120,000 x *g* for 60 min, resuspended in room temperature water and washed three to four more times by centrifugation and resuspension as above. Before resuspension, the supernatant was assayed for SDS using methylene blue and chloroform (227) and washed repeatedly until no SDS was detected. When SDS was undetectable, the pellet was resuspended in 1 mL of water, with Tris-HCl (pH 7.5) added to a final concentration of 100 mM and $MgSO_4$ added to a concentration of 20 mM, then treated with 10 µg DNase I and 50 µg RNase A for 2 hours at 37°C. Samples were then treated with 100 µg of Trypsin, $CaCl_2$ was added to a final concentration of 10 mM. Samples were then incubated overnight at 37°C, and then centrifuged at 15,880 x *g* for 10 minutes, after which pellets were resuspended in 1% SDS. The solution was incubated in a 95°C hot water bath for twenty minutes, diluted into warm water, and then centrifuged at 120,000 x *g* for 60 minutes at room temperature. The pellet was then washed with warm water and centrifuged as above, until SDS-free. Subsequent pellets were then resuspended in 12.5 mM $NaPO_4$ (pH 5.5) and digested with 125 units of Mutanolysin at 37°C overnight. Insoluble material was removed by centrifugation at 15,880 x *g* for 15 minutes. The muropeptide-containing supernatant was transferred to a new tube, lyophilized until dry, and stored at -20°C until analysis. Amino acid (228) and muropeptide (229) analyses were performed using HPLC as previously described.

Time-lapse microscopy of D-ala auxotrophic bacteria. MC13 cells were initially cultured at 28°C in LBS medium supplemented with 400 µg/mL of D-ala, until the bacterial population reached exponential phase, with OD_{600} between 0.4 and 0.8. Cells

were harvested by centrifugation at 7000 x *g* for 1 minute at room temperature, then resuspended in LBS without D-ala supplementation. A 1 µL aliquot of cells was carefully placed onto a pad containing 1.0% agarose in LBS and sealed with a coverslip. Time-lapse images were captured at 5-minute intervals over a period of two hours, by an inverted Zeiss LSM 980 microscope equipped with a Plan Apochromat 1.4NA 100x oil Phase 3 objective at the Caltech Biological Imaging Facility. The acquired time-lapse sequences were subsequently processed and visualized in ImageJ, enabling generation of a comprehensive image montage.

Squid colonization assay. *V. fischeri* ES114 was cultured overnight at 28°C in LBS medium, and D-ala auxotrophic strain MC13 carrying *gfp*-expressing plasmid pVSV102 was grown in LBS with 400 µg/mL of D-ala and 100 µg/mL km for plasmid retention. Overnight cultures were diluted 100-fold into Seawater Tryptone (SWT) liquid medium and allowed to grow until mid-exponential phase at 28°C, then diluted to a final inoculum concentration of ~5000 CFU/mL in 100 mL of filter-sterilized ocean water (FSW). ES114 was inoculated into FSW alone, while MC13 was supplemented with 50 µg/mL D-ala. Newly hatched *E. scolopes* were introduced into these mixtures and allowed to colonize overnight under a 12/12-hour day-night cycle. After about 16 hours, squid were transferred into individual vials with fresh water. ES114-inoculated squid were placed into FSW; half of the MC13-inoculated squid were transferred into FSW alone, while the other half were transferred into FSW supplemented with 50 µg/mL D-ala. At 24 hours post-inoculation, luminescence was measured using a TD 20/20 luminometer (Turner Designs, Sunnyvale, CA), after which the squid were either

transferred to fresh FSW with D-ala as needed, or frozen at -80°C in 700 µL of FSW until ready for use. Most squid were individually homogenized, then dilution plated to LBS agar medium, and the number of CFU/mL was determined. Five squid from each treatment (D-ala or no D-ala) were fixed in 4% paraformaldehyde solution in 1x marine PBS (mPBS) for microscopy, as previously described (283).

Light microscopy and fluorescence imaging. PFA-fixed juvenile *E. scolopes* were dissected, treated with TO-PRO-3 Iodide (Thermo Fisher Scientific) to stain nuclei, and permeabilized overnight in 0.1% Triton X-100 in mPBS (mPBST). Squid were washed in mPBST for 15 minutes, and then mounted in Vectashield (Vector Laboratories, Burlingame, CA) for imaging. Imaging was conducted using a Zeiss LSM 980 confocal microscope equipped with Zeiss Plan Apochromat 1.4NA 63x oil objective lens at the Caltech Biological Imaging Facility.

ACKNOWLEDGEMENTS

This work was supported by the NSF grant IOS-1557964 awarded to EVS and DLP. We would like to thank the Caltech Biological Imaging center where we performed the microscopy imaging.

CHAPTER 5

CONCLUSIONS AND FUTURE DIRECTIONS

The goal of this dissertation was to study the evolution of PG structure and biosynthesis in *Vibrio fischeri*. *V. fischeri* is a perfect system for these studies, as it parallels PG-induced virulence mechanisms of two pathogens, *Neisseria gonorrhoeae* and *Bordetella pertussis*, while itself being non-pathogenic. *V. fischeri* and its host *Euprymna scolopes* are both tractable in laboratory settings, allowing for experimental control and observation of these mechanisms. Additionally, *V. fischeri* shares the wild-type PG structure with most Gram-negative bacteria, and has a simple PG biosynthesis proteome, with only one canonical racemase each for D-ala and D-glu, and one predicted epimerase for *meso*-diaminopimelic acid (*m*DAP). These studies can further our understanding of host-microbe interactions, as well as bacterial evolution and the constraints on PG structure.

To explore the essentiality of *V. fischeri*'s PG peptide structure, and the constraints on evolution of this structure, mutants lacking racemases necessary for PG biosynthesis were generated, and suppressors of these strains were isolated. Chapters 2 and 3 describe studies of suppressor strains that were isolated by plating a D-glu auxotrophic parent strain on media without supplemented D-glu. Attempts to isolate suppressors on unsupplemented media did not yield colonies, so the approach was adjusted to attempt suppressor selection on media supplemented with structural

variants of D-glu. Chapter 2 describes a strain isolated on iso-D-gln, while the suppressors in Chapter 3 were isolated on medium with a very low concentration of D-glu. This difficultly to select suppressor mutations was not encountered in Chapter 4, where I detail my work with D-ala auxotrophy and suppression. D-ala auxotrophic *V. fischeri* was further explored for the ability to develop a model of transient colonization of *E. scolopes* in the described collaborative work.

As outlined in chapter 1, *V. fischeri* has a mutually beneficial partnership with the Hawaiian bobtail squid *E. scolopes*. Throughout the colonization of the *E. scolopes* light organ, *V. fischeri* uses signaling molecules to communicate with the squid. One of these signals is a biologically active monomer of PG, referred to as TCT. Both TCT and polymeric PG are common MAMPs. Although the structure of PG is largely conserved among bacteria, this study sought to alter the structure through variation of the DAAs in its peptide. DAAs are ubiquitous in nature and are commonly produced and released by bacteria. In *V. fischeri*, two of the PG-specific DAAs, D-ala and D-glu, are each produced from their corresponding L-isomers by a specific racemase: D-glu is produced by MurI and D-ala by Alr (158). The final DAA utilized in PG, *m*DAP, is produced by a single epimerase. The goal for my research was to investigate how and if *V. fischeri* could evolve to produce D-glu or D-ala without the necessary racemase, and/or evolve PG with a substituted amino acid. Evolution of PG structure or biosynthesis would inform our understanding of how bacteria adapt to environmental stressors, including antibacterial drugs.

ALTERING THE BROAD-SPECTRUM RACEMASE, BSRF

In Chapter 2, I discuss the selection and characterization of one spontaneous mutant of D-glu auxotrophy, allowing it to grow in both rich and minimal media without exogenous D-glu. This rare mutant contained a genetic amplification and concomitant gene fusion, apparently burying the secretion signal sequence of a periplasmic broad-spectrum racemase, BsrF. The engineered ΔSS-*bsrF* allele deleted that signal sequence, presumably sequestering BsrF in the cytoplasm and allowed the cells to produce both D-glu and D-ala needed for PG biosynthesis, a pathway that wild-type BsrF usually does not affect. By producing sufficient D-ala, cytoplasmic BsrF increases *V. fischeri*'s tolerance for D-cycloserine (DCS), an antibiotic that inhibits both alanine racemase and D-ala:D-ala ligase (189).

The findings of this study are of particular interest, as bacterial racemases are popular targets for antibacterial drug discovery. Specifically, researchers have been testing small molecules for inhibition against glutamate and alanine racemases. DCS is currently the only racemase-targeting antibiotic that has been used medicinally. This study illuminates one concern against relying on racemase inhibition as antimicrobial drugs, specifically by showing how a broad-spectrum racemase can lead to antimicrobial resistance. This resistance mechanism is especially concerning as we continue discovering broad-spectrum racemases in more species, many of which are found in known pathogens. Broad-spectrum racemases have wider substrate ranges, so have greater potential to compensate for loss of specific racemases when under nutrient starvation or other environmental stressors.

The most obvious continuation of this work will be in the further characterization of BsrF. Though we first assumed that BsrF would have similar activities and phenotypic effects as its orthologue in *Vibrio cholerae*, we have now seen enough significant divergence between their activities that BsrF merits further investigation. For example, BsrV of *V. cholerae* has been studied both *in vivo* and *in vitro*, and in neither case does it appear able to racemize glutamate (156). However, as shown by its ability to suppress D-glu auxotrophy while allowing production of wild-type PG structure, BsrF likely does racemize glutamate. BsrF and the altered ΔSS-BsrF protein deserve continued attention, with *in vivo* and *in vitro* studies to determine their exact substrate range. Additionally, BsrV from *V. cholerae* has been shown to affect PG structure in stationary phase (77, 99, 100, 103), which in turn determines how well *V. cholerae* can withstand osmotic pressure (77). Although we found that expressing ΔSS-BsrF in a background with *bsrF* does not alter PG structure, we do not yet know if the wild-type BsrF enzyme does affect PG structure. Preliminary data suggests that BsrF's canonical activity within the periplasm can also lead to altered PG structure, but more studies need to be done.

CHARACTERIZATION OF MUTANTS WITH ALTERED GLUTAMATE TRANSPORT

Chapter 3 explores mutants that suppress D-glu auxotrophy through mutation that altered a putative sodium:glutamate symporter, GltS. Alteration of the symporter allowed utilization of lower concentrations of D-glu in rich medium. *In trans* overexpression of either of two mutant alleles (*gltS*^{C1092T} and *gltS*^{C490T}) leads to growth in rich medium without exogenous D-glu, increased sensitivity to homocysteic acid, and altered PG peptides. These data led us to the discovery that, contrary to our prior

assumptions, LBS contains low but significant amounts of DAAs. Although the final concentrations are too low to be utilized by wild type, we have demonstrated that alteration of a glutamate transporter can allow access to these nutrients. More trials are needed to quantify DAAs from LBS and its components, to ensure the result is reproducible. If verified, this knowledge could lend itself to research of transport for both D-ala and D-glu in *V. fischeri*.

Altered PG structure in the D-glu auxotrophic strain over-expressing *gltS*^{C490T} led us to hypothesize that the cells were importing so much glutamine that some was replacing D-ala in the fifth position of the PG peptide chain. It was therefore surprising that the suppressors instead had incorporated lysine at the fifth position of the peptide. Future work is necessary to determine whether this is D- or L-lys, and how and why the cells are adding lysine onto their PG. Is it being incorporated into the nascent PG strand during cytoplasmic biosynthesis? Does it get added to the end of mature peptides within the periplasm? Preliminary data suggests that peptides containing lysine are still involved in some amount of crosslinking, but is there any difference in crosslink pattern or amount? One hypothesis is that the periplasmic BsrF produces D-lys during its normal activity, and cells that are stressed by dwindling D-glu availability are adding it to the mature PG as a way to add stability to the cell wall. To test this possibility, PG sacculi would need to be isolated from a *murI racD bsrF* triple mutant strain that is overexpressing GltS. The PG peptide would then be assessed for the presence or absence or lysine. Absence of lysine would indicate that BsrF produces the D-lys that is incorporated, while presence would indicate that BsrF is uninvolved.

Based on preliminary results, the D-glu auxotroph expressing *gltS*^{C1092T} may also have a non-canonical DAA incorporated into its PG peptide, though in even lower proportion than the strain mentioned above. In-depth analysis on sacculi of this strain is needed to verify if these data are correct. I would speculate that it also has lysine in the fifth amino acid position, as this PG alteration appears to be due to cellular stress rather than due the specific activities of the mutant symporter, which is not known to transport lysine. Additionally, since these strains appear to have altered PG structure, the impact of mutant GltS on antibiotic sensitivities is worth exploring, both those that target mature PG and PG biosynthesis in the cytoplasm. I also demonstrated that, although it has altered PG structure, the D-glu auxotroph expressing mutant GltS is able to colonize *E. scolopes* to the same level as wild type when it is provided with D-glu. This is however unsurprising, as we know that only a subset of the PG in this strain appears to have lysine. To determine if the lysine actually affects colonization, one would need to elute and purify this specific peak during HPLC analysis. Such experiments would give insight as to whether an amino acid, especially a non-canonical amino acid, affects recognition and binding of host PG recognition proteins.

In addition to the altered glutamate symporter, many of the D-glu auxotrophic suppressors had other mutations. Two of these, VF_0468^{A699G} and *gacS*^{G644C}, were recovered independently from two mutants each. GacS is a sensor kinase within a broad regulon that is known to affect colonization of many Proteobacteria (252), while VF_0468 is an essential gene that appears to encode an orthologue of LspA, a prolipoprotein signal peptidase that often plays a role in synthesis of the cell envelope and PG (178, 309). Both mutations warrant further study within the context of D-glu

auxotrophy and transport, and LspA could be an interesting target for further squid-*Vibrio* colonization studies.

D-ALA AUXOTROPHY IN CULTURE AND IN SYMBIOSIS

Chapter 4 describes my work with the D-ala branch of PG biosynthesis. The study began by creating D-ala auxotrophic strains by deleting the gene encoding the canonical alanine racemase used for PG biosynthesis, *alr*. From our work in chapter two and the published literature, we knew that BsrF can compensate for D-ala auxotrophy when relegated to the cytoplasm, and that MetC of *E. coli* can rescue D-ala auxotrophy by producing D-ala (157, 292), so we created further deletions in the Δ*alr* background. Ultimately four D-ala auxotrophic strains were investigated to determine if suppressors of D-ala auxotrophy could be selected. The first strain, MC6 (Δ*alr*) generated ten suppressors out of 10^{10} CFU plated, while plating of similar CFU counts yielded no prototrophic suppressors from the other three auxotrophs (MC13, Δ*alr* Δ*bsrF*; MC24, Δ*alr* Δ*metC*; and MC27, Δ*alr* Δ*bsrF* Δ*metC*). These results are consistent with the possibility that suppressors generated from MC6 likely involve *metC* and/or *bsrF* and strengthen speculation that these three proteins are the only examples in the *V. fischeri* proteome with canonical racemase activity. Future characterization of these ten prototrophic suppressors can be done via qRT-PCR to check expression levels of *metC* and *bsrF*, and through whole genome resequencing to determine the genetics underpinning suppression. Though we do expect to see mutations involving *metC* or *bsrF* in these strains, it is possible that they will have alterations in some other, unexpected gene or pathway.

Finally, this chapter introduced a new method for achieving transient colonization of *V. fischeri* within *E. scolopes*. We found that a D-ala auxotroph can effectively colonize the *E. scolopes* light organ when D-ala is present in the seawater, and then the bacteria are cleared when D-ala supplementation is removed. This method accomplishes transient colonization that can be controlled experimentally and could be a useful complementary option to the use of antibiotics, with less potential impact on the health of the squid. Although antibiotic treatments effectively can abolish viable CFU in the light organ and do not outwardly harm juvenile squid, there has not been significant research on possible off-target effects. Additionally, antibiotic use is not feasible with adult squid, as the drugs could disrupt the microbiomes in their guts and/or accessory nidamental glands. Curing of *V. fischeri* via limitation of a key nutrient like D-ala, however, is not likely to affect other microbes within the host.

However, more studies need to be performed with DAA auxotrophies within the squid-*Vibrio* mutualism before this method can be widely used. In the current study, the concentration of D-ala used appears to be somehow toxic to juvenile *E. scolopes*, who did not live more than one day after D-ala treatment. Interestingly this problem was not encountered with D-glu, in which squid survived through the full 96 hours of experimentation. The D-glu studies of Chapter 3 used much lower concentrations of the amino acid, only 1 or 5 μg/mL, as opposed to the 50 μg/mL used for the D-ala studies. This high concentration could be the culprit, so the first step to investigating this problem will be finding a lower concentration of D-ala that supports growth of a D-ala auxotroph without being toxic to squid.

FUTURE STUDY OF THE DAP BRANCH OF PG BIOSYNTHESIS

Notably missing from this dissertation is a chapter about *m*DAP auxotrophy. Previously in our lab, Dr. R. M. Jones generated a *V. fischeri* strain auxotrophic for mDAP, and isolated derivatives that had suppressed DAP auxotrophy (190). However, the work he did was not without difficulties. Dr. Jones was unable to generate the *m*DAP auxotroph on rich medium, though he was able to isolate the strain with minimal medium. Isolation of suppressors also required minimal medium. The suppressors that were isolated did have interesting genotypes, with one ultimately having altered PG structure (190). As is seen naturally in *Fusobacterium nucleatum* (79, 80), and experimentally in *Escherichia coli* (76) and *Mycobacterium smegmatis* (86), this suppressor incorporated lanthionine in the third position of its PG peptide. The strain had altered cell morphology and increased sensitivity to osmotic challenge, and we were interested to see how the altered PG structure would affect signaling in the squid-*Vibrio* symbiosis.

Future studies in Dr. Jones' strains would likely begin with serial passage of the altered-PG suppressor strain, to ameliorate some of the negative growth defects it experiences. This would hopefully give rise to an evolved strain with better growth rate, and possibly allow for growth on rich medium. Since the strain is sensitive to NaCl, work should be done to determine if there is a salt concentration that both squid and the strain can tolerate, in order to conduct colonization experiments with this altered PG strain.

Another approach that could be taken is creating a new *m*DAP auxotrophic parent strain. The original strain made by Dr. Jones has a deletion of most of the *dapF*

gene, which encodes *N*-succinyl-L,L-diaminopimelic acid desuccinylase. Since the strain was made, our lab has begun using overlap extension PCR (SOE-PCR), which greatly reduces the time needed to make chromosomal deletions in *V. fischeri*. Future work could therefore be to delete *dapF* in its entirety, or perhaps delete *dapE*, the gene encoding the putative *m*DAP epimerase (14, 15). Any new strains created could still have the same growth phenotypes as the original *dapF* mutant, but this could lead to determination of why and how *m*DAP auxotrophs are specifically unable to grow on rich medium.

FINAL CONCLUSIONS

The PG cell wall has been a hot topic of research for many years, as it is highly conserved throughout the Bacterial Kingdom. Through this work, we have increased the understanding of the mechanisms and constraints of PG variation and evolution. The work described here has important implications for the inherent necessity of D-glu and D-ala in the PG peptide chain, which can inform future work with antibiotic drugs that target cell wall synthesis. We have also introduced a novel method of transient colonization of *E. scolopes*, that could be more effective in curing *V. fischeri* and healthier for the hosts. My results have opened up fascinating new research directions, some of which are described in this chapter.

REFERENCES

1. Heddi A, Zaidman-Remy A. 2018. Endosymbiosis as a source of immune innovation. C R Biol 341:290-296.
2. Ruby EG, McFall-Ngai MJ. 1992. A squid that glows in the night: development of an animal-bacterial mutualism. J Bacteriol 174:4865-70.
3. Koropatnick TA, Engle JT, Apicella MA, Stabb EV, Goldman WE, McFall-Ngai MJ. 2004. Microbial factor-mediated development in a host-bacterial mutualism. Science 306:1186-8.
4. Wei SL, Young RE. 1989. Development of symbiotic bacterial bioluminescence in a nearshore cephalopod, *Euprymna scolopes*. Mar Biol 103:541-546.
5. Boettcher KJ, Ruby EG. 1990. Depressed light emission by symbiotic *Vibrio fischeri* of the sepiolid squid *Euprymna scolopes*. J Bacteriol 172:3701-3706.
6. McFall-Ngai MJ, Montgomery MK. 1990. The anatomy and morphology of the adult bacterial light organ of the *Euprymna scolopes* berry (Cephalopoda:Sepiolidae). Biol Bull 179:332-339.
7. Kishitani T. 1928. Ueber das Leuchtorgan von *Euprymna morsei* Verrill und die symbiotischen Leuchtbakterien. Proc Imp Acad 4:306-309.
8. Nyholm SV, Stabb EV, Ruby EG, McFall-Ngai M. 2000. Establishment of an animal-bacterial association: Recruiting symbiotic *Vibrios* from the environment. Proc Natl Acad Sci U S A 97:102321-102325.
9. McFall-Ngai MJ, Ruby EG. 1998. Sepiolids and Vibrios: when they first meet. Biosci 48:257-265.

10. Foster JS, Apicella MA, McFall-Ngai MJ. 2000. *Vibrio fischeri* lipopolysaccharide induces developmental apoptosis, but not complete morphogenesis, of the *Euprymna scolopes* symbiotic light organ. Dev Biol 226:242-254.

11. Montgomery MK, McFall-Ngai M. 1994. Bacterial symbionts induce host organ morphogenesis during early postembryonic development of the squid *Eurprymna scolopes*. Development 120:1719-1729.

12. Koropatnick TA, Kimbell JR, McFall-Ngai MJ. 2007. Responses of host hemocytes during the initiation of the squid-Vibrio symbiosis. Biol Bull 212:29-39.

13. Truong TV, Holland DB, Madaan S, Andreev A, Keomanee-Dizon K, Troll JV, Koo DES, McFall-Ngai MJ, Fraser SE. 2020. High-contrast, synchronous volumetric imaging with selective volume illumination microscopy. Commun Biol 3:74.

14. Ruby EG, Urbanowski M, Campbell J, Dunn A, Faini M, Gunsalus R, Lostroh P, Lupp C, McCann J, Millikan D, Schaefer A, Stabb E, Stevens A, Visick K, Whistler C, Greenberg EP. 2005. Complete genome sequence of *Vibrio fischeri*: a symbiotic bacterium with pathogenic congeners. Proc Natl Acad Sci U S A 102:3004-9.

15. Mandel MJ, Stabb EV, Ruby EG. 2008. Comparative genomics-based investigation of resequencing targets in *Vibrio fischeri*: focus on point miscalls and artefactual expansions. BMC Genomics 9:138.

16. Mandel MJ, Wollenberg MS, Stabb EV, Visick KL, Ruby EG. 2009. A single regulatory gene is sufficient to alter bacterial host range. Nature 458:215-218.

17. Gyllborg MC, Sahl JW, Cronin DC, Rasko DA, Mandel MJ. 2012. Draft genome sequence of *Vibrio fischeri* SR5, a strain isolated from the light organ of the Mediterranean squid *Sepiola robusta*. J Bacteriol 194:1639-1639.
18. Bongrand C, Koch EJ, Moriano-Gutierrez S, Cordero OX, McFall-Ngai M, Polz MF, Ruby EG. 2016. A genomic comparison of 13 symbiotic *Vibrio fischeri* isolates from the perspective of their host source and colonization behavior. ISME J 10:2907-2917.
19. Bultman KM, Cecere AG, Miyashiro T, Septer AN, Mandel MJ. 2019. Draft genome sequences of Type VI secretion system-encoding *Vibrio fischeri* strains FQ-A001 and ES401. Microbiol Resour Announc 8.
20. Christensen DG, Tepavčević J, Visick KL. 2020. Genetic manipulation of *Vibrio fischeri*. Curr Protoc Microbiol 59:e115.
21. Dunn AK, Millikan DS, Adin DM, Bose JL, Stabb EV. 2006. New rfp- and pES213-derived tools for analyzing symbiotic *Vibrio fischeri* reveal patterns of infection and *lux* expression *in situ*. Appl Environ Microbiol 72:802-810.
22. McFall-Ngai MJ, Ruby EG. 1991. Symbiont recognition and subsequent morphogenesis as early events in an animal-bacterial mutualism. Science 254:1491-1494.
23. Norsworthy A, Visick K. 2013. Gimme shelter: how *Vibrio fischeri* successfully navigates an animal's multiple environments. Front Microbiol 4.
24. Aschtgen M-S, Brennan CA, Nikolakakis K, Cohen S, McFall-Ngai M, Ruby EG. 2019. Insights into flagellar function and mechanism from the squid–Vibrio symbiosis. NPJ Biofilms Microbiomes 5:32.

25. Adin DM, Engle JT, Goldman WE, McFall-Ngai MJ, Stabb EV. 2009. Mutations in *ampG* and lytic transglycosylase genes affect the net release of peptidoglycan monomers from *Vibrio fischeri*. J Bacteriol 191:2012-2022.

26. Doino Lemus J, McFall-Ngai MJ. 2000. Alterations in the proteome of the *Euprymna scolopes* light organ in response to symbiotic *Vibrio fischeri*. Appl Environ Microbiol 66:4091-7.

27. Chun CK, Scheetz TE, Bonaldo MdF, Brown B, Clemens A, Crookes-Goodson WJ, Crouch K, DeMartini T, Eyestone M, Goodson MS, Janssens B, Kimbell JL, Koropatnick TA, Kucaba T, Smith C, Stewart JJ, Tong D, Troll JV, Webster S, Winhall-Rice J, Yap C, Casavant TL, McFall-Ngai MJ, Soares MB. 2006. An annotated cDNA library of juvenile *Euprymna scolopes* with and without colonization by the symbiont *Vibrio fischeri*. BMC Genom 7:154.

28. Schleicher TR, Nyholm SV. 2011. Characterizing the host and symbiont proteomes in the association between the bobtail squid, Euprymna scolopes, and the bacterium, Vibrio fischeri. PLoS One 6:e25649.

29. Thompson LR, Nikolakakis K, Pan S, Reed J, Knight R, Ruby EG. 2017. Transcriptional characterization of *Vibrio fischeri* during colonization of juvenile *Euprymna scolopes*. Environ Microbiol 19:1845-1856.

30. Nyholm SV, McFall-Ngai MJ. 2021. A lasting symbiosis: how the Hawaiian bobtail squid finds and keeps its bioluminescent bacterial partner. Nat Rev Microbiol 19:666-679.

31. Rouressol L, Briseno J, Vijayan N, Chen GY, Ritschard EA, Sanchez G, Nyholm SV, McFall-Ngai MJ, Simakov O. 2023. Emergence of novel genomic regulatory

regions associated with light-organ development in the bobtail squid. iScience 26:107091.

32. Aschtgen MS, Lynch JB, Koch E, Schwartzman J, McFall-Ngai M, Ruby E. 2016. Rotation of *Vibrio fischeri* flagella produces outer membrane vesicles that induce host development. J Bacteriol 198:2156-65.

33. Aschtgen MS, Wetzel K, Goldman W, McFall-Ngai M, Ruby EG. 2016. *Vibrio fischeri*-derived outer membrane vesicles trigger host development. Cell Microbiol 18:488-499.

34. Osborn MJ. 1969. Structure and biosynthesis of the bacterial cell wall. Annu Rev Biochem 38:501-38.

35. Vollmer W, Blanot D, de Pedro MA. 2008. Peptidoglycan structure and architecture. FEMS Microbiol Rev 32:149-167.

36. Melly MA, McGee ZA, Rosenthal RS. 1984. Ability of monomeric peptidoglycan fragments from *Neisseria gonorrhoeae* to damage human fallopian-tube mucosa. J Infect Dis 149:378-86.

37. Rosenthal RS, Nogami W, Cookson BT, Goldman WE, Folkening WJ. 1987. Major fragment of soluble peptidoglycan released from growing *Bordetella pertussis* is tracheal cytotoxin. Infect Immun 55:2117-20.

38. Rietschel ET, Kirikae T, Schade FU, Mamat U, Schmidt G, Loppnow H, Ulmer AJ, Zähringer U, Seydel U, Di Padova F, et al. 1994. Bacterial endotoxin: molecular relationships of structure to activity and function. FASEB J 8:217-25.

39. Shibata S, Visick KL. 2012. Sensor kinase RscS induces the production of antigenically distinct outer membrane vesicles that depend on the symbiosis polysaccharide locus in *Vibrio fischeri*. J Bacteriol 194:185-94.

40. Beveridge TJ. 1999. Structures of Gram-negative cell walls and their derived membrane vesicles. J Bacteriol 181:4725-33.

41. Czuprynski CJ, Welch RA. 1995. Biological effects of RTX toxins: the possible role of lipopolysaccharide. Trends Microbiol 3:480-3.

42. Norimatsu M, Ono T, Aoki A, Ohishi K, Takahashi T, Watanabe G, Taya K, Sasamoto S, Tamura Y. 1995. Lipopolysaccharide-induced apoptosis in swine lymphocytes *in vivo*. Infect Immun 63:1122-1126.

43. Zychlinsky A, Thirumalai K, Arondel J, Cantey JR, Aliprantis AO, Sansonetti PJ. 1996. In vivo apoptosis in *Shigella flexneri* infections. Infect Immun 64:5357-5365.

44. Hotchkiss RS, Swanson PE, Freeman BD, Tinsley KW, Cobb JP, Matuschak GM, Buchman TG, Karl IE. 1999. Apoptotic cell death in patients with sepsis, shock, and multiple organ dysfunction. Crit Care Med 27:1230-51.

45. Bannerman DD, Goldblum SE. 2003. Mechanisms of bacterial lipopolysaccharide-induced endothelial apoptosis. Am J Physiol 284:L899-L914.

46. George L, Ramasamy T, Sirajudeen K, Manickam V. 2019. LPS-induced apoptosis is partially mediated by hydrogen sulfide in RAW 264.7 murine macrophages. Immunol Invest 48:451-465.

47. Nyholm SV, Deplancke B, Gaskins HR, Apicella MA, McFall-Ngai MJ. 2002. Roles of *Vibrio fischeri* and nonsymbiotic bacteria in the dynamics of mucus

secretion during symbiont colonization of the *Euprymna scolopes* light organ. Appl Environ Microbiol 68:5113-22.

48. Troll JV, Adin DM, Wier AM, Paquette N, Silverman N, Goldman WE, Stadermann FJ, Stabb EV, McFall-Ngai MJ. 2009. Peptidoglycan induces loss of a nuclear peptidoglycan recognition protein during host tissue development in a beneficial animal-bacterial symbiosis. Cell Microbiol 11:1114-27.

49. Nyholm SV, Stewart JJ, Ruby EG, McFall-Ngai MJ. 2009. Recognition between symbiotic *Vibrio fischeri* and the haemocytes of *Euprymna scolopes*. Environ Microbiol 11:483-93.

50. Nyholm SV, McFall-Ngai MJ. 1998. Sampling the light-organ microenvironment of *Euprymna scolopes*: description of a population of host cells in association with the bacterial symbiont *Vibrio fischeri*. Biol Bull 195:89-97.

51. McAnulty SJ, Nyholm SV. 2016. The role of hemocytes in the Hawaiian bobtail squid, *Euprymna scolopes*: A model organism for studying beneficial host-microbe interactions. Front Microbiol 7:2013.

52. Van Heijenoort J. 1994. Biosynthesis of the bacterial peptidoglycan unit, p 39-54, New Comprehensive Biochemistry, vol 27. Elsevier.

53. Barreteau H, Kovac A, Boniface A, Sova M, Gobec S, Blanot D. 2008. Cytoplasmic steps of peptidoglycan biosynthesis. FEMS Microbiol Rev 32:168-207.

54. Bouhss A, Trunkfield AE, Bugg TD, Mengin-Lecreulx D. 2008. The biosynthesis of peptidoglycan lipid-linked intermediates. FEMS Microbiol Rev 32:208-233.

55. Sauvage E, Kerff F, Terrak M, Ayala JA, Charlier P. 2008. The penicillin-binding proteins: structure and role in peptidoglycan biosynthesis. FEMS Microbiol Rev 32:234-258.

56. Scheurwater E, Reid CW, Clarke AJ. 2008. Lytic transglycosylases: bacterial space-making autolysins. Int J Biochem Cell Biol 40:586-91.

57. Vollmer W, Joris B, Charlier P, Foster S. 2008. Bacterial peptidoglycan (murein) hydrolases. FEMS Microbiol Rev 32:259-286.

58. Jacobs C, Huang L, Bartowsky E, Normark S, Park JT. 1994. Bacterial cell wall recycling provides cytosolic muropeptides as effectors for β-lactamase induction. EMBO J 13:4684-4694.

59. Parquet C, Flouret B, Leduc M, Hirota Y, van Heijenoort J. 1983. N-acetylmuramoyl-L-alanine amidase of *Escherichia coli* K12. Possible physiological functions. Eur J Biochem 133:371-7.

60. Goodell EW, Higgins CF. 1987. Uptake of cell wall peptides by *Salmonella typhimurium* and *Escherichia coli*. J Bacteriol 169:3861-3865.

61. Goodell EW. 1985. Recycling of murein by *Escherichia coli*. J Bacteriol 163:305-310.

62. Goldman WE, Klapper DG, Baseman JB. 1982. Detection, isolation, and analysis of a released *Bordetella pertussis* product toxic to cultured tracheal cells. Infect Immun 36:782-794.

63. Lyons RS. 2001. Tracheal cytotoxin production by the Bordetellae. Ph.D. Washington University, St. Louis, MO.

64. Cloud-Hansen KA, Hackett KT, Garcia DL, Dillard JP. 2008. *Neisseria gonorrhoeae* uses two lytic transglycosylases to produce cytotoxic peptidoglycan monomers. J Bacteriol 190:5989-94.

65. Garcia DL, Dillard JP. 2008. Mutations in *ampG* or *ampD* affect peptidoglycan fragment release from *Neisseria gonorrhoeae*. J Bacteriol 190:3799-3807.

66. Chan JM, Dillard JP. 2016. *Neisseria gonorrhoeae* crippled its peptidoglycan fragment permease to facilitate toxic peptidoglycan monomer release. J Bacteriol 198:3029-3040.

67. Schleifer KH, Kandler O. 1972. Peptidoglycan types of bacterial cell walls and their taxonomic implications. Bacteriol Rev 36:407-77.

68. Vollmer W. 2008. Structural variation in the glycan strands of bacterial peptidoglycan. FEMS Microbiol Rev 32:287-306.

69. Strominger JL, Birge CH. 1965. Nucleotide accumulation induced in *Staphylococcus aurus* by glycine. J Bacteriol 89:1124-1127.

70. Knüsel F, Nüesch J, Scherrer M, Schmid K. 1967. Effect of lanthionine on the growth of a diaminopimelic acid-heterotrophic mutant of *Escherichia coli*. Pathol Microbiol (Basel) 30:871-9.

71. Schleifer KH, Hammes WP, Kandler O. 1976. Effect of endogenous and exogenous factors on the primary structures of bacterial peptidoglycan. Adv Microb Physiol 13:245-92.

72. Tsuruoka T, Tamura A, Miyata A, Takei T, Iwamatsu K, Inouye S, Matsuhashi M. 1984. Penicillin-insensitive incorporation of D-amino acids into cell wall

peptidoglycan influences the amount of bound lipoprotein in *Escherichia coli*. J Bacteriol 160:889-94.

73. Tsuruoka T, Tamura A, Miyata A, Takei T, Inouye S, Matsuhashi M. 1985. Second lytic target of beta-lactam compounds that have a terminal D-amino acid residue. Eur J Biochem 151:209-16.

74. Mengin-Lecreulx D, Blanot D, van Heijenoort J. 1994. Replacement of diaminopimelic acid by cystathionine or lanthionine in the peptidoglycan of *Escherichia coli*. J Bacteriol 176:4321-4327.

75. Mainardi JL, Villet R, Bugg TD, Mayer C, Arthur M. 2008. Evolution of peptidoglycan biosynthesis under the selective pressure of antibiotics in Gram-positive bacteria. FEMS Microbiol Rev 32:386-408.

76. Richaud C, Mengin-Lecreulx D, Pochet S, Johnson EJ, Cohen GN, Marlière P. 1993. Directed evolution of biosynthetic pathways. Recruitment of cysteine thioethers for constructing the cell wall of *Escherichia coli*. J Biol Chem 268:26827-26835.

77. Lam H, Oh DC, Cava F, Takacs CN, Clardy J, de Pedro MA, Waldor MK. 2009. D-amino acids govern stationary phase cell wall remodeling in bacteria. Science 325:1552-1555.

78. Horcajo P, de Pedro MA, Cava F. 2012. Peptidoglycan plasticity in bacteria: stress-induced peptidoglycan editing by noncanonical D-amino acids. Microb Drug Resist 18:306-313.

79. Kato K, Umemoto T, Sagawa H, Kotani S. 1979. Lanthionine as an essential constituent of cell wall peptidoglycan of *Fusobacterium nucleatum*. Curr Microbiol 3:147-151.

80. Vasstrand EN, Hofstad T, Endresen C, Jensen HB. 1979. Demonstration of lanthionine as a natural constituent of the peptidoglycan of *Fusobacterium nucleatum*. Infect Immun 25:775-780.

81. Kato K, Umemoto T, Fukuhara H, Sagawa H, Kotani S. 1981. Variation of dibasic amino acid in the cell wall peptidoglycan of bacteria of genus Fusobacterium. FEMS Microbiol Lett 10:81-85.

82. Vasstrand EN, Jensen HB, Miron T, Hofstad T. 1982. Composition of peptidoglycans of Bacteroidaceae: Determineation and distribution of lanthionine. Infect Immun 36:114-122.

83. Boniface A, Parquet C, Arthur M, Mengin-Lecreulx D, Blanot D. 2009. The elucidation of the structure of *Thermotoga maritima* peptidoglycan reveals two novel types of cross-link. J Biol Chem 284:21856-21862.

84. Guinand M, Ghuysen JM, Schleifer KH, Kandler O. 1969. The peptidoglycan in walls of *Butyribacterium rettgeri*. Biochemistry 8:200-7.

85. Mengin-Lecreulx D, Michaud C, Richaud C, Blanot D, van Heijenoort J. 1988. Incorporation of LL-diaminopimelic acid into peptidoglycan of *Escherichia coli* mutants lacking diaminopimelate epimerase encoded by *dapF*. J Bacteriol 170:2031-9.

86. Consaul SA, Wright LF, Mahapatra S, Crick DC, Pavelka MS, Jr. 2005. An unusual mutation results in the replacement of diaminopimelate with lanthionine

in the peptidoglycan of a mutant strain of *Mycobacterium smegmatis*. J Bacteriol 187:1612-20.

87. Jones RM, Jr., Popham DL, Schmidt AL, Neidle EL, Stabb EV. 2018. *Vibrio fischeri* DarR directs responses to D-aspartate and represents a group of similar LysR-type transcriptional regulators. J Bacteriol 200:e00773-17.

88. Weidel W, Pelzer H. 1964. Bagshaped macromolecules—a new outlook on bacterial cell walls. Adv Enzymol Relat Subj Biochem 26:193-232.

89. Brückner H, Westhauser T. 2003. Chromatographic determination of L- and D-amino acids in plants. Amino Acids 24:43-55.

90. Azúa I, Goiriena I, Baña Z, Iriberri J, Unanue M. 2014. Release and consumption of D-amino acids during growth of marine prokaryotes. Microb Ecol 67:1-12.

91. Kubota T, Kobayashi T, Nunoura T, Maruyama F, Deguchi S. 2016. Enantioselective utilization of D-amino acids by deep-sea microorganisms. Front Microbiol 7:511.

92. Radkov AD, McNeill K, Uda K, Moe LA. 2016. D-amino acid catabolism is common amond soil-dweling bacteria. Microbes Environ 31:165-8.

93. Drechsel H, Jung G. 1998. Peptide siderophores. J Pept Sci 4:147-181.

94. Peypoux F, Bonmatin JM, Wallach J. 1999. Recent trends in the biochemistry of surfactin. Appl Microbiol Biotechnol 51:553-63.

95. Martínez-Rodríguez S, Martínez-Gómez AI, Rodríguez-Vico F, Clemente-Jiménez JM, Las Heras-Vázquez FJ. 2010. Natural occurence and industrial applications of D-amino acids: a review. Chem Biodivers 7:1531-1548.

96. Fang W-Y, Dahiya R, Qin H-L, Mourya R, Maharaj S. 2016. Natural proline-rich cyclopeptides from marine organisms: chemistry, synthetic methodologies and biological status. Mar Drugs 14:194.

97. Rogers HJ. 1974. Peptidoglycans (mucopeptides): structure, function and variations. Ann NY Acad Sci 235:29-51.

98. Candela T, Fouet A. 2006. Poly-gamma-glutamate in bacteria. Mol Microbiol 60:1091-1098.

99. Cava F, de Pedro MA, Lam H, Davis BM, Waldor MK. 2011. Distinct pathways for modification of the bacterial cell wall by non-canonical D-amino acids. EMBO J 30:3442-3453.

100. Cava F, Lam H, de Pedro MA, Waldor MK. 2011. Emerging knowledge of regulatory roles of D-amino acids in bacteria. Cell Mol Life Sci 68:817-831.

101. Lupoli TJ, Tsukamoto H, Doud EH, Wang T-SA, Walker S, Kahne D. 2011. Transpeptidase-mediated incorporation of D-amino acids into bacterial peptidoglycan. J Am Chem Soc 133:10748-10751.

102. Luo Z, Guo Y, Liu J, Qiu H, Zhao M, Zou W, Li S. 2016. Microbial synthesis of poly-γ-glutamic acid: current progress, challenges, and future perspectives. Biotechnol Biofuel 9:134.

103. Espaillat A, Carrasco-Lopez C, Bernardo-Garcia N, Rojas-Altuve A, Klett J, Morreale A, Hermoso JA, Cava F. 2021. Binding of non-canonical peptidoglycan controls *Vibrio cholerae* broad spectrum racemase activity. Comput Struct Biotechnol J 19:1119-1126.

104. Caparrós M, Pisabarro AG, MA dP. 1992. Effect of D-amino acids on structure and synthesis of peptidoglycan in *Escherichia coli*. J Bacteriol 174:5549-5559.

105. Reynolds PE, Snaith HA, Maguire AJ, Dutka-Malen S, Courvalin P. 1994. Analysis of peptidoglycan precursors in vancomycin-resistant *Enterococcus gallinarum* BM4174. Biochem J 301:5-8.

106. Friedman M. 1999. Chemistry, nutrition, and microbiology of D-amino acids. J Agric Food Chem 47:3457-3479.

107. Radkov AD, Moe LA. 2014. Bacterial synthesis of D-amino acids. Appl Microbiol Biotechnol 98:5363-5374.

108. Konz D, Klens A, Schörgendorfer K, Marahiel MA. 1997. The bacitracin biosynthesis operon of *Bacillus licheniformis* ATCC 10716: molecular characterization of three multi-modular peptide synthetases. Chem Biol 4:927-37.

109. Vahdati SN, Behboudi H, Navasatli SA, Tavakoli S, Safavi M. 2022. New insights into the inhibitory roles and mechanisms of D-amino acids in bacterial biofilms in medicine, industry, and agriculture. Microbiol Res 263:127107.

110. Irukayama-Tomobe Y, Tanaka H, Yokomizo T, Hashidate-Yoshida T, Yanagisawa M, Sakurai T. 2009. Aromatic D-amino acids act as chemoattractant factors for human leukocytes through a G protein-coupled receptor, GPR109B. Proc Natl Acad Sci U S A 106:3930-4.

111. Nakade Y, Iwata Y, Furuichi K, Mita M, Hamase K, Konno R, Miyake T, Sakai N, Kitajima S, Toyama T. 2018. Gut microbiota–derived D-serine protects against acute kidney injury. JCI Insight 3.

112. Sasabe J, Suzuki M. 2018. Emerging role of D-amino acid metabolism in the innate defense. Front Microbiol 9:933.

113. Suzuki M, Sujino T, Chiba S, Harada Y, Goto M, Takahashi R, Mita M, Hamase K, Kanai T, Ito M, Waldor MK, Yasui M, Sasabe J. 2021. Host-microbe cross-talk governs amino acid chirality to regulate survival and differentiation of B cells. Science Advances 7:eabd6480.

114. Raterman EL, Welch RA. 2013. Chemoreceptors of *Escherichia coli* CFT073 play redundant roles in chemotaxis toward urine. PLoS One 8:e54133.

115. Cerna-Vargas JP, Santamaría-Hernando S, Matilla MA, Rodríguez-Herva JJ, Daddaoua A, Rodríguez-Palenzuela P, Krell T, López-Solanilla E. 2019. Chemoperception of specific amino acids controls phytopathogenicity in *Pseudomonas syringae* pv. tomato. mBio 10:10.1128/mbio.01868-19.

116. Irazoki O, ter Beek J, Alvarez L, Mateus A, Colin R, Typas A, Savitski MM, Sourjik V, Berntsson RPA, Cava F. 2023. D-amino acids signal a stress-dependent run-away response in *Vibrio cholerae*. Nat Microbiol 8:1549-1560.

117. Kolodkin-Gal I, Romero D, Cao S, Clardy J, Kolter R, Losick R. 2010. D-amino acids trigger biofilm disassembly. Science 328:627-9.

118. Hochbaum AI, Kolodkin-Gal I, Foulston L, Kolter R, Aizenberg J, Losick R. 2011. Inhibitory Effects of D-Amino Acids on *Staphylococcus aureus* Biofilm Development. J Bacteriol 193:5616-5622.

119. Leiman SA, May JM, Lebar MD, Kahne D, Kolter R, Losick R. 2013. D-amino acids indirectly inhibit biofilm formation in *Bacillus subtilis* by interfering with protein synthesis. J Bacteriol 195:5391-5.

120. Sanchez Z, Tani A, Kimbara K. 2013. Extensive reduction of cell viability and enhanced matrix production in *Pseudomonas aeruginosa* PAO1 flow biofilms treated with a D-amino acid mixture. Appl Environ Microbiol 79:1396-9.

121. Ramón-Peréz ML, Diaz-Cedillo F, Ibarra JA, Torales-Cardeña A, Rodríguez-Martínez S, Jan-Roblero J, Cancino-Diaz ME, Cancino-Diaz JC. 2014. D-amino acids inhibit biofilm formation in *Staphylococcus epidermidis* strains from ocular infections. J Med Microbiol 63:1369-1376.

122. Sarkar S, Pires MM. 2015. D-amino acids do not inhibit biofilm formation in *Staphylococcus aureus*. PLoS One 10:e0117613.

123. Bucher T, Kartvelishvily E, Kolodkin-Gal I. 2016. Methodologies for studying *B. subtilis* biofilms as a model for characterizing small molecule biofilm inhibitors. J Vis Exp doi:10.3791/54612.

124. Rumbo C, Vallejo JA, Cabral MP, Martínez-Guitián M, Pérez A, Beceiro A, Bou G. 2016. Assessment of antivirulence activity of several D-amino acids against *Acinetobacter baumannii* and *Pseudomonas aeruginosa*. J Antimicrob Chemother 71:3473-3481.

125. Kao WT, Frye M, Gagnon P, Vogel JP, Chole R. 2017. D-amino acids do not inhibit *Pseudomonas aeruginosa* biofilm formation. Laryngoscope Investig Otolaryngol 2:4-9.

126. Su X, Cheng X, Wang Y, Luo J. 2021. Effect of different D-amino acids on biofilm formation of mixed microorganisms. Water Sci Technol 85:116-124.

127. Hishinuma F, Izaki K, Takahashi H. 1969. Effects of glycine and D-amino acids on growth of various microorganisms. Agric Biol Chem 33:1577-1586.

128. Giegé R, Sissler M, Florentz C. 1998. Universal rules and idiosyncratic features in tRNA identity. Nucleic Acids Res 26:5017-5035.

129. Soutourina J, Plateau P, Blanquet S. 2000. Metabolism of D-aminoacyl-tRNAs in *Escherichia coli* and *Saccharomyces cerevisiae* cells. J Biol Chem 275:32535-32542.

130. Soutourina O, Soutourina J, Blanquet S, Plateau P. 2004. Formation of d-Tyrosyl-tRNATyr accounts for the toxicity of D-tyrosine toward *Escherichia coli*. J Biol Chem 279:42560-42565.

131. Englander MT, Avins JL, Fleisher RC, Liu B, Effraim PR, Wang J, Schulten K, Leyh TS, Gonzalez RL, Jr., Cornish VW. 2015. The ribosome can discriminate the chirality of amino acids within its peptidyl-transferase center. Proc Natl Acad Sci U S A 112:6038-43.

132. Alvarez L, Aliashkevich A, de Pedro MA, Cava F. 2018. Bacterial secretion of D-arginine controls environmental microbial biodiversity. ISME J 12:438-450.

133. Arkin H, Grossowicz N. 1970. Inhibition by D-glutamate of growth and glutamate dehydrogenase activity of *Neurospora crassa*. J Gen Microbiol 61:255-61.

134. Dörr T, Lam H, Alvarez L, Cava F, Davis BM, Waldor MK. 2014. A novel peptidoglycan binding protein crucial for PBP1A-mediated cell wall biogenesis in *Vibrio cholerae*. PLoS Genet 10:e1004433.

135. Hills GM. 1949. Chemical factors in the germination of spore-bearing aerobes; the effects of amino acids on the germination of *Bacillus anthracis*, with some observations on the relation of optical form to biological activity. Biochem J 45:363-70.

136. Fey G, Gould GW, Hitchins AD. 1964. Identification of D-Alanine as the auto-inhibitor of germination of *Bacillus globigii* spores. Microbiology 35:229-236.

137. Yasuda Y, Tochikubo K. 1984. Relation between D-glucose and L- and D-alanine in the initiation of germination of *Bacillus subtilis* spore. Microbiol Immunol 28:197-207.

138. Hu H, Sa Q, Koehler TM, Aronson AI, Zhou D. 2006. Inactivation of *Bacillus anthracis* spores in murine primary macrophages. Cell Microbiol 8:1634-1642.

139. Hu H, Emerson J, Aronson AI. 2007. Factors involved in the germination and inactivation of *Bacillus anthracis* spores in murine primary macrophages. FEMS Microbiol Lett 272:245-250.

140. Wood WA, Gunsalus IC. 1951. D-Alanine formation; a racemase in *Streptococcus faecalis*. J Biol Chem 190:403-16.

141. Narrod S, Wood W. 1952. Evidence for a glutamic acid racemase in *Lactobacillus arabinosus*. Arch Biochem Biophys 35:462-463.

142. Antia M, Hoare DS, Work E. 1957. The stereoisomers of α∈-diaminopimelic acid. 3. Properties and distribution of diaminopimelic acid racemase, an enzyme causing interconversion of the ll and meso isomers. Biochem J 65:448-459.

143. Fischer C, Ahn Y-C, Vederas JC. 2019. Catalytic mechanism and properties of pyridoxal 5′-phosphate independent racemases: how enzymes alter mismatched acidity and basicity. Nat Prod Rep 36:1687-1705.

144. Liang J, Han Q, Tan Y, Ding H, Li J. 2019. Current advances on structure-function relationships of pyridoxal 5'-phosphate-dependent enzymes. Front Mol Biosci 6:4.

145. Adams E. 1972. Amino Acid Racemases and Epimerases, p 479-507. *In* Boyer PD (ed), The Enzymes, vol 6. Academic Press.

146. Yoshimura T, Esaki N. 2003. Amino acid racemases: functions and mechanisms. J Biosci Bioeng 96:103-109.

147. Conti P, Tamborini L, Pinto A, Blondel A, Minoprio P, Mozzarelli A, De Micheli C. 2011. Drug Discovery Targeting Amino Acid Racemases. Chem Rev 111:6919-6946.

148. Bellais S, Arthur M, Dubost L, Hugonnet JE, Gutmann L, van Heijenoort J, Legrand R, Brouard JP, Rice L, Mainardi JL. 2006. Aslfm, the D-aspartate ligase responsible for the addition of D-aspartic acid onto the peptidoglycan precursor of *Enterococcus faecium*. J Biol Chem 281:11586-94.

149. Chen IC, Lin WD, Hsu SK, Thiruvengadam V, Hsu WH. 2009. Isolation and characterization of a novel lysine racemase from a soil metagenomic library. Appl Environ Microbiol 75:5161-6.

150. Miyamoto T, Katane M, Saitoh Y, Sekine M, Homma H. 2017. Identification and characterization of novel broad-spectrum amino acid racemases from *Escherichia coli* and *Bacillus subtilis*. Amino Acids 49:1885-1894.

151. Soda K, Osumi T. 1971. Amino acid racemase (*Pseudomonas striata*). Methods Enzymol 17:629-636.

152. Lim YH, Yokoigawa K, Esaki N, Soda K. 1993. A new amino acid racemase with threonine alpha-epimerase activity from *Pseudomonas putida*: purification and characterization. J Bacteriol 175:4213-7.

153. Matsui D, Oikawa T, Arakawa N, Osumi S, Lausberg F, Stabler N, Freudl R, Eggeling L. 2009. A periplasmic, pyridoxal-5'-phosphate-dependent amino acid racemase in *Pseudomonas taetrolens*. Appl Microbiol Biotechnol 83:1045-54.

154. Kuan Y-C, Kao C-H, Chen C-H, Chen C-C, Hu H-Y, Hsu W-H. 2011. Biochemical characterization of a novel lysine racemase from *Proteus mirabilis* BCRC10725. Process Biochem 46:1914-1920.

155. Kato S, Hemmi H, Yoshimura T. 2012. Lysine racemase from a lactic acid bacterium, *Oenococcus oeni*: structural basis of substrate specificity. J Biochem 152:505-508.

156. Espaillat A, Carrasco-Lopez C, Bernardo-Garcia N, Pietrosemoli N, Otero LH, Alvarez L, de Pedro MA, Pazos F, Davis BM, Waldor MK, Hermoso JA, Cava F. 2014. Structural basis for the broad specificity of a new family of amino-acid racemases. Acta Crystallogr D Biol Crystallogr 70:79-90.

157. Miyamoto T, Katane M, Saitoh Y, Sekine M, Homma H. 2018. Cystathionine beta-lyase is involved in D-amino acid metabolism. Biochem J 475:1397-1410.

158. Lyell NL, Septer AN, Dunn AK, Duckett D, Stoudenmire JL, Stabb EV. 2017. An expanded transposon mutant library reveals that *Vibrio fischeri* δ-aminolevulinate auxotrophs can colonize *Euprymna scolopes*. Appl Environ Microbiol 83:e02470-16.

159. Inagaki K, Tanizawa K, Tanaka H, Soda K. 1984. Purification and properties of amino acid racemase from *Aeromonas punctata* subsp. *caviae*. Prog Clin Biol Res 144a:355-63.

160. Inagaki K, Tanizawa K, Tanaka H, Soda K. 1987. Purification and Characterization of Amino Acid Racemase with Very Broad Substrate Specificity from *Aeromonas caviae*. Agric Biol Chem 51:173-180.

161. Badet B, Lee K, Floss HG, Walsh CT. 1984. Stereochemical studies of processing of D- and L-isomers of suicide substrates by an amino acid racemase from *Pseudomonas striata*. J Chem Soc Chem Commun doi:10.1039/C39840000838:838-840.

162. Kino K, Sato M, Yoneyama M, Kirimura K. 2007. Synthesis of DL-tryptophan by modified broad specificity amino acid racemase from *Pseudomonas putida* IFO 12996. Appl Microbiol Biotechnol 73:1299-305.

163. Radkov AD, Moe LA. 2013. Amino acid racemization in *Pseudomonas putida* KT2440. J Bacteriol 195:5016-24.

164. Radkov AD, Moe LA. 2018. A broad spectrum racemase in *Pseudomonas putida* KT2440 plays a key role in amino acid catabolism. Front Microbiol 9:1343.

165. Teufel F, Almagro Armenteros JJ, Johansen AR, Gíslason MH, Pihl SI, Tsirigos KD, Winther O, Brunak S, von Heijne G, Nielsen H. 2022. SignalP 6.0 predicts all five types of signal peptides using protein language models. Nat Biotechnol 40:1023-1025.

166. Yorifuji T, Ogata K, Soda K. 1971. Arginine racemase of *Pseudomonas graveolens*: I. Purification, crystallization, and properties. J Biol Chem 246:5085-5092.

167. Yamauchi T, Choi SY, Okada H, Yohda M, Kumagai H, Esaki N, Soda K. 1992. Properties of aspartate racemase, a pyridoxal 5'-phosphate-independent amino acid racemase. J Biol Chem 267:18361-4.

168. Mutaguchi Y, Ohmori T, Wakamatsu T, Doi K, Ohshima T. 2013. Identification, purification, and characterization of a novel amino acid racemase, isoleucine 2-epimerase, from *Lactobacillus* species. J Bacteriol 195:5207-15.

169. Fisher SL. 2008. Glutamate racemase as a target for drug discovery. Microb Biotechnol 1:345-360.

170. Zhou J, Cai Y, Liu Y, An H, Deng K, Ashraf MA, Zou L, Wang J. 2022. Breaking down the cell wall: still an attractive antibacterial strategy. Front Microbiol 13:952633.

171. Azam MA, Jayaram U. 2016. Inhibitors of alanine racemase enzyme: a review. J Enzyme Inhib Med Chem 31:517-26.

172. Strominger JL, Ito E, Threnn RH. 1960. Competitive inhibition of enzymatic reactions by oxamycin. J Am Chem Soc 82:998-999.

173. Stabb EV. 2006. The *Vibrio fischeri-Euprymna scolopes* light organ symbiosis, p 204-218. *In* al FTe (ed), The Biology of Vibrios. ASM Press, Washington, DC.

174. Stabb EV, Visick KL. 2013. *Vibrio fischeri*: A bioluminescent light-organ symbiont of the bobtail squid *Euprymna scolopes*, p 497-532. *In* E R, Delong EF, Lory S, Stackebrandt E, Thompson F (ed), The Prokaryotes: Prokaryotic biology and symbiotic associations, Fourth ed. SpringerReference.

175. Visick KL, Stabb EV, Ruby EG. 2021. A lasting symbiosis: how *Vibrio fischeri* finds a squid partner and persists within its natural host. Nat Rev Microbiol 19:654-665.

176. Doublet P, van Heijenoort J, Bohin J, Mengin-Lecreulx D. 1993. The *murI* gene of *Escherichia coli* is an essential gene that encodes a glutamate racemase activity. J Bacteriol 175:2970-2979.

177. Morayya S, Awasthy D, Yadav R, Ambady A, Sharma U. 2015. Revisiting the essentiality of glutamate racemase in *Mycobacterium tuberculosis*. Gene 555:269-276.

178. Brooks II JF, Gyllborg MC, Cronin DC, Quillin SJ, Mallama CA, Foxall R, Whistler C, Goodman AL, Mandel MJ. 2014. Global discovery of colonization determinants in the squid symbiont *Vibrio fischeri*. Proc Natl Acad Sci U S A 111:17284-17289.

179. Doublet P, van Heijenoort J, Mengin-Lecreulx D. 1992. Identification of the *Escherichia coli* murI gene, which is required for the biosynthesis of D-glutamic acid, a specific component of bacterial peptidoglycan. J Bacteriol 174:5772-9.

180. El Zoeiby A, Sanschagrin F, Levesque RC. 2003. Structure and function of the Mur enzymes: development of novel inhibitors. Mol Microbiol 47:1-12.

181. Mahapatra S, Yagi T, Belisle JT, Espinosa BJ, Hill PJ, McNeil MR, Brennan PJ, Crick DC. 2005. Mycobacterial lipid II is composed of a complex mixture of modified muramyl and peptide moieties linked to decaprenyl phosphate. J Bacteriol 187:2747-2757.

182. Lyell NL, Dunn AK, Bose JL, Vescovi SL, Stabb EV. 2008. Effective mutagenesis of *Vibrio fischeri* by using hyperactive mini-Tn*5* derivatives. Appl Environ Microbiol 74:7059-7063.

183. Sega GA. 1984. A review of the genetic effects of ethyl methanesulfonate. Mutat Res 134:113-142.

184. Chen L, Duan L, Sun M, Yang Z, Li H, Hu K, Yang H, Liu L. 2022. Current trends and insights on EMS mutagenesis application to studies on plant abiotic stress tolerance and development. Front Plant Sci 13:1052569.

185. Bernardo-Garcia N, Sánchez-Murcia P, Gago F, Cava F, Hermoso JA. 2016. Structural bioinformatics in broad-spectrum racemases: a new path in antimicrobial research. Curr Org Chem 20:1222-1231.

186. Cava F. 2017. Divergent functional roles of D-amino acids secreted by *Vibrio cholerae*. Int Microbiol 20:149-150.

187. Aliashkevich A, Alvarez L, Cava F. 2018. New insights into the mechanisms and biological roles of D-amino acids in complex eco-systems. Front Microbiol 9:683.

188. Nielsen H, Tsirigos KD, Brunak S, von Heijne G. 2019. A brief history of protein sorting prediction. Protein J 38:200-216.

189. Strominger JL, Threnn RH, Scott SS. 1959. Oxamycin, a competitive antagonist of the incorporation of D-alanine into a uridine nucleotide in *Staphylococcus aureus*. J Am Chem Soc 81:3803-3804.

190. Jones RM, Jr. 2017. Characterization of *Vibrio fischeri* mutants with altered amino acid metabolism and peptidoglycan biosynthesis. Doctor of Philosophy. University of Goergia.

191. Zhao Y, Liu Y, Li N, Muhammad M, Gong S, Ju J, Cai T, Wang J, Zhao B, Liu D. 2022. Significance of broad-spectrum racemases for the viability and pathogenicity of *Aeromonas hydrophila*. Future Microbiol 17:251-265.

192. Guex N, Peitsch MC, Schwede T. 2009. Automated comparative protein structure modeling with SWISS-MODEL and Swiss-PdbViewer: a historical perspective. Electrophoresis 30 Suppl 1:S162-73.

193. Bienert S, Waterhouse A, de Beer TA, Tauriello G, Studer G, Bordoli L, Schwede T. 2017. The SWISS-MODEL Repository-new features and functionality. Nucleic Acids Res 45:D313-d319.

194. Waterhouse A, Bertoni M, Bienert S, Studer G, Tauriello G, Gumienny R, Heer FT, de Beer TAP, Rempfer C, Bordoli L, Lepore R, Schwede T. 2018. SWISS-MODEL: homology modelling of protein structures and complexes. Nucleic Acids Res 46:W296-W303.

195. Epstein IG, Nair KG, Boyd LJ. 1955. Cycloserine, a new antibiotic, in the treatment of human pulmonary tuberculosis: a preliminary report. Antibiotic Med Clin Ther (New York) 1:80-93.

196. de Chiara C, Homsak M, Prosser GA, Douglas HL, Garza-Garcia A, Kelly G, Purkiss AG, Tate EW, de Carvalho LPS. 2020. D-Cycloserine destruction by alanine racemase and the limit of irreversible inhibition. Nat Chem Biol 16:686-694.

197. de Chiara C, Prosser GA, Ogrodowicz R, de Carvalho LPS. 2023. Structure of the D-cycloserine-resistant variant D322N of alanine racemase from *Mycobacterium tuberculosis*. ACS Bio Med Chem Au 3:233-239.

198. Prosser GA, Rodenburg A, Khoury H, de Chiara C, Howell S, Snijders AP, de Carvalho LP. 2016. Glutamate racemase is the primary target of β-chloro-D-alanine in *Mycobacterium tuberculosis*. Antimicrob Agents Chemother 60:6091-6099.

199. Pawar A, Jha P, Konwar C, Chaudhry U, Chopra M, Saluja D. 2019. Ethambutol targets the glutamate racemase of *Mycobacterium tuberculosis*-an enzyme involved in peptidoglycan biosynthesis. Appl Microbiol Biotechnol 103:843-851.

200. Pawar A, Jha P, Chopra M, Chaudhry U, Saluja D. 2020. Screening of natural compounds that targets glutamate racemase of *Mycobacterium tuberculosis* reveals the anti-tubercular potential of flavonoids. Sci Rep 10:949.

201. Bongaerts N, Edoo Z, Abukar AA, Song X, Sosa-Carrillo S, Haggenmueller S, Savigny J, Gontier S, Lindner AB, Wintermute EH. 2022. Low-cost anti-mycobacterial drug discovery using engineered *Escherichia coli*. Nat Commun 13:3905.

202. Kumar A, Singh E, Jha RK, Khan RJ, Jain M, Varshney S, Muthukumaran J, Singh AK. 2023. Targeting multi-drug-resistant *Acinetobacter baumannii*: a structure-based approach to identify the promising lead candidates against glutamate racemase. J Mol Model 29:188.

203. Stogios PJ, Savchenko A. 2020. Molecular mechanisms of vancomycin resistance. Protein Sci 29:654-669.

204. Adin DM, Visick KL, Stabb EV. 2008. Identification of a cellobiose utilization gene cluster with cryptic beta-galactosidase activity in *Vibrio fischeri*. Appl Environ Microbiol 74:4059-4069.

205. Bassis CM, Visick KL. 2010. The cyclic-di-GMP phosphodiesterase BinA negatively regulates cellulose-containing biofilms in *Vibrio fischeri*. J Bacteriol 192:1269-78.

206. Lyell NL, Dunn AK, Bose JL, Stabb EV. 2010. Bright mutants of *Vibrio fischeri* ES114 reveal conditions and regulators that control bioluminescence and expression of the *lux* operon. J Bacteriol 192:5103-14.

207. Miyashiro T, Klein W, Oehlert D, Cao X, Schwartzman J, Ruby EG. 2011. The *N*-acetyl-D-glucosamine repressor NagC of *Vibrio fischeri* facilitates colonization of *Euprymna scolopes*. Mol Microbiol 82:894-903.

208. Post DM, Yu L, Krasity BC, Choudhury B, Mandel MJ, Brennan CA, Ruby EG, McFall-Ngai MJ, Gibson BW, Apicella MA. 2012. O-antigen and core carbohydrate of *Vibrio fischeri* lipopolysaccharide: composition and analysis of their role in *Euprymna scolopes* light organ colonization. J Biol Chem 287:8515-30.

209. Ray VA, Visick KL. 2012. LuxU connects quorum sensing to biofilm formation in *Vibrio fischeri*. Mol Microbiol 86:954-70.

210. Brennan CA, Mandel MJ, Gyllborg MC, Thomasgard KA, Ruby EG. 2013. Genetic determinants of swimming motility in the squid light-organ symbiont *Vibrio fischeri*. MicrobiologyOpen 2:576-94.

211. Lyell NL, Stabb EV. 2013. Symbiotic characterization of *Vibrio fischeri* ES114 mutants that display enhanced luminescence in culture. Appl Environ Microbiol 79:2480-3.

212. Visick KL, Quirke KP, McEwen SM. 2013. Arabinose induces pellicle formation by *Vibrio fischeri*. Appl Environ Microbiol 79:2069-80.

213. Eickhoff MJ, Bassler BL. 2020. *Vibrio fischeri* siderophore production drives competitive exclusion during dual-species growth. Mol Microbiol 114:244-261.

214. Fidopiastis PM, Mariscal V, McPherson JM, McAnulty S, Dunn A, Stabb EV, Visick KL. 2021. *Vibrio fischeri* amidase activity is required for normal cell division, motility, and symbiotic competence. Appl Environ Microbiol 87:e02109-20.

215. Smith S, Salvato F, Garikipati A, Kleiner M, Septer AN. 2021. Activation of the Type VI secretion system in the squid symbiont *Vibrio fischeri* requires the transcriptional regulator TasR and the structural proteins TssM and TssA. J Bacteriol 203:e0039921.

216. Dunn AK, Martin MO, Stabb EV. 2005. Characterization of pES213, a small mobilizable plasmid from *Vibrio fischeri*. Plasmid 54:114-134.

217. Getz LJ, Thomas NA. 2018. The transcriptional regulator HlyU positively regulates expression of *exsA*, leading to Type III secretion system 1 activation in *Vibrio parahaemolyticus*. J Bacteriol 200:e00653-17.

218. Stoudenmire JL, Black M, Fidopiastis PM, Stabb EV. 2019. Mutagenesis of *Vibrio fischeri* and other marine bacteria using hyperactive mini-Tn*5* derivatives, p 87-104, Microbioal Transposon Mutagenesis: Protocols and Applications. Springer New York.

219. Hu M, Zhang H, Gu D, Ma Y, Zhou X. 2020. Identification of a novel bacterial receptor that binds tail tubular proteins and mediates phage infection of *Vibrio parahaemolyticus*. Emerg Microbes Infect 9:855-867.

220. Tchelet D, Salomon D. 2022. A rapid fluorescence-based screen to identify regulators and components of interbacterial competition mechanisms in bacteria, p 11-24. *In* Gal-Mor O (ed), Bacterial Virulence: Methods and Protocols doi:10.1007/978-1-0716-1971-1_2. Springer US, New York, NY.

221. Miller JH. 1992. A short course in bacterial genetics: a laboratory manual and handbook for *Escherichia coli* and related bacteria. Cold Spring Harbor Laboratory Press, Plainview, N.Y.

222. Stabb EV, Ruby EG. 2002. RP4-based plasmids for conjugation between *Escherichia coli* and members of the Vibrionaceae. Methods Enzymol 358:413-426.

223. Hanahan D. 1983. Studies on transformation of *Escherichia coli* with plasmids. J Mol Biol 166:557-80.

224. Septer AN, Wang Y, Ruby EG, Stabb EV, Dunn AK. 2011. The haem-uptake gene cluster in *Vibrio fischeri* is regulated by Fur and contributes to symbiotic colonization. Environ Microbiol 13:2855-2864.

225. Visick KL, Hodge-Hanson KM, Tischler AH, Bennett AK, Mastrodomenico V. 2018. Tools for rapid genetic engineering of *Vibrio fischeri*. Appl Environ Microbiol 84:e00850-18.

226. Pollack-Berti A, Wollenberg MS, Ruby EG. 2010. Natural transformation of *Vibrio fischeri* requires *tfoX* and *tfoY*. Environ Microbiol 12:2302-2311.

227. Hayashi K. 1975. A rapid determination of sodium dodecyl sulfate with methylene blue. Anal Biochem 67:503-506.

228. Gonzalez-Castra MJ, Lopez-Hernandez J, Simal-Lozano J, Oruna-Concha MJ. 1997. Determination of amino acids in green beans by derivatization of phenylisothiociante and high-performace liquid chromatography with ultraviolet detection. J Chromatogr Sci 35:181-185.

229. Popham DL, Helin J, Costello CE, Setlow P. 1996. Analysis of the peptidoglycan structure of *Bacillus subtilis* endospores. J Bacteriol 178:6451-6458.

230. Girardin SE, Travassos LH, Hervé M, Blanot D, Boneca IG, Philpott DJ, Sansonetti PJ, Mengin-Lecreulx D. 2003. Peptidoglycan molecular requirements allowing detection by Nod1 and Nod2. J Biol Chem 278:41702-41708.

231. Lim J-H, Kim M-S, Kim H-E, Yano T, Oshima Y, Aggarwal K, Goldman WE, Silverman N, Kurata S, Oh B-H. 2006. Structural basis for preferential recognition of diaminopimelic acid-type peptidoglycan by a subset of peptidoglycan recognition proteins. J Biol Chem 281:8286-8295.

232. Grimes CL, Ariyananda LDZ, Melnyk JE, O'Shea EK. 2012. The innate innume protein Nod2 binds directly to MDP, a bacterial cell wall fragment. J Am Chem Soc 134:13535-13537.

233. Tanaka M, Kato Y, Kinoshita S. 1961. Glutamic acid racemase from *Lactobacillus fermenti* purification and properties. Biochem Biophys Res Comm 4:114-117.

234. Miyamoto T, Homma H. 2021. D-Amino acid metabolism in bacteria. J Biochem 170:5-13.

235. Cabral MP, Garcia P, Beceiro A, Rumbo C, Perez A, Moscoso M, Bou G. 2017. Design of live attenuated bacterial vaccines based on D-glutamate auxotrophy. Nat Commun 8:15480.

236. Muhammad M, Bai J, Alhassan AJ, Sule H, Ju J, Zhao B, Liu D. 2020. Significance of glutamate racemase for the viability and cell wall integrity of *Streptococcus iniae*. Biochemistry 85:248-256.

237. Hoffmann B, Messer W, Schwarz U. 1972. Regulation of polar cap formation in the life cycle of *Escherichia coli*. J Supramol Struct 1:29-37.

238. Dougherty TJ, Thanassi JA, Pucci MJ. 1993. The *Escherichia coli* mutant requiring D-glutamic acid is the result of the mutations in two distinct genetic loci. J Bacteriol 175:111-116.

239. Marcus M, Halpern YS. 1967. Genetic analysis of glutamate transport and glutamate decarboxylase in Escherichia coli. J Bacteriol 93:1409-1415.

240. Marcus M, YS H. 1969. Genetic analysis of the glutamate permease in *Escherichia coli* K-12. J Bacteriol 97:1118-1128.

241. Essenberg RC. 1984. Use of homocysteic acid for selecting mutants at the *gltS* locus of *Escherichia coli* K12. J Gen Microbiol 130:1311-1314.

242. Altschul SF, Gish W, Miller W, Myers EW, Lipman DJ. 1990. Basic local alignment search tool. J Mol Biol 215:403-10.

243. Altschul SF. 1991. Amino acid substitution matrices from an information theoretic perspective. J Mol Biol 219:555-565.

244. Altschul SF, Gish W. 1996. Local alignment statistics, p 460-480, Methods Enzymol, vol 266. Academic Press.

245. Deguchi Y, Yamato I, Y A. 1989. Molecular cloning of *gltS* and *gltP*, which encode glutamate carriers of *Escherichia coli* B. J Bacteriol 171:1314-1319.

246. Dobrowolski A, Sobczak-Elbourne I, Lolkema JS. 2007. Membrane topology prediction by hydropathy profile alignment: membrane topology of the Na+-glutamate transporter GltS. Biochemistry 46:2326-2332.

247. Szvetnik A, Gal J, Kalman M. 2007. Membrane topology of the GltS Na+/glutamate permease of *Escherichia coli*. FEMS Microbiol Lett 275:71-79.

248. Yu NY, Wagner JR, Laird MR, Melli G, Rey S, Lo R, Dao P, Sahinalp SC, Ester M, Foster LJ, Brinkman FSL. 2010. PSORTb 3.0: improved protein subcellular localization prediction with refined localization subcategories and predictive capabilities for all prokaryotes. Bioinformatics 26:1608-1615.

249. Krupnik T, Sobczak-Elbourne I, Lolkema JS. 2011. Turnover and accessibility of a reentrant loop of the Na+-glutamate transporter GltS are modulated by the central cytoplasmic loop. Mol Membr Biol 28:462-472.

250. Höltje J-V. 1998. Growth of the stress-bearing and shape-maintaining murein sacculus of *Escherichia coli*. Microbiol Mol Biol Rev 62:181-203.

251. Whistler CA, Ruby EG. 2003. GacA regulates symbiotic colonization traits of *Vibrio fischeri* and facilitates a beneficial association with an animal host. J Bacteriol 185:7202-7212.

252. Song H, Li Y, Wang Y. 2023. Two-component system GacS/GacA, a global response regulator of bacterial physiological behaviors. Eng Microbiol 3:100051.

253. Miner KM, L F. 1974. Sodium-stimulated glutamate transport in osmotically shocked cells and membrane vesicles of *Escherichia coli*. J Bacteriol 117:1093-1098.

254. Fujimura T, Yamato I, Y A. 1983. Mechanism of glutamate transport in *Escherichia coli* B. 1. Proton-dependent and sodium ion dependent binding of glutamate to a glutamate carrier in the cytoplasmic membrane. Biochemistry 22:1954-1959.

255. Fujimura T, Yamato I, Anraku Y. 1983. Mechanism of glutamate transport in *Escherichia coli* B. 2. Kinetics of glutamate transport driven by artificially imposed proton and sodium ion gradients across the cytoplasmic membrane. Biochemistry 22:1959-1965.

256. Booth IR, Kleppang KE, Kempsell KE. 1989. A Genetic Locus for the GltII-GIutamate Transport System in *Escherichia coli*. Microbiol Res 135:2767-2774.

257. Kalman M, Gentry DR, M C. 1991. Characterization of the *Escherichia coli* K12 *gltS* glutamate permease gene. Mol Gen Genet 225:379-386.

258. Hille B. 1978. Ionic channels in excitable membranes. Current problems and biophysical approaches. Biophys J 22:283-294.

259. MacKinnon R. 1995. Pore loops: an emerging theme in ion channel structure. Neuron 14:889-92.

260. Doyle DA, Morais Cabral J, Pfuetzner RA, Kuo A, Gulbis JM, Cohen SL, Chait BT, MacKinnon R. 1998. The structure of the potassium channel: molecular basis of K+ conduction and selectivity. Science 280:69-77.

261. Murata K, Mitsuoka K, Hirai T, Walz T, Agre P, Heymann JB, Engel A, Fujiyoshi Y. 2000. Structural determinants of water permeation through aquaporin-1. Nature 407:599-605.

262. van der Cruijsen EA, Nand D, Weingarth M, Prokofyev A, Hornig S, Cukkemane AA, Bonvin AM, Becker S, Hulse RE, Perozo E, Pongs O, Baldus M. 2013. Importance of lipid-pore loop interface for potassium channel structure and function. Proc Natl Acad Sci U S A 110:13008-13.

263. Wientjes FB, Woldringh CL , N N. 1991. Amount of peptidoglycan in cell walls of Gram-negative bacteria. J Bacteriol 173:7684-7691.

264. Bada JL. 1982. Racemization of amino acids in nature. Interdiscip Sci Rev 7:30-46.

265. Zagon J, Dehne L-I, Bögl K-W. 1994. D-amino acids in organisms and food. Nutr Res 14:445-463.

266. Marcone GL, Rosini E, Crespi E, Pollegioni L. 2020. D-amino acids in foods. Appl Microbiol Biotechnol 104:555-574.

267. Khan K, Elia M. 1991. Factors affecting the stability of L-glutamine in solution. Clin Nutr 10:186-192.

268. Robinson NE, Robinson AB. 2001. Prediction of protein deamidation rates from primary and three-dimensional structure. Proc Natl Acad Sci U S A 98:4367-4372.

269. Robinson NE, Robinson ZW, Robinson BR, Robinson AL, Robinson JA, Robinson ML, Robinson AB. 2004. Structure-dependent nonenzymatic

deamidation of glutaminyl and asparaginyl pentapeptides. J Pept Res 63:426-436.

270. Serra A, Gallart-Palau X, Wei J, Sze SK. 2016. Characterization of glutamine deamidation by long-length electrostatic repulsion-hydrophilic interaction chromatography-tendem mass spectrometry (LERLIC-MS/MS) in shotgun proteomics. Anal Chem 88:10573-10582.

271. Riggs DL, Silzel JW, Lyon YA, Kang AS, Julian RR. 2019. Analysis of glutamine deamidation: products, pathways, and kinetics. Anal Chem 91:13032-13038.

272. Asai H, Kato K, Nakayoshi T, Ishikawa Y, Kurimoto E, Oda A, Fukuishi N. 2021. Nonenzymatic deamidation mechanism on a glutamine residue with a C-terminal adjacent glycine residue: a computational mechanistic study. Appl Chem 1:142-155.

273. White PJ. 1979. Inhibition by D-glutamate as the cause of diphasic growth of diphasic growth of *Bacillus megaterium* NCIB 7581 with glycerol plus DL-glutamic acid. J Gen Microbiol 114:149-158.

274. White PJ. 1979. Effects of D-glutamate on enzymes of ammonia assimilation in *Bacillus megaterium* NCIB 7581. J Gen Microbiol 114:159-168.

275. Pratviel-Sosa F, Acher F, Trigalo F, Blanot D, Azerad R, J vH. 1994. Effect of various analogues of D-glutamic acid on the D-glutamate-adding enzyme from *Escherichia coli*. FEMS Microbiol Lett 115:223-228.

276. DeHart TG, Kushelman MR, Hildreth SB, Helm RF, Jutras BL. 2021. The unusual cell wall of the Lyme disease spirochaete *Borrelia burgdorferi* is shaped by a tick sugar. Nat Microbiol 6:1583-1592.

277. Jones BW, Nishiguchi MK. 2004. Counterillumination in the Hawaiian bobtail squid, *Euprymna scolopes* Berry (Mollusca: Cephalopoda). Mar Biol 144:1151-1155.

278. Stabb EV, Millikan DS. 2009. Is the *Vibrio fischeri-Euprymna scolopes* symbiosis a defensive mutualism?, p 103-116, Defensive Mutualism in Microbial Symbiosis. CRC Press.

279. Boettcher KJ, Ruby EG, McFall-Ngai MJ. 1996. Bioluminescence in the symbiotic squid *Euprymna scolopes* is controlled by a daily biological rhythm. J Comp Physiol A 179:65-73.

280. Montgomery MK, McFall-Ngai M. 1993. Embryonic Development of the Light Organ of the Sepiolid Squid *Euprymna scolopes* Berry. Biol Bull 184:296-308.

281. Sycuro LK, Ruby EG, McFall-Ngai M. 2006. Confocal microscopy of the light organ crypts in juvenile *Euprymna scolopes* reveals their morphological complexity and dynamic function in symbiosis. J Morphol 267:555-68.

282. Essock-Burns T, Bongrand C, Goldman WE, Ruby EG, McFall-Ngai MJ. 2020. Interactions of symbiotic partners drive the development of a complex biogeography in the squid-*Vibrio* symbiosis. mBio 11:e00853-20.

283. Essock-Burns T, Lawhorn S, Wu L, McClosky S, Moriano-Gutierrez S, Ruby EG, McFall-Ngai MJ. 2023. Maturation state of colonization sites promotes symbiotic resiliency in the *Euprymna scolopes-Vibrio fischeri* partnership. Microbiome 11:68.

284. Doino JA, McFall-Ngai MJ. 1995. A transient exposure to symbiosis-competent bacteria induces light organ morphogenesis in the host squid. Biol Bull 189:347-355.

285. Lamarcq LH, MJ M-N. 1998. Induction of a gradual, reversible morphogenesis of its host's epithelial brush border by *Vibrio fischeri*. Infect Immun 66:777-785.

286. Kerwin AH, Gromek SM, Suria AM, Samples RM, Deoss DJ, O'Donnell K, Frasca S, Jr., Sutton DA, Wiederhold NP, Balunas MJ, Nyholm SV. 2019. Shielding the next generation: symbiotic bacteria from a reproductive organ protect bobtail squid eggs from fungal fouling. mBio 10.

287. Kerwin AH, McAnulty SJ, Nyholm SV. 2021. Development of the accessory nidamental gland and associated bacterial community in the Hawaiian bobtail squid, *Euprymna scolopes*. Biol Bull 240:205-218.

288. McAnulty SJ, Kerwin AH, Koch E, Nuttall B, Suria AM, Collins AJ, Schleicher TR, Rader BA, Nyholm SV. 2023. "Failure To launch": development of a reproductive organ linked to symbiotic bacteria. mBio 14:e02131-22.

289. Hapfelmeier S, Lawson MA, Slack E, Kirundi JK, Stoel M, Heikenwalder M, Cahenzli J, Velykoredko Y, Balmer ML, Endt K, Geuking MB, Curtiss R, 3rd, McCoy KD, Macpherson AJ. 2010. Reversible microbial colonization of germ-free mice reveals the dynamics of IgA immune responses. Science 328:1705-9.

290. Cuenca M, Pfister SP, Buschor S, Bayramova F, Hernandez SB, Cava F, Kuru E, Van Nieuwenhze MS, Brun YV, Coelho FM, Hapfelmeier S. 2016. D-alanine-controlled transient intestinal mono-colonization with non-laboratory-adapted commensal *Escherichia coli* strain HS. PLoS One 11:e0151872.

291. Moscoso M, García P, Cabral MP, Rumbo C, Bou G. 2018. A D-Alanine auxotrophic live vaccine is effective against lethal infection caused by *Staphylococcus aureus*. Virulence 9:604-620.

292. Kang L, Shaw AC, Xu D, Xia W, Zhang J, Deng J, Woldike HF, Liu Y, Su J. 2011. Upregulation of MetC is essential for D-alanine-independent growth of an *alr/dadX*-deficient *Escherichia coli* strain. J Bacteriol 193:1098-1106.

293. Graf J, Ruby EG. 1998. Host-derived amino acids support the proliferation of symbiotic bacteria. Proc Natl Acad Sci U S A 95:1818-1822.

294. Shaku M, Ealand C, Matlhabe O, Lala R, Kana BD. 2020. Peptidoglycan biosynthesis and remodeling revisited, p 67-103. *In* Gadd GM, Sariaslani S (ed), Advances in Applied Microbiology, vol 112. Academic Press.

295. Tomasz A. 1979. The mechanism of the irreversible antimicrobial effects of penicillins: how the beta-lactam antibiotics kill and lyse bacteria. Annu Rev Microbiol 33:113-137.

296. Kuru E, Radkov A, Meng X, Egan A, Alvarez L, Dowson A, Booher G, Breukink E, Roper DI, Cava F, Vollmer W, Brun Y, VanNieuwenhze MS. 2019. Mechanisms of incorporation for D-amino acid probes that target peptidoglycan biosynthesis. ACS Chem Biol 14:2745-2756.

297. Walsh CT. 1989. Enzymes in the D-alanine branch of bacterial cell wall peptidoglycan assembly. J Biol Chem 264:2393-2396.

298. Hols P, Defrenne C, Ferain T, Derzelle S, Delplace B, Delcour J. 1997. The alanine racemase gene is essential for growth of *Lactobacillus plantarum*. J Bacteriol 179:3804-7.

299. Strych U, Huang HC, Krause KL, Benedik MJ. 2000. Characterization of the alanine racemases from *Pseudomonas aeruginosa* PAO1. Curr Microbiol 41:290-4.

300. Milligan DL, Tran SL, Strych U, Cook GM, Krause KL. 2007. The alanine racemase of *Mycobacterium smegmatic* is essential for growth in the absence of D-alanine. J Bacteriol 189:8381-8386.

301. Awasthy D, Bharath S, Subbulakshmi V, Sharma U. 2012. Alanine racemase mutants of *Mycobacterium tuberculosis* require D-alanine for growth and are defective for survival in macrophages and mice. Microbiol 158:319-327.

302. Wei Y, Qiu W, Zhou XD, Zheng X, Zhang KK, Wang SD, Li YQ, Cheng L, Li JY, Xu X, Li MY. 2016. Alanine racemase is essential for the growth and interspecies competitiveness of *Streptococcus mutans*. Int J Oral Sci 8:231-238.

303. Wasserman SA, Walsh CT, Botstein D. 1983. Two alanine racemase genes in *Salmonella typhimurium* that differ in structure and function. J Bacteriol 153:1439-1450.

304. Wild J, Hennig J, Lobocka M, Walczak W, Klopotowski T. 1985. Identification of the *dadX* gene coding for the predominant isozyme of alanine racemase in *Escherichia coli* K12. Mol Gen Genet 198:315-322.

305. Dodds D, Bose JL, Deng M-D, Dubé GR, Grossman TH, Kaiser A, Kulkarni K, Leger R, Mootien-Boyd S, Munivar A, Oh J, Pestrak M, Rajpura K, Tikhonov AP, Turecek T, Whitfill T. 2020. Controlling the growth of the skin commensal *Staphylococcus epidermidis* using D-alanine auxotrophy. mSphere 5:10.1128/msphere.00360-20.

306. Fuentes-Valverde V, García P, Moscoso M, Bou G. 2022. Double auxotrophy to improve the safety of a live anti-*Pseudomonas aeruginosa* vaccine. Vaccines 10:1622.

307. García P, Moscoso M, Fuentes-Valverde V, Rodicio MR, Herrera-León S, Bou G. 2023. A highly-safe live auxotrophic vaccine protecting against disease caused by non-typhoidal *Salmonella Typhimurium* in mice. J Microbiol Immunol Infect 56:324-336.

308. Stabb EV, Reich KA, Ruby EG. 2001. *Vibrio fischeri* genes *hvnA* and *hvnB* encode secreted NAD(+)-glycohydrolases. J Bacteriol 183:309-317.

309. Yamagata H, Taguchi N, Daishima K, Mizushima S. 1983. Genetic characterization of a gene for prolipoprotein signal peptidase in *Escherichia coli*. Mol Gen Genet 192:10-14.